Analysis of T Cell Activation Regulators in Autoimmune Hepatitis

Dissertation for obtaining the degree of

Doctor rerum naturalium at the

Faculty of Mathematics, Informatics, and Natural Sciences,

Department of Biology, University Hamburg

submitted by

Pamela Twumwaa Filpe

Hamburg 2020

The following evaluators recommend the admission of this dissertation:

1. **Prof. Dr. rer. nat. Johannes Herkel**

University Medical Center Hamburg-Eppendorf, Department of Internal Medicine I
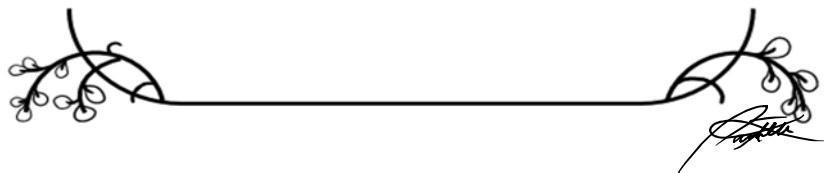
2. **Prof. Dr. rer. nat. Susanne Dobler**

University Hamburg, Department of Biology, Institute of Zoology

Date of oral defence: 15th May, 2020.

I will praise thee;

for I am fearfully and wonderfully made:

marvellous *are* thy works;

and *that* my soul knoweth right well.

Psalm 139: 14, King James Bible

Table of contents

I   List of figures

II List of tables

1.   Introduction

1.1   Autoimmune Hepatitis

Autoimmune hepatitis (AIH) is a chronic inflammatory disease of the liver. The immune response of AIH is directed against hepatocytes. In clinical terms, AIH presents heterogeneously with fluctuating periods of increased and decreased activity. Moreover, the clinical appearance of AIH is characterised by elevation of immunoglobulin G (IgG) and the presence of circulating autoantibodies (e.g. antinuclear antibodies (ANA), anti-smooth muscle antigen (anti-SMA) and anti-soluble liver antigen/liver pancreas antigen (anti-SLA/LP) antibodies) in the serum. Further diagnostic hallmark is the elevation of serum transaminases aspartate aminotransferase (AST) and alanine aminotransferase (ALT), indicating liver damage [1, 2]. In histology, livers of AIH patients show intrahepatic mononuclear lymphocytic infiltration in the portal and periportal regions. The portal mononuclear infiltration is mainly composed by plasma cells, T cells, macrophages and monocytes [3]. A histological key feature of AIH is interface hepatitis, which describes lympho-plasmacytic infiltrates extending from the portal tracts into hepatic lobules [2, 4; *figure 1*]. If AIH is left untreated, development of fibrosis and progression to liver cirrhosis occurs.

AIH is more common in females, however it affects children and adults of both sexes, all ages and different ethnic groups [5, 6, 7]. The appearance of AIH is clinically subdivided into adult-predominant AIH type 1, AIH type 2 which is paediatric-predominant and AIH type 3. The determination of the three subtypes is mainly dependent on the pattern of autoantibodies. Type 1 AIH is characterised by the presence of serum ANA, SMA and occasionally perinuclear anti-neutrophil cytoplasmic antibodies (pANCA), whereas AIH type 2 is characterised by anti-liver kidney microsomal type 1 (LKM1) and anti-liver cytosol type 1 (LC1) antibodies. AIH type 3 is characterised by the presence of anti SLA/LP antibodies, at times accompanied by ANA antibodies [2, 8, 9, 10, 11]. As compared to type 2 and type 3 AIH, disease severity of type 1 AIH is mild to moderate with rare occurrence of liver failure. AIH type 2 or type 3 have been associated with frequent relapse [12, 13].

Progression to liver cirrhosis and liver failure in AIH can only be prevented by lifelong use of immunosuppressive drugs. Currently, non-selective immunosuppression with prednisolone for initial treatment and azathioprine for maintenance treatment is the standard therapy for AIH. This standard therapy can achieve remission in 70-80% of cases but if no remission was achieved and relapse occurs, e.g. because patients do not tolerate or respond to the drugs, second-line treatment with stronger immunosuppression is needed. Good response to treatment, defined by normalisation of transaminases and IgG and/or resolution of liver inflammation,

stops the progression of AIH and can prevent liver transplantation [14, 15, 16, 17]. Unfortunately, initial and maintenance regimens with standard and second-line therapy often lead to side effects, such as steroid-induced osteoporosis or azathioprine-induced bone marrow suppression [8, 18].

The aetiology and the immunopathogenesis of AIH remains unclear. Genome-wide association studies and other genetic human studies reported an association of AIH with human leukocyte antigens (HLA)-DR3 and HLA-DR4 [19, 20, 21, 22]. This suggests that AIH might be driven by self-antigen presentation in terms of adaptive immunity. Highly activated T effector cells seem to play an essential role by mediating hepatic inflammation and hepatocellular damage. It is assumed that immune regulations of activated T effector cells are impaired in AIH [9]. Regulatory T cells (Tregs) can mediate inhibition of activated T effecter cells and immune tolerance to self-antigens. Previous studies suggested that the frequency and function of Tregs are diminished in AIH patients [1, 9]. However, in contrast, other studies showed that Tregs were not reduced in frequency and were not dysfunctional in AIH patients [23].
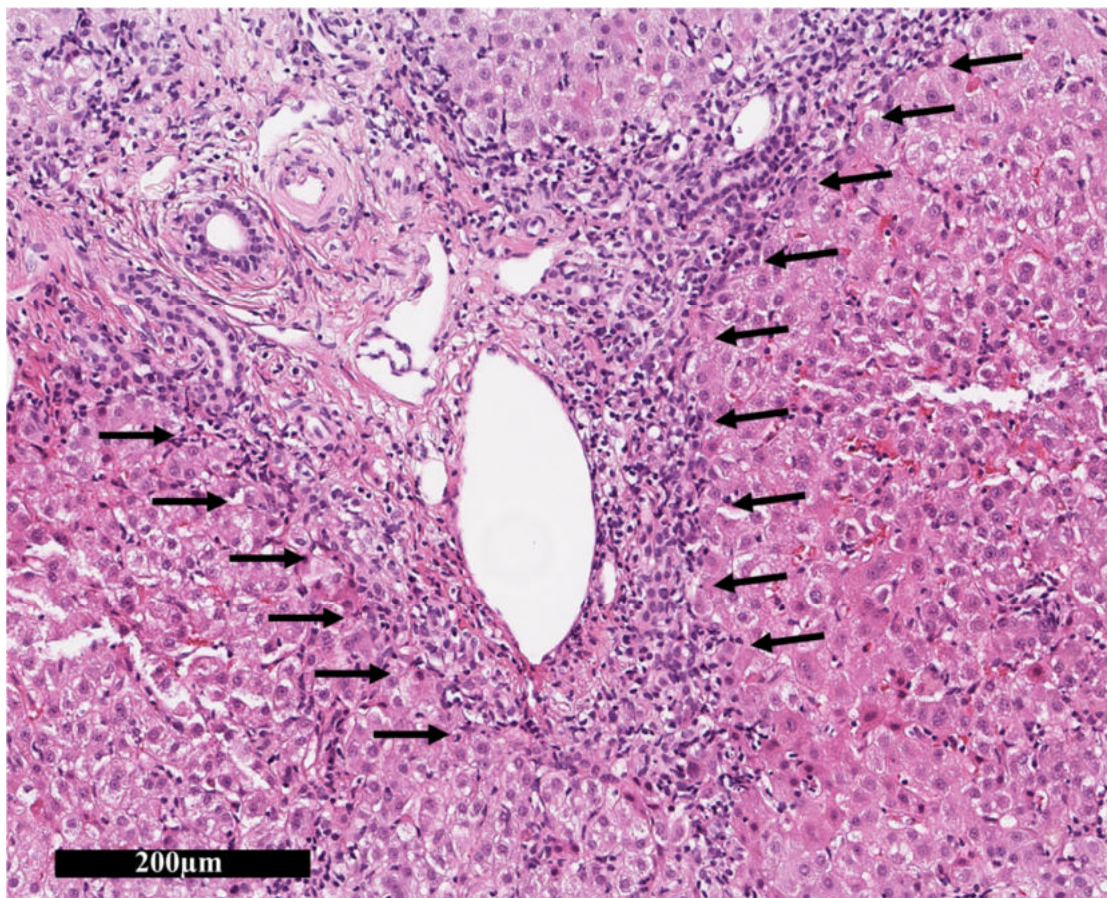
Figure 1 **Interface hepatitis in AIH.** Liver tissue sample of patient with AIH was stained with haematoxylin and eosin (HE). Portal inflammation extend into the lobule (arrows). Figure is from personal collection.

1.2 Autoimmune cholestatic liver diseases

Primary biliary cirrhosis (PBC) and primary sclerosing cholangitis (PSC) are main autoimmune cholestatic liver diseases. Patients with PBC or PSC exhibit impaired bile flow and accumulation of toxic bile acids due to immune response against endogenous bile duct cells (cholangiocytes).

1.2.1 Primary biliary cholangitis

Primary biliary cholangitis (PBC, former: primary biliary cirrhosis) is a chronic inflammatory autoimmune liver disease, which is characterised by the progressive destruction of small intrahepatic bile ducts, resulting in an impairment of bile flow (cholestasis). Untreated PBC leads to fibrosis, which progresses to liver cirrhosis and liver failure [24, 25]. PBC predominantly affects middle-aged women [26] and it is diagnosed by the presence of anti-mitochondrial antibodies (AMA), which are the serological hallmark for PBC, and elevated serum alkaline phosphatase (AP or ALP) [27]. Patients with PBC show histological evidence of chronic non-suppurative destructive cholangitis, formation of granulomas within the liver, degeneration and necrosis of biliary epithelial cells (BECs) and destruction of interlobular bile ducts [28, 29, 30, 31]. Regarding the pathogenesis of PBC, it was reported that T cell-mediated inflammatory responses play a crucial role in the production of AMA against dihydrolipoamide acetyltransferase (E2) subunit of pyruvate dehydrogenase complex (PDC-E2) in the inner mitochondrial membrane of BECs [29, 32, 33; *figure 2*]. Besides, PDC-E2 molecules and apoptotic bodies released from BECs stimulate inflammatory macrophages to secrete pro-inflammatory cytokines [34, 35]. In addition, previous studies showed that expression of anion exchanger 2 (AE2) was reduced in patients with PBC. Reduced expression of AE2 might contribute to the impaired secretion of biliary bicarbonate by cholangiocytes and thus, benefit the pathology of PBC [36, 37, 38, 39]. Ursodeoxycholic acid (UDCA) is the approved drug for PBC treatment. Treatment with UDCA prevents progression to PBC-mediated liver cirrhosis and liver failure. Thereby, reducing the numbers of liver transplantation performed on patients due to PBC [25, 40].
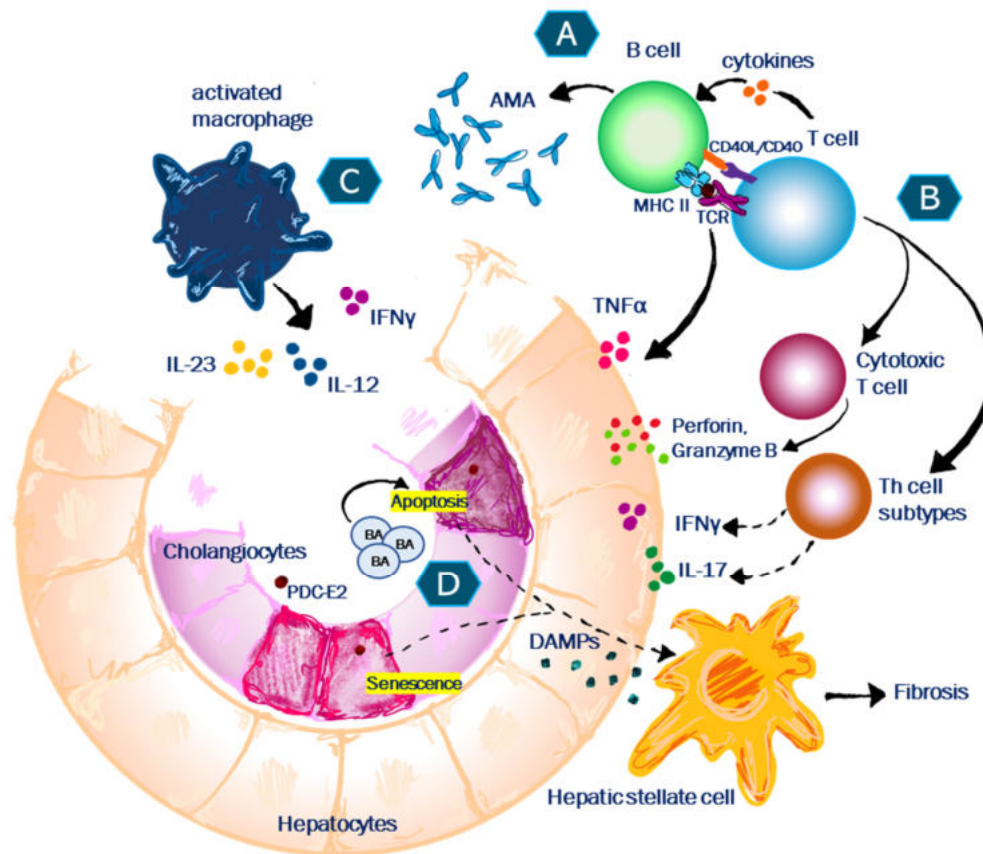
Figure 2 **Pathogenesis of PBC.** (A) T helper (Th) cell interaction with B cell induces B cell activation and production of anti-mitochondrial antibodies (AMA) that are specific to PDC-E2. (B) Pro-inflammatory cytokines induce the recruitment of Th cell subsets and cytotoxic T lymphocytes (CTLs). CTLs and Th cells produce cytokines that promote apoptosis or senescence of BECs. (C) Stimulated immune cells, like macrophages, secrete pro-inflammatory cytokines, contributing to the damage of BECs. (D) Unchaperoned bile acids (BA) directly interfere with BECs, promoting apoptosis and senescence. Injured BECs secrete damage-associated molecular patterns (DAMPs) that maintain inflammation and stimulate hepatic stellate cells, which induce fibrosis. Figure is from personal collection.

BECs, biliary epithelial cells; CD, cluster of differentiation; IFNγ, interferon-gamma; IL, interleukin; MHC II, major histocompatibility complex class II; PDC-E2, pyruvate dehydrogenase complex E2 subunit; TCR, T cell receptor; TNFα, tumour necrosis factor-alpha.

1.2.2 Primary sclerosing cholangitis

Primary sclerosing cholangitis (PSC) is a chronic inflammatory cholestatic liver disease, which is characterised by progressive fibrotic strictures of larger bile ducts and suppurative lesions of the bile duct mucosa, leading to biliary cirrhosis and malignancy. Patients who are diagnosed with PSC are at increased risk for cholangiocarcinoma and cancers of the gallbladder and colon [41, 42, 43]. PSC predominantly affects middle-aged men, especially patients that are diagnosed with ulcerative colitis (UC) or Crohn`s disease. UC and Crohn`s disease are described as

inflammatory bowel diseases (IBD) and patients with PSC are strongly associated with IBD. Reasons for the direct association with IBD are not yet clearly defined [43, 44].

PSC is clinically tested with magnetic resonance cholangiopancreatography (MRCP). MRCP generates a cholangiogram, which images the patient`s bile ducts. A cholangiogram of PSC patients features narrowings, known as strictures, which are multifocal and ring-shaped (annular) within the bile ducts. Alternation of normal and slightly dilated structure segments of the bile ducts appears as "beads-on-a-string" [45; *figure 3*]. Elevated levels of anti-smooth muscle antibodies (ASMA), pANCA and ANA are present in PSC patients [46, 47, 48]. In addition, serum levels of AP (or ALP), ALT and AST are elevated in PSC patients [49, 50].

Histologically, concentric fibrotic rings form around the bile ducts (onion-skinning) and eventually leads to loss of interlobular bile ducts. Furthermore, lymphocytic infiltration, portal inflammation and periductal oedema are manifested in liver tissue of PSC patients [44].

Although the aetiology and pathogenesis of PSC remains uncertain, according to genetic studies, HLA-A1 B8 DR3, HLA-D2 and HLA-DR6 are strongly associated with PSC. This indicates an immune-mediated pathology of the disease [51, 52]. Next-generation sequencing (NGS) studies revealed that as compared to healthy individuals, patients with PSC have an altered gut bacterial microbiome in the oral cavity, duodenal fluid and mucosa as well as in the ductal bile [43, 53, 54]. In addition, it has been proposed that components of microbial origin may trigger pro-inflammatory immune responses by leaking from the bowel to the liver through portal circulation. Currently, PSC is treated with UDCA with the intention of reducing elevated cholestatic liver enzymes and delay of inevitable liver transplantation; however, its prognostic benefit is still uncertain [55, 56, 57].
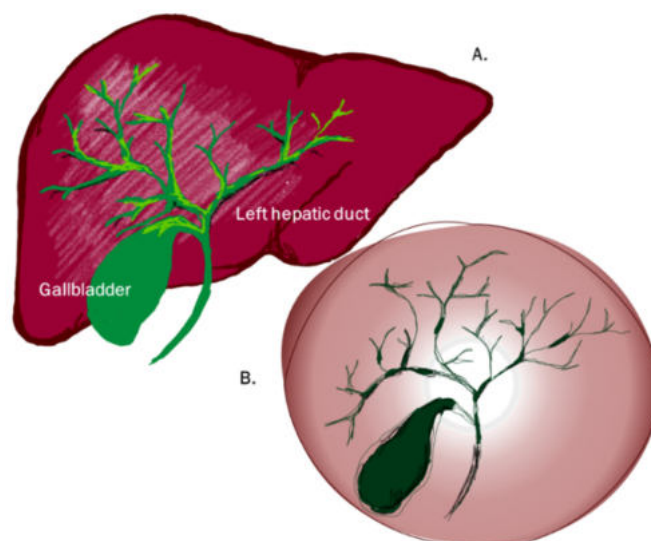
Figure 3 **Bile ducts in PSC.** Schematic representation of healthy gallbladder and bile duct (A). Schematic representation of bile ducts in PSC (B). In PSC, bile ducts exhibit strictures that lead to "beads-on-a-string" appearance. Figure is from personal collection.

1.3 Non-autoimmune liver diseases

1.3.1 Drug-induced liver injury

Drug-induced liver injury (DILI) is a non-autoimmune condition of the liver, which spectrum of manifestations ranges from moderate increase of liver enzymes to acute liver failure. The effect of drug agents on liver toxicity and DILI can be subdivided in either intrinsic or idiosyncratic form. Following drug intake, drug-induced hepatotoxicity can occur in a predictable manner due to a clear dose-dependency, resulting in intrinsic DILI. In contrast, idiosyncratic DILI is defined as dose-independent, unpredictable and more individual course [59, 60, 61, 62, 63]. DILI has been associated to multiple drugs, causing their non-approval or withdrawal during or after clinical trials [64, 65].

Causality assessment of the Council for International Organizations of Medical Sciences/Roussel-Uclaf causality assessment method (CIOMS/RUCAM) proposes older age as a possible risk factor for DILI [66]. In addition, female gender (age over 60) has been associated with cholestatic DILI [67]. Because the diagnosis of DILI is challenging, causality scores such as RUCAM are intended to confirm or exclude the diagnostic suspicion of DILI [66, 68, 69]. Since clinical features of DILI, such as elevated levels of serum ALT and AST, are not DILI-specific, current diagnosis of IDILI mainly depends on expert opinion [70]. For proper diagnosis, the causative agent and the onset of liver injury after drug intake as well as the resolution of liver enzymes after drug withdrawal, and recurrence on re-exposure must be identified [71, 72]. DILI can resemble the clinical appearance of AIH regarding elevated AST, ALT, IgG, autoantibodies and lymphocytic infiltration of the liver [59]. However, a lack of recurrence following weaning of corticosteroid treatment strongly supports the diagnosis of AIH. In uncertain cases, liver biopsy can be relevant to assess alternative diagnoses [72, 73].

Recently, genetic studies have identified protein tyrosine phosphatase non-receptor type 22 (PTPN22) as non-HLA autoimmunity risk gene for IDILI [74, 75]. Furthermore, genetic polymorphism of cytochrome p450 enzymes (CYPs) may affect metabolism of toxic drugs or accelerate production of drug metabolites [76, 77]. The pathogenesis of DILI depends on lipophilicity and metabolism in the liver of the drug argent. In terms of metabolism, the liver is exposed to bioactive metabolites that are potentially toxic and can interact with various proteins, activate signal transduction pathways and induce oxidative stress [63]. Nevertheless, many pathogenetic pathways at the molecular level remain unknown.

1.3.2 Non-alcoholic steatohepatitis

Non-alcoholic steatohepatitis (NASH) is the progressed form of non-alcoholic fatty liver disease (NAFLD) and it is characterised by steatosis (abnormal accumulation of lipids within cells or organ), hepatic inflammation, hepatocyte cell ballooning and varying degrees of liver fibrosis. NAFLD describes the spectrum that comprises varying conditions of liver injury from non-inflammatory, isolated steatosis to NASH. Moreover, NASH predisposes to the development of liver cirrhosis and hepatocellular carcinoma [78, 79, 80]. Diagnostic identification of hepatic steatosis is enabled through imaging, for instance, through ultrasound or magnetic resonance imaging (MRI). However, the diagnosis of NASH requires liver biopsy [80]. Risk factors for NASH are metabolic disorders, such as dyslipidaemia (elevated amount of lipids in blood), type 2 diabetes mellitus and insulin resistance. Furthermore, sedentary lifestyle in combination with excessive caloric intake are risk factors for NAFLD and NASH [81, 82, 83]. Several genes were associated with elevated levels of steatosis in NAFLD, such as PNPLA3 [84, 85, 86].

Medical management of NASH is based on healthy weight loss and changes in lifestyle [87]. Unfortunately, there is no approved therapeutic drug agent for the treatment of NASH.

Previous studies defined the pathologic progression of NAFLD to NASH with either the "two-hit" hypothesis or the "multiple-parallel hit" hypothesis. The first "hit" of the "two-hit" hypothesis is defined by insulin resistance. Insulin resistance may account for elevated levels of serum free fatty acid (FFA), leading to accumulation of hepatic triglyceride and resulting in an increase of liver fat. Hepatic steatosis is reached, when hepatic fat exceeds more than 5% of the liver [88, 89]. Accumulation of hepatic triglyceride enhances oxidative stress, the second "hit", which promotes the release of pro-inflammatory cytokines and mitochondrial damage. Progression of steatosis and inflammation with formation of hepatocellular damage results in NASH [90]. The "multiple-parallel hit" hypothesis describes NASH as a consequence of several intra- and extracellular processes that run in parallel, including insulin resistance, hepatocellular injury and death through induction of oxidative stress as well as endoplasmatic reticulum (ER) stress caused by excessive accumulation of toxic lipid metabolites in the liver [91, 92, 93].

1.4 Activation of T lymphocytes

T cell activation initially requires interaction of the T cell receptor (TCR)/CD3 complex with antigen peptides presented on professional Antigen presenting cells (APCs), such as dendritic cells (DCs), B cells and macrophages. APCs present antigen peptides on human leukocyte antigen (HLA) complexes to naive CD4$^+$ or CD8$^+$ T lymphocytes. HLA complexes are major histocompatibility complexes (MHC), which are subdivided in MHC class I or MHC class II. Isotypes of MHC class I or II molecules are diverse in function and in polymorphism. A single individual can express nine MHC class I and six MHC class II isotypes [94, 95, 96]. MHC class I presentation of antigen peptides is restricted to CD8$^+$ T cells and MHC class II presentation is restricted to CD4$^+$ T cells. TCR/CD3 and co-receptor CD8 or CD4 ligation to MHC class I or class II provides "signal 1", whereas "signal 1" by itself is insufficient to enable full T cell activation. Upon ligation cytoplasmic protein kinases Lck is recruited to the TCR/CD3 complex and phosphorylates immunoreceptor tyrosine-based activation motifs (ITAMs) in the cytoplasmic tail of CD3 and in the associated ζ chain (CD247). Lck activates protein kinase ZAP-70, which then binds to phosphorylated ITAMs on the ζ chain and transmits further activating signal transduction onwards [94, 97; *figure 4*]. Co-stimulation of T cell activation is assured, when the homodimeric co-receptor CD28 binds to its ligands B7-1 (CD80) or B7-2 (CD86). CD80 and CD86 are expressed on APCs [98, 99]. Autocrine production of inflammatory cytokines, such as interleukin 2 (IL-2), provide the "signal 3" by activating cytokine signalling pathways that promote T cell proliferation and differentiation into T effector cells [94, 100, 101].

Differentiation of CD4$^+$ T cells into distinct effector subtypes depends mainly on the secreted cytokine milieu and on specific transcription factors (*figure 5*). Activated cytokine signalling pathways and activation of lineage-specific transcription factors induce T cell differentiation into distinct T effector cell phenotypes [100, 102]. Activated CD4$^+$ T cells can differentiate into CD4$^+$ T effector cells subtypes with diverse immune functions. Interleukin 12 (IL-12) and interferon γ (IFNγ) as well as transcription factor T-box transcription factor (T-bet) play an essential role for the differentiation of CD4$^+$ T cells into classical T helper 1 (Th1) cells. Th1 cells produce IFNy, IL-2 and tumour necrosis factor α (TNFα) to activate macrophages and cell-mediated immune responses against bacterial and viral infections [103]. Classical Th2 cell differentiation is prompted by IL-4, IL-2 and transcription regulator GATA3. Secretion of IL-4, IL-5 and IL-13 by Th 2 cells prime B cell class switching, recruit eosinophils and induce degranulation of basophils and mast cells [103, 104]. Differentiation of activated CD4$^+$ T cells into IL-9 producing Th9 cells is induced by the presence of transforming growth factor β

(TGFβ) and IL-4. IL-4 downstream signalling activates key transcription factor interferon response factor 4 (IRF4). Given to the multiple function of IL-9, Th9 cells are present in various inflammatory processes [105, 106]. For differentiation into Th17 cells, IL-6, IL-21, IL-23 as well as TGFβ signalling pathways are essential. Retinoic acid receptor-related orphan receptor gamma-T (RORγt) functions as the master transcription factor for the Th17 cell subset. Th17 cells produce IL-17, IL-21 and IL-22 and are involved in the host defence against viral and extracellular bacterial infections [107]. Follicular helper T cell (Tfh) differentiation is promoted by IL-6 and IL-21 cytokine signalling. Transcription factor B cell lymphoma 6 (Bcl6) drives Tfh differentiation. Tfh cells are located in secondary lymphoid organs, such as lymph nodes, and contribute to the development of antigen-specific B cells into plasma cells or memory
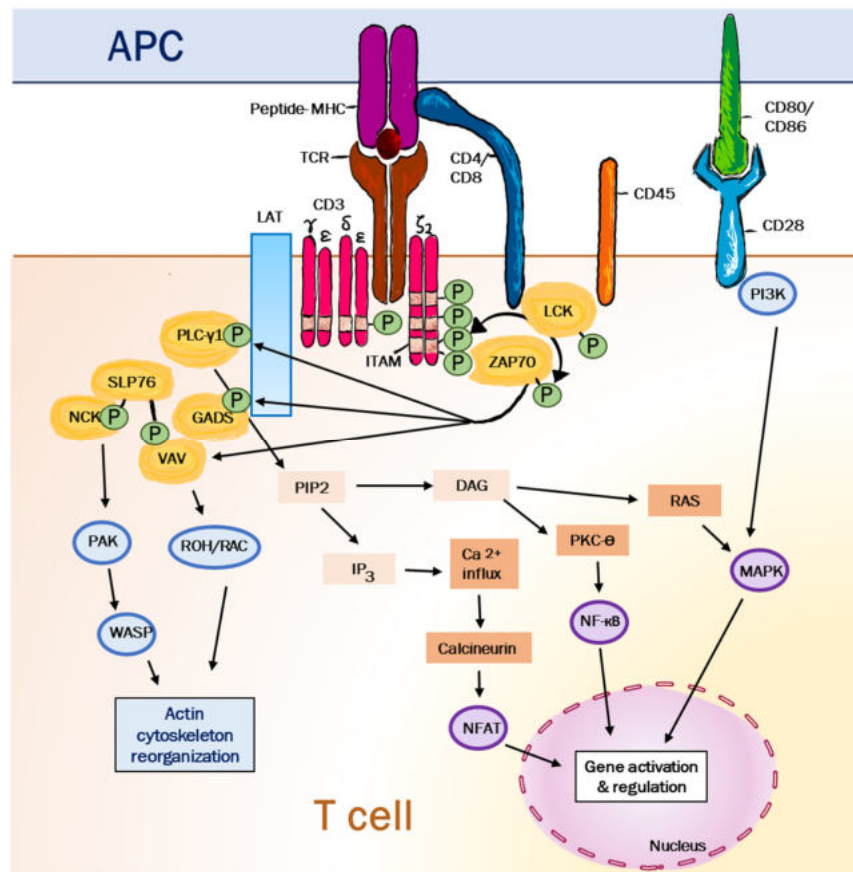
Figure 4 **TCR-depending signalling pathways.** Antigen presenting cell (APC) presents antigen derived peptide to T cell. TCR engages MHC-peptide complex and CD28 co-receptor engages CD80/CD86. This promotes activation of protein kinase LCK which phosphorylate the ITAMs of CD3ζ-and CD3ε-chains. Activated ZAP-70 binds phosphorylated ITAMs and thereby provide downstream signalling transduction that leads to activation of multiple molecules such as transcription factors. Figure is from personal collection.

DAG: diacylglycerol; ITAM: immunoreceptor tyrosine-based activation motifs; IP3: inositol-1,4,5-trisphosphate; PI3K: Phosphoinositide 3-kinases; PIP2: phosphatidylinositol-4,5-bisphosphate; PKCθ: protein kinase C theta; PLCγ: phospholipase C gamma**.**

B cells [108]. In the presence of TGFβ and IL-2 signalling, activated CD4$^+$ T cells can differentiate into peripheral T regulatory cells (pTregs), which originate from the periphery and not from the thymus (thymic-derived T cells, tTregs). pTregs are positive for transcription factor Forkhead-Box-Protein P3 (FOXP3). By secretion of TGFβ and IL-10, pTregs inhibit functions of T effector cells and thus, contribute to immune regulation of inflammatory processes [109].

Activated CD8$^+$ T cells exposed to autocrine or paracrine secreted IL-2, differentiate into CD8$^+$ cytotoxic T lymphocytes (CTLs). CTLs recognize and eliminate intracellular pathogens, such as bacteria, viruses and protozoan parasites (*figure 5*). In addition, CTLs play a key role in tumour surveillance by killing of damaged cells and tumorous cells. CTLs secret TNFα as well as IFNγ, and they are capable to release perforins and granzymes. The release of perforins and granzymes cytotoxic granules induces apoptosis of the target cell. Another pathway of CTL-mediated cell death is through Fas ligand (FasL) and Fas receptor (Fas) interactions. FasL on the cell surface of CTL binds to Fas, which is expressed on the cell surface of the target cell.
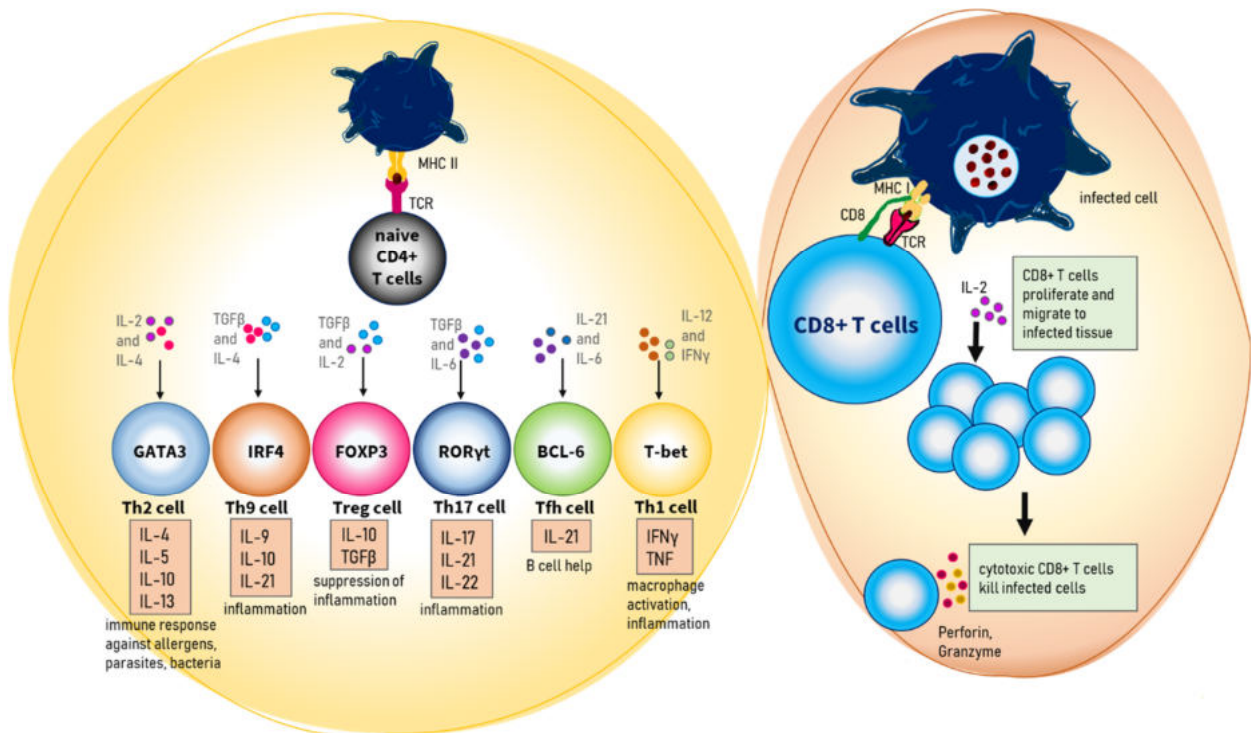
Figure 5 **Polarisation of naive T cells into activated T effector cells**. Activated naive CD4$^+$ T cells differentiate mainly into T helper cell subsets with different responsibilities that help innate and adaptive immune responses against foreign molecules (left panel). Activated naive CD8$^+$ T cells mainly differentiate into cytotoxic T cell that provide cytotoxic T cell-mediated anti-viral immune responses and immune defence against intracellular pathogens, bacteria and parasites (right panel). Figure from personal collection.

BCL-6: B cell lymphoma 6; FOXP3: forkhead box P3; GATA3: GATA-binding protein 3; IRF4: interferon regulatory factor 4; RORγt: retinoic acid receptor-related orphan receptor-γt; T-bet: T-box transcription factor; TCR: T cell receptor; TGFβ: transforming growth factor-β; TNF: tumour necrosis factor.

FasL/Fas ligation induces downstream signalling to activate caspase cascade, resulting in apoptosis of the target cell [110, 111]. Recent studies have identified peripherally induced CD8$^+$ Tregs (CD8$^+$ pTregs). Similar to CD4$^+$ pTregs, CD8$^+$ pTreg derive from the periphery upon stimulation [112, 113]. However, the function of CD8$^+$ pTregs remains to be clarified.

1.5   T cell co-stimulatory and co-inhibitory molecules

TCR/CD3 engagement ("signal 1"), ligation of co-stimulatory receptor CD28 with its ligand ("signal 2") and intracellular IL-2 cytokine signalling pathways ("signal 3") are essential for sufficient T cell activation. For additional T cell stimulating signalling, T cell co-stimulatory receptors, such as Inducible T cell co-stimulator (ICOS), bind to their appropriate ligands. Co-stimulatory receptors do not necessarily have to associate with the TCR/CD3 complex in order to induce complementary T cell stimulation. Moreover, co-stimulatory receptors can transduce intracellular signals to stimulate TCR signalling [114, 115, 116].

Co-receptors that induce signalling to prohibit continuous T cell activation are called co-inhibitory receptors. Co-inhibitory receptors, such as cytotoxic T lymphocyte-associated protein 4 (CTLA-4) and programmed cell death protein 1 (PD-1) are expressed on activated T cells. Co-inhibitory receptors increase the activation threshold of T effector cells by binding to their specific ligands. Hence, T cell co-stimulatory and co-inhibitory receptors regulate T cell activation and contribute to a balanced immune response [117]. In addition to co-stimulatory and co-inhibitory receptors, T cells inherent intracellular molecules, such as casitas B-lineage lymphoma proto-oncogene-b (CBL-B), which are involved in the suppression or stimulation of T effector cell activation. These molecules are as well activation regulators that support well-balanced T effector cell immune responses. Impaired co-stimulatory or co-inhibitory regulators of T cell activation result in altered T effector cell functions and may cause aberrant immune responses.

1.5.1 ICOS

Inducible T cell co-stimulator (ICOS), also named CD278, is a co-stimulatory molecule expressed on the surface of T cells following activation. ICOS is an homodimeric protein, which belongs to the B7-CD28 family of proteins. ICOS shares structural similarities with CD28; however, ICOS lacks the specific MYPPPY motif, which is relevant for the binding of CD80 and CD86 [118]. ICOS owns the specific FDPPPF motif that is necessary to interact with ICOS ligand B7-H (CD275, ICOSL). ICOSL is expressed at low levels on APCs, such as B cells, macrophages, monocytes and DCs, but it can be quickly upregulated when APCs become activated, for instance, in presence of inflammatory cytokines [114, 119, 120]. Similar to CD28 signalling, ligation of ICOS with ICOSL intracellularly recruits class IA phosphatidylinositol 3-kinase (PI3K). Signalling molecule PI3K is a heterodimer with regulatory p50α, p85α and catalytic p110δ subunits. Through phosphorylation, PI3K converts membrane-bound phosphatidyl-inositol 4,5-bisphosphate (PIP2) into phosphatidylinositol 3,4,5-trisphosphate (PIP3), leading to the activation of protein kinase AKT. AKT induces downstream signals, which promotes cellular growth, proliferation and survival [121, 122]. In contrast to CD28 ligation, ICOS ligation leads to an increased expression of AKT because the YMFM Src homology 2 domain-binding motif in ICOS preferentially recruits the regulatory p50α of PI3K, which has greater lipid kinase activity compared to p85α [122, 123].

ICOS signalling in activated T cells leads to the production of IL-4, IL-10 and IL-21 but not IL-2 [114, 118]. Co-stimulation by ICOS seems to favour CD4$^+$ T cell proliferation and differentiation into Tfh, Th2 and Th17 cells [119]. Previous *in-vitro* and *in-vivo* studies revealed that ICOS deficiency in T cells resulted in impaired T cell proliferation [124, 125].

1.5.2 CTLA-4

Cytotoxic T lymphocyte antigen-4 (CTLA-4, CD152) is a co-inhibitory molecule that belongs to the B7-CD28 family of proteins. Moreover, genes of CTLA-4 and CD28 are located next to each other on the human chromosome 2q33. Like CD28, CTLA-4 form homodimers and uses its highly conserved MYPPPY motif to bind the ligands CD80 and CD86 on APCs [114, 126]. CTLA-4 binds to the ligand CD80 with higher affinity as compared to the co-receptor CD28 ligation and thus, directly competes with CD28 [127]. CD28 is mainly expressed on resting and activated T cells, whereas CTLA-4 is constitutively expressed exclusive on Tregs. CTLA-4 expression on T effector cell surface is induced in response to TCR ligation with CD28 co-stimulation [128]. CTLA-4 trafficking to T effector cell surface is not fully understood;

however, it seems that for externalisation, intracellular CTLA-4 binds to the transmembrane adapter T cell receptor-interacting molecule (TRIM) and to linker for activation of X cells (LAX) in the trans-Golgi network (TGN). Binding to TRIM and LAX induces the formation of CTLA-4-containing vesicles and enables their transport to the cell surface [128, 129; *figure 6*].

Previous studies showed that CTLA-4-mediated inhibitory effect on T cell responses can be either cell-intrinsic or cell-extrinsic. Cell-intrinsic describes the direct influence of CTLA-4 on intracellular processes of the CTLA-4 expressing cell. For instance, the tyrosine-phosphorylated cytoplasmic domain of CTLA-4 associates with protein phosphatases SHP-2 and PP2A to modulate TCR/CD3 signalling [130], it inhibits ZAP-70 [131] and activates E3 ubiquitin ligases [132, 133]. Cell-extrinsic effects of CTLA-4 include the binding of CD80/CD86, the downregulation of CD80/CD86 on APCs [134], the modulation of Treg functions on T effector cells [135, 136] and the induction of indoleamine 2,3-dioxygenase (IDO) production by APCs to limit T cell proliferation [137, 138, 139]. However, the distinct mechanisms by which CTLA-4 supresses T effector cells that have been activated through TCR/CD3 and CD28 stimulation are not fully understood.

Studies in CTLA-4 deficient (*CTLA-4-/-*) mice reported on a hyperproliferative phenotype of T effector cells and enhanced tissue infiltration by lymphocytes. Moreover, *CTLA-4-/-* mice showed pronounced organ destruction [140, 141, 142]. Thus, the co-inhibitory receptor CTLA-4 may play a key role in regulating the activation threshold of T effector cells by dampen their activation and thereby prohibiting tissue damage.
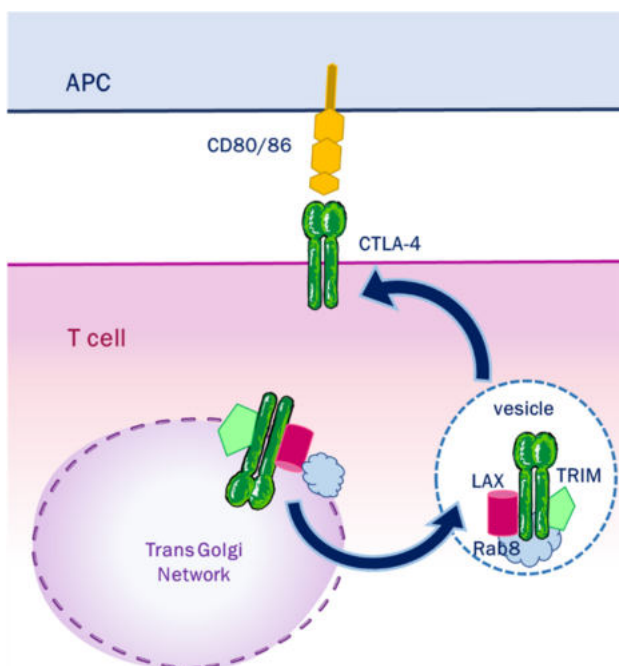
Figure 6 **CTLA-4 trafficking to T cell surface**. In activated T effector cells, transmembrane adapter LAX binds to Ras8 which is a member of the Ras superfamily and regulates protein transport [143, 144]. Transmembrane adaptor TRIM and LAX bind to the cytoplasmic tail of CTLA-4 and thereby form a multimeric complex in TGN. Interaction of LAX with Rab8 is a necessity for the formation and maintenance of the complex. The complex facilitates the transport of synthesized CTLA-4 to the cell surface. Figure is from personal collection.

CTLA-4: cytotoxic T-lymphocyte antigen-4
LAX: linker for activation of X cells
TGN: Trans-Golgi network
TRIM: transmembrane adapter T cell receptor-interacting molecule

1.5.3 PD-1

Programmed cell death protein 1 (PD-1, CD279) is a member of the CD28 superfamily of immunoglobulin receptors. PD-1 expression on T cells can be induced upon T cell activation through TCR/CD3 or cytokine stimulation [145, 146]. PD-1 binds to two ligands, programmed death-ligand 1 (PD-L1) and programmed cell death ligand 2 (PD-L2) [147]. PD-L2 expression is mainly restricted to DCs [148, 149], whereas PD-L1 is expressed by many hematopoietic cells, such as APCs and non-hematopoietic cells, such as epithelial cells and tumorous cells. Moreover, PD-L1 expression can be induced during inflammation [148].

The cytoplasmic tail of PD-1 contains immunoreceptor tyrosine-based inhibition motif (ITIM) and immunoreceptor tyrosine-based switch motif (ITSM). Upon PD-1 engagement with PD-L1 or PD-L2 ITIM (Y223) and ITSM (Y248) become phosphorylated. As a consequence, Src homology region 2 domain-containing phosphatases SHP-2 and SHP-1 are recruited (*figure 7*). SHP-2 and SHP-1 dephosphorylate PKCθ, ZAP-70 and PI3K, resulting in downregulation of TCR signalling. Dephosphorylation of PI3K leads to its inhibition and hence, prevents the expression of PIP3, which activates AKT (PI3K-AKT pathway). In addition, SHP-2 de-phosphorylation of phospholipase C gamma 1 (PLCγ1) leads to inhibition of diacyl glycerol (DAG) and inositol 1,4,5-triphosphate (IP3) production and further, to the inhibition of signal transduction through the Ras-MEK-ERK pathway [150, 151, 152]. Consequently, PD-1 ligation results in inhibition of the PI3K-Akt and Ras-MEK-ERK pathways, in suppression of NF-κB activation by PKCθ and downstream signalling through ZAP-70. In these mechanisms, PD-1 ligation supresses cytokine production, cell proliferation and decreases nuclear transcription factors.

In cancer research, PD-1 has been described as an important T cell activation checkpoint as the blockade of PD-1 and PD-L1 ligation with so called checkpoint inhibitor agents is effective in patients with various types of cancer [153, 154, 155, 156].
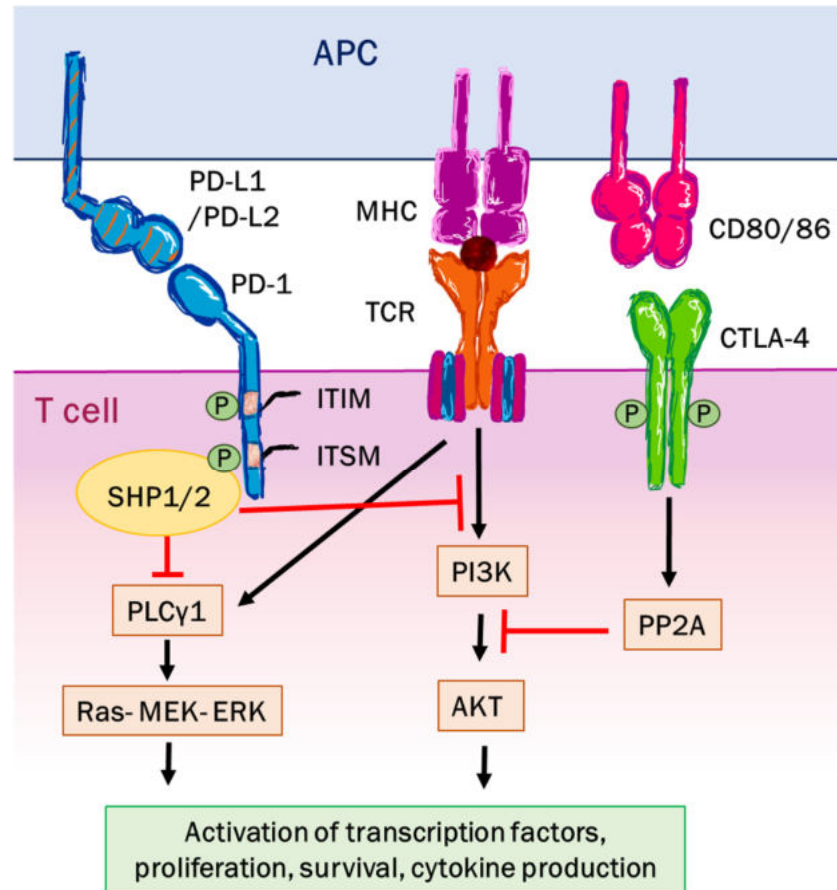
Figure 7 **Intracellular signalling upon PD-1 ligation.** PD-1 ligation with PD-L1 or PD-L2 drives phosphorylation dependent inhibition of TCR stimulation. PD-1 engagement leads to phosphorylation of ITSM/ITIM motifs in the PD-1 cytoplasmic domain and to the recruitment of the tyrosine phosphatases SHP1 and 2 (SHP1/2). SHP1/2 dephosphorylate TCR signalling molecules PI3K and PLCγ1, leading to their inhibition. In this way, PD-1 ligation has inhibitory effects on PI3K-AKT signalling and downstream Ras-MEK-ERK signalling. In contrast, CTLA-4 engagement activates phosphatase PP2A, which leads to direct inhibition of AKT activation. However, PI3K activity is maintained during CTLA-4 mediated signalling and CTLA-4 does not inhibit Ras-MEK-ERK and PLCγ1 signalling. Figure from personal collection.

1.5.4   CBL-B

E3 ubiquitin-protein ligase casitas B-lineage lymphoma proto-oncogene b (CBL-B) can modulate the activation threshold of T effector cells and therefore, CBL-B can affect the adaptive immune response.

CBL-B is a member of the casitas B-lineage lymphoma (CBL) family and functions as a Really Interesting New Gene (RING)-type E3 ubiquitin-protein ligase for the mechanism of ubiquitination [157]. Ubiquitination allows post-transcriptional alterations of intracellular pathways. Thereby, ubiquitin activating enzyme (E1), ubiquitin conjugating enzyme (E2) and ubiquitin ligase (E3) form the ubiquitination cascade. The ubiquitination cascade initiates with

E1 binding to the 76 amino acid peptide ubiquitin by thioester linkage between the C-terminus of ubiquitin and the active site cysteine of E1. Activated ubiquitin is then transferred to the active site of E2 by the manner of transthiolation. E3 ligase binds to E2 with conjugated ubiquitin and to the target protein. E3 ligase catalyses the iso-peptide bond between ubiquitin and a specific lysine residue of the target protein. As a result, ubiquitin is directly transferred from E2 to the target protein. E3 also mediates the formation of multi- or poly-ubiquitin chains on target proteins [158, 159, 160]. Post-translational modification of target proteins by ubiquitination changes fate and function of the target proteins. Ubiquitination modifies target proteins for many cellular processes, such as degradation by the proteasome, transcriptional regulation, signal transduction and even DNA repair.

CBL-B negatively regulates T cell stimulation by TCR signalling [158, 161, 162, 163]. Thereby, CBL-B influences multiple intracellular processes in a proteolysis-dependent or -independent manner, leading to an increase of the T cell activation threshold. For instance, CBL-B can regulate phosphorylation and activation of PLCγ-1, which is essential for signal transduction through the Ras-MEK-ERK pathway [158, 161]. Moreover, CBL-B negatively influences the PLCγ1-regulated calcium influx. In addition, the proline-rich N-terminus of CBL-B interacts directly with Vav Guanine Nucleotide Exchange Factor 1 (Vav1) to associate with PKCθ and thus, supressing NF-κB activation by PKCθ [162]. Furthermore, the p85α regulatory subunit of PI3K was identified as target protein of CBL-B; therefore, CBL-B associates with PI3K-AKT pathway [163]. Upon TCR and co-receptor CD28 stimulation, CBL-B is post-transcriptionally degraded by CD28 mediated downstream signalling. In addition, PKCθ and the E3 ligase neural precursor cell-expressed developmentally downregulated gene 4 (NEDD4) are capable of inducing the degradation of CBL-B [164].

In previous mouse studies, CBL-B deficient (*CBL-B*-/-) mice developed spontaneous and antigen-induced experimental autoimmune diseases. These studies reported on massive tissue infiltration of activated T and B cells. Furthermore, *CBL-B*-/- mice showed hyperproliferative T cells that expanded upon TCR stimulation alone, without any further co-stimulation [158, 165, 166]. Therefore, CBL-B seems to play a crucial role in maintaining well-balanced immune responses by T effector cells.

1.5.5   Other regulatory molecules of T cell activation

GRAIL, ITCH and NEDD4 are E3 ubiquitin ligases that modulate T cell activation. GRAIL is a transmembrane protein, which belongs to the E3 RING-type family and it is known to negatively regulate TCR responsiveness and T cell activation. Previous *in-vitro* studies with mouse T cells revealed that *GRAIL*-deficient T cells were hypersusceptible to TCR and CD28 stimulation [167, 168]. *In-vivo* mouse studies showed that *GRAIL*-deficient mice exhibited hyperproliferative T cells with excessive activation and these mice were more susceptible to autoimmune diseases, as compared to wildtype control mice [169].

ITCH and NEDD4 are homologous to E6-AP carboxy terminus (HECT)-type E3 ubiquitin ligases of the NEDD4 family. In contrast to Ring-type E3 ubiquitin ligases, HECT-type E3 ubiquitin ligases possess protein-interacting WW-domains for binding the target protein and the catalytic HECT domain directly transfers activated ubiquitin to target protein [170, 171]. ITCH becomes activated through serine/threonine phosphorylation by c-Jun N-terminal kinase (JNK). Activated ITCH targets JunB transcription factor of the activator protein-1 (AP-1) family for ubiquitination and subsequent proteasomal degradation. This negatively affects the expression of Th2 cytokine IL-4 [172, 173]. ITCH facilitates the degradation of PLCγ1 and PKCθ; thus, suppressing TCR downstream signalling and negatively regulating T cell activation. *ITCH*-deficient T cells displayed enhanced activation and proliferation; furthermore, IL-4 and IL-5 expression was enhanced, indicating that Th2 differentiation was augmented. In addition, *ITCH*-deficient mice exhibited inflammatory diseases and itching of the skin [172]. Although NEDD4 and ITCH belong to the same protein family, NEDD4 has different target proteins and therefore, its function varies from that of ITCH. *In-vivo* studies showed that in *NEDD4*-deficient foetal liver chimeras, *NEDD4*-deficient T cells poorly proliferated and were hyporesponsive towards antigen stimulation. Hence, NEDD4 facilitates and positively regulates T cell activation. It is assumed that NEDD4 positively affect T cell activation because NEDD4 targets CBL-B for ubiquitination and proteasomal degradation [174, 175]. Thereby, it is suggested that serine/threonine protein kinase C-theta (PKCθ) phosphorylates CBL-B upon TCR/CD28 stimulation, promoting CBL-B ubiquitination by NEDD4 [176].

PKCθ is composed of an N-terminal regulatory domain and a highly homologous conserved C-terminal kinase domain. PKCθ exhibit multiple phosphorylation sites contributing to the PKCθ kinase activity and translocation to T cell membrane upon TCR/CD28 stimulation. PKCθ downstream signalling leads to activation of nuclear transcription factors NF-κB, NFAT and AP-1. In this manner, PKCθ is involved in T cell activation, proliferation and cytokine

production [177, 178, 179, 180]. Previous studies revealed that *PKCθ*-deficient mice exhibited impaired T cell activation and defective T cell differentiation into Th2 and Th17 cells, suggesting that PKCθ plays a crucial role in T cell differentiation [181, 182, 183].

Another regulatory molecule of T cell activation is tumour necrosis factor (TNF) receptor-associated factor 6 (TRAF6). TRAF6 is an adaptor protein that mediates protein-protein interactions in various intracellular signalling pathways. TRAF6 associates with receptors, such as TNF receptor, IL-1 receptor (IL-1R), IL-17R and transforming growth factor receptor (TGF-βR), which are involved in T cell immune responses and inflammatory processes. In addition, TRAF6 engages activation of nuclear transcription factor NF-κB [184, 185, 186]. Previous studies in *Traf6*-ΔT mice revealed that activated *TRAF6*-deficient T cells were resistant to Treg-mediated inhibition, resulting in multiorgan inflammatory disease [187, 188].

T cell co-receptor OX40 is a transmembrane protein and belongs to the TNFR superfamily. OX40 expression on T cell surface is induced upon TCR engagement with peptide-MHC complex. OX40 ligation to OX40 ligand (OX40L) activates downstream signalling, enhancing T cell stimulation, survival and thus, T cell immune responses. More precisely, TRAF molecules are recruited to the cytoplasmic tail of OX40 upon OX40-OX40L ligation. TRAF molecules bind to activated OX40, which leads to the activation of NF-κB downstream signalling pathways [189, 190]. Furthermore, OX40-OX40L interaction activates PI3K-AKT pathway and transcription factor NFAT. Previous studies associated OX40-positive T cells with several human autoimmune diseases, such as colitis or Multiple sclerosis (MS) as well as with animal models of autoimmune-mediated inflammation [191, 192, 193].

1.6   Aim of study

The aetiology and pathogenesis of autoimmune hepatitis (AIH) is not fully understood. It is assumed that hepatic inflammation and hepatocyte damage are mediated by activated T effector cells [194]. Thus, activated T effector cells seem to play a crucial role in the immunopathogenesis of AIH. Previous studies revealed that Tregs, which extrinsically mediate immune regulation by suppressing activated T effector cells were not reduced in frequency and were not dysfunctional in AIH patients [23]. Other, intrinsic mechanisms that regulate T cell activation are mediated by molecules which provide T effector cell co-stimulation or co-inhibition, thereby regulating the activation thresholds of T effector cells and consequently affecting T cell immune responses (see chapter 1.5).

We hypothesise that an impaired intrinsic regulation of T cell activity and aberrant expression of co-stimulatory or co-inhibitory molecules in T cells, may account for inappropriately controlled T cell activation in AIH, allowing T effector cells to escape immune regulation and leading to enhanced T cell immune responses in AIH. Thus, the aim of this study was to analyse intrinsic regulatory molecules of T cell activation in peripheral blood and in livers of patients with AIH. Therefore, we intended to apply real-time quantitative PCR and RNA *in-situ* hybridisation to analyse *CBL-B*, *CTLA-4*, *GRAIL*, *ICOS*, *ITCH*, *NEDD4*, *OX40*, *PD-1*, *PKCθ*, *TRAF6* RNA expression in blood and livers of AIH patients. Furthermore, protein expression should be analysed by use of flow cytometry. Moreover, we aimed to correlate the expression of intrinsic T cell activation regulators with disease activity. We also planned to examine the secretory cytokine profile of T effector cells in AIH. In this study, healthy control subjects, patients with other autoimmune liver disorders, such as PBC or PSC, and patients with non-autoimmune-mediated liver diseases such as DILI or NASH served as study control groups.

2.   Materials and Methods

2.1   Materials

2.1.1   Antibodies

Table 1 **Primary and secondary antibodies**

primary antibodies	clonality	supplier	catalogue number
anti- human CBLB, unconjugated	polyclonal rabbit IgG	Proteintech	12781-1-AP (IF, FC)
anti- human CD3, unconjugated	monoclonal mouse IgG1 clone F7.2.38	Thermo Fisher Scientific	MA5-12577 (IHC-P)
anti- human CD3, AF488	Monoclonal mouse IgG Clone UCHT1	Biolegend	BLD-300454 (IF)
anti- human CD3, LEAF™ purified	monoclonal mouse IgG2a clone OKT3	Biolegend	BLD - 317302
anti- human CD3, brilliant violet 510™	monoclonal mouse IgG2a clone OKT3	Biolegend	BLD-317332 (FC)
anti- human CD3, PECy7	monoclonal mouse IgG clone SK7	Biolegend	BLD-344816 (FC)
anti- human CD4, pacific blue™	monoclonal mouse IgG clone RPA-T4	Biolegend	BLD-300521 (FC)
anti- human CD8, Alexa Fluor 700	monoclonal mouse IgG clone RPA-T8	BD Pharmingen™	557945 (FC)
anti- humuan CD14, APC	monoclonal mouse IgG clone HCD14	Biolegend	BLD-325608 (FC)
anti- human CD19, PE/Cy5	monoclonal mouse IgG1 clone HIB19	Biolegend	BLD-302210 (FC)
anti- human CD25 AF700	monoclonal mouse IgG1 clone BC96	Biolegend	BLD-302622 (FC)
Anti-human CD69 PE	monoclonal mouse IgG1 clone FN50	Biolegend	BLD-310905 (FC)
anti- human CD28, LEAF™ purified	monoclonal mouse IgG1 clone CD28	Biolegend	BLD-302914

anti- human CD134, PE	monoclonal mouse IgG1 clone Ber-ACT35	Biolegend	BLD-350003 (IF)
anti- human CD152, unconjugated	monoclonal rabbit IgG	Thermo Fisher Scientific	702534 (IF)
anti- human CD152, APC	monoclonal mouse IgG1 clone L3D10	Biolegend	BLD-349907 (FC)
anti-human CD127 PerCP Cy5.5	monoclonal mouse IgG1 clone CDhIL-7R-M21	BD Pharmingen™	557938 (FC)
anti- human CD278, brilliant violent 605™	monoclonal mouse IgG1 clone DX29	BD Biosciences	745100 (FC)
anti- human CD279, brilliant violet 711™	monoclonal mouse IgG1 clone EH12.2H7	Biolegend	BLD-329927 (FC)
anti- human FOXP3, PE/Dazzle 594™	monoclonal mouse IgG clone 206D	Biolegend	BLD-320126 (FC)
secondary antibodies	**clonality**	**supplier**	**catalogue number**
anti- mouse IgG H&L, horseradish peroxidase	polyclonal goat IgG	Abcam	Ab205719 (IHC-P)
anti- rabbit IgG, Dylight 488	polyclonal donkey IgG	Dianova	711-485-152 (FC)
anti- rabbit IgG H&L, AF488	polyclonal rabbit IgG	Invitrogen	A-21206 (FC/IF)
anti- rabbit IgG H&L, PE	polyclonal goat IgG	Invitrogen	P2771MP (IF)

FC: flow cytometry

IHC-P: immunohistochemistry on paraffin-embedded sections;

IF: immunofluorescence;

Table 2 **Isotype controls for flow cytometry**

isotype controls	clonality	supplier	catalogue number
rabbit IgG isotype, AF488	polyclonal IgG	Dianova	011-000-003
mouse IgG isotype, APC	monoclonal mouse IgG1 clone MOPC-21	BD Pharmingen™	554681
mouse IgG isotype, BV605	monoclonal mouse IgG1 clone X40	BD Biosciences	562652
mouse IgG isotype, BV711	monoclonal mouse IgG1 clone X40	BD Biosciences	563044
mouse IgG isotype, PE	monoclonal mouse IgG1 clone MOPC-21	Biolegend	400112

2.1.2 Sequence based reagents

Table 3 **Probes for quantitative real-time polymerase chain reaction**

gene name	sequence/assay ID	supplier
human CD3D	Hs00174158_m1	Thermo Fisher Scientific
human CD4	Hs01058407_m1	Thermo Fisher Scientific
human CD8A	Hs00233520_m1	Thermo Fisher Scientific
human CD28	Hs01007422_m1	Thermo Fisher Scientific
human CBL-B	Hs00180288_m1	Thermo Fisher Scientific
human CTLA-4	Hs00175480_m1	Thermo Fisher Scientific
human GRAIL (RNF128)	HS00226053_m1	Thermo Fisher Scientific
human ICOS	Hs00359999_m1	Thermo Fisher Scientific
human IFNγ	Hs00989291_m1	Thermo Fisher Scientific
human ITCH	Hs01008308_m1	Thermo Fisher Scientific
human NEDD4	Hs00406454_m1	Thermo Fisher Scientific
human PD-1 (PDCD1)	Hs01550088_m1	Thermo Fisher Scientific
human TNF	Hs01113624_g1	Thermo Fisher Scientific
human TRAF6	Hs00939742_g1	Thermo Fisher Scientific

human TNFRSF4 (OX40)	Hs00937195_g1	Thermo Fisher Scientific
human PKCθ (PRKCQ-AS1)	Hs00292281_m1	Thermo Fisher Scientific
human HPRT1	Hs02800695_m1	Thermo Fisher Scientific

Table 4 **Probes for RNA *in-situ* hybridisation**

gene name	supplier	catalogue number
Hs- CBLB	Advanced Cell Diagnostics	530811
HS-CTLA4	Advanced Cell Diagnostics	55431
HS-ICOS	Advanced Cell Diagnostics	460441
Hs-NEDD4	Advanced Cell Diagnostics	533881
Hs-TNFRSF4	Advanced Cell Diagnostics	412381
Hs-PDCD1	Advanced Cell Diagnostics	602021
Negative control Probe-DapB	Advanced Cell Diagnostics	310043
Positive control Probe-Hs-PPIB	Advanced Cell Diagnostics	313901

2.1.3   KITS

Table 5 **Kits**

Kit name	supplier	catalogue number
DAB Substrate Kit	Abcam	ab64238
ELISA Human IL-4	Invitrogen	BMS225-2
ELISA Human IL-6	Invitrogen	EH2IL6
ELISA Human IL-8	Invitrogen	KHC0081
ELISA Human IL-10	Invitrogen	BMS215-2
ELISA Human IL-21	Affymetrix eBioscience	BMS2043
ELISA Human TNF alpha	Invitrogen	BMS223-4
high capacity cDNA Reverse Transcription Kit	Applied Biosystems	4368813

Legendplex^{TM} HU Essential Immune Response Panel	Biolegend	740930
Legendplex^{TM} Human T Helper Cytokine Panel	Biolegend	700047/700790
NucleoSpin® RNA	Macherey-Nagel	740955.250
Pan T cell Isolation Kit, human	Miltenyi Biotec	130-096-535
RNAscope® 2.5 HD Detection Reagents- RED	Advanced Cell Diagnostics	322360
RNAscope® H202 & Protease Plus	Advanced Cell Diagnostics	32233

2.1.4   Reagents and buffers

Table 6 **Reagents and buffers**

name	supplier	catalogue number
aceton	Th Geyer GmbH, Renningen	2654.1000
Alexa Fluor™ 750 NHS Ester	Thermo Fisher Scientific	A20011
antifect	Schülke & Mayr GmbH	113940
aqua	B. Braun, Melsungen	75/12600521212
aquatex aqueus mounting medium	Merck- Millipore, Darmstadt	1085620050
beta-Mercaptoethanol	Sigma-Aldrich Chemie	60242
bovine serum albumin (BSA)	Sigma-Aldrich Chemie	9048-46-8
dimethylsulfoxid (DMSO)	Serva, Heidelberg	20385
Dako envision system HRP rabbit	Dako, Jena	K4003
Dako fluorescent mounting medium	Dako, Jena	S3023
DPBS	Gibco, USA	14190-094
EDTA ultra pure	Life technologies, USA	15576028
ethanol 99,8% mit ca. 1% MEK ; 2,5L	Carl Roth, Karlsruhe	K928.3
Entellan (mounting medium for microscopy)	Merck-Millipore, Darmstadt	1.07961.0100
eosin-G solution	Carl Roth, Karlsruhe	X883.2

(0,5% aqueous for microscopy)		
FACS™ lysing solution	BD Biosciences, Heidelberg	349202
fecal calf serum	Gibco, USA	10270106
Fc Receptor Binding Inhibitor	eBioscience, UK	14-9161-73
Ficoll-Paque PLUS	GE Healthcare Life Sciences	17-1440-03
hemalum solution acidic according to Mayer	Carl Roth, Karlsruhe	T865
Hoechst pentahydrate (bis-benzimide)	Invitrogen, USA	H3569
IC fixation buffer	eBioscience, UK	00-8222-49
KAPA probe fast universal	KAPA Biosystems, USA	KK4715
nitrogen liquid	German-Cryo, Jüchen	CYL 120/4 SB
normal donkey serum	Merck-Millipore, Darmstadt	566460-5ML
normal goat serum	Merck-Millipore, Darmstadt	S30-100ML
OneComp eBeads™ compensation	eBioscience, UK	01-1111
Pacific Orange™ succinimidyl ester	Thermo Fisher Scientific	P30253
penicillin-streptomycin (10,000 U/mL)	Gibco, USA	15140122
roti-Histofix (formaldehyde 4 %)	Carl Roth, Karlsruhe	P087.3
ROX low fluorescence reference dye	KAPA Biosystems, USA	KD4705
TaqMan™ Universal PCR Master Mix	Applied Biosystems, Darmstadt	4304437
Trition- X 100	Carl Roth, Karlsruhe	3051.2
trypan blue solution (0,4 %)	Invitrogen, USA	10702404
Tween®20	Sigma-Aldrich Chemie	P9416
xylene	Th Geyer Gmbh, Renningen	371-5L

2.1.5 Devices and software

Table 7 **Technical devices**

technical device	supplier
CO_2 incubator	Sanyo Denki K.K, Moriguchi; Japan
CryoStar NX50 HOPD cryostat	Thermo Fisher Scientific, USA
centrifuge 5417R	Eppendorf AG, Hamburg
centrifuge 5810R	Eppendorf AG, Hamburg
ELISA reader INFINITY F50	Tecan, Männedorf; Switzerland
HL-2000 Hybrilinker hybridisation oven	UVP Laboratory Products, Jena
HybEZ Oven	Advanced Cell Diagnostics; UK
LSR II, LSR Fortessa (flow cytometer)	BD Biosciences, Heidelberg
LSR II, FACS Canto (flow cytometer)	BD Biosciences, Heidelberg
MACS® MultiStand	Miltenyi Biotec, Bergisch Gladbach
microbiological safety cabinet MSC 1.8	Thermo Fischer Scientific, USA
microbiological safety cabinet DLF BSS6	Clean Air Technique B.V., Netherlands
microscope BH-2	Olympus, Tokio; Japan
microscope BZ-9000	Keyence, Osaka; Japan
microscope BZ-X700	Keyence, Osaka; Japan
microtome	Slee medical, Mainz
microwave	Bosch, Munich
Nanodrop™ 2000	Thermo Fischer Scientific, USA
Neubauer hemocytometer Marienfeld Superior	Paul Marienfeld GmbH & Co. KG, Lauda Königshofen
PCR/Thermo Cycler peqSTAR 2x universal gradient	VWR Peqlab, Pennsylvania; USA
precision scales Sartorius analytics A200s	Sartorius AG, Göttingen
pipetboy	Integra Biosciences AG, Zizers; Schweiz
platform shaker	Heidolph Instruments GmbH & Co.KG, Schwabach
ViiA7™ Real-Time PCR System	Applied Biosystems, California; USA
vortex, Reax 2000	Heidolph Instruments GmbH
water bath	GFL, Großburgwedel

Table 8 **Disposables**

name	supplier
96 well plates round bottom	Sarstedt, Nürmbrecht
96 well plate V bottom, flat bottom	Greiner Bio-One, Frickenhausen
cover slip, 24mm x 50mm #1	Carl Roth, Karlsruhe
cryo reagent tubes	Sarstedt, Nürmbrecht
EDTA KE 9 mL tube	Sarstedt, Nürmbrecht
flow cytometry reaction tubes	Sarstedt, Nürmbrecht
ImmEdge pen H4000	Vector Laboratories Inc., California
LS-Columns	Miltenyi Biotec, Bergisch Gladbach
MACS®Pre-Separation Filters 30 µm	Miltenyi Biotec, Bergisch Gladbach
MaxiSorp micro plate	Nunc, Schwerte
micro Amp^{TM} fast 96-well reaction plate	Applied Biosystems, Darmstadt
micro Amp^{TM} optical adhesive film	Applied Biosystems, Darmstadt
micro pestle	Carl Roth, Karlsruhe
micro reagent tubes 1.5 mL, 2 mL	Sarstedt, Nürmbrecht
microscope slides superfrost	Menzel GmbH, Braunschweig
multichannel pipettors 300 µL	Eppendorf AG, Hamburg
nylon mesh cell strainer 100 µm	BD Biosciences, Heidelberg
petri dish	Sarstedt, Nürmbrecht
pipettes 1 mL, 200 µL, 100 µL, 10 µL	Eppendorf AG, Hamburg
pipettes serological 2 mL, 5 mL, 10 mL, 25 mL	Greiner Bio-One, Frickenhausen
pasteur pipettes	Sarstedt, Nürmbrecht
reaction tubes polypropylene 15 mL, 50 mL	Greiner Bio-One, Frickenhausen
reagent reservoirs	VWR north American, USA
vacuum filtration unit Filtropur V50, 500 ml	Sarstedt, Nürmbrecht
weighing boats	Carl Roth, Karlsruhe

Table 9 **Software**

name	supplier	version
Aperio image scope	Leica Biosystems pathology imaging	12.3.3.5048
BZ II Viewer und Analyzer	Keyence	2.2
FACSDiva	BD Biosciences	8
FlowJo	BD Biosciences	10
GraphPad Prism	GraphPad Software Inc.	6
ImageJ	Fiji	1.51s
Ink scape	Tarmjong Bah	0.92
LEGENDplex	Biolegend	8
Magelan F50	Tecan Corperation	V7.0
Nano Drop 2000	Thermo Fischer Scientific	1.6.198
ViiA 7 RUO Software	Applied Biosystems	1.2.4

2.2 Methods

2.2.1 Human subjects

Blood and liver tissue samples of AIH, DILI, NASH, PBC, PSC patients and healthy control subjects were tested for this study. Human samples of 42 patients with treatment-naive AIH, 37 patients with AIH under immunosuppressive treatment, 35 DILI patients, 17 patients with NASH, 13 PBC and 18 PSC patients were analysed. In addition, samples of 44 healthy control subjects were applied. Thereby, healthy margin resection of 8 patients with liver adenomas served for analyses of healthy livers. Patients with liver adenomas underwent surgery in the Department of Hepatobiliary Surgery and Transplantation at the University Medical Centre Hamburg-Eppendorf. Moreover, liver tissue samples of 9 patients who underwent bariatric surgery at the University Medical Centre Hamburg-Eppendorf, were applied as healthy controls. Furthermore, diagnosis of DILI was based on the RUCAM score [66, 195].

Clinical data of AIH patients and control groups were listed in table 10. The gender distribution (female; male) in treatment-naive AIH study group was 69% female patients versus (vs.) 31% male patients. Moreover, gender distribution in other study groups, such as patients with AIH under immunosuppressive treatment (65% vs. 35%), healthy control subjects (59% vs. 40%), patients with DILI (66% vs. 34%), NASH (65% vs. 35%), PBC (46% vs. 54%) or PSC (61% vs. 39%) was displayed in *figure 8*.

Table 10 **Clinical parameters of patient and control cohort.** Values are expressed in mean (range) and ANA titer in median (range). Standard values for men and women ($\male$;$\female$) are shown.

Study group	Healthy controls	AIH naive	AIH steroid treated	DILI	NASH	PBC	PSC
number n	**44**	**42**	**37**	**35**	**17**	**13**	**18**
age	37 (23-79)	46 (18-79)	48 (18-27)	47 (21-79)	52 (21-71)	63 (41-88)	45 (21-68)
AST U/L ($\male$10-50; $\female$10-35)	**45** (16-114)	**596** (34-2359)	**52** (18-251)	**607** (38-2871)	**56** (25-95)	**33** (14-132)	**38** (12-147)
ALT U/L ($\male$10-50; $\female$10-35)	61 (11-145)	755 (27-2368)	62 (18-279)	992 (17-3634)	94 (27-290)	42 (15-198)	67 (17-322)
AP U/L ($\male$30-129; $\female$30-104)	**73** (49-105)	**152** (58-376)	**94** (17-223)	**193** (25-310)	**100** (46-268)	**156** (57-590)	**192** (44-402)
GGT U/L ($\male$<60; $\female$<40)	95 (14-483)	226 (42-568)	102 (14-560)	420 (14-2557)	208 (34-767)	139 (17-343)	178 (13-502)
IgG g/L (7-16)	**-**	**18.5** (8.31-33.8)	**15.3** (2-27.3)	**11.2** (5.19-18.3)	**10.5** (6-15.8)	**13.8** (10.1-19)	**14.5** (8.6-20.6)
Leukocytes Mrd/L (3.8-11)	12 (7.3-18)	7.8 (3.1-20.5)	6.9 (2-13.6)	9.2 (1-27.3)	7.9 (3.8-17.7)	9.0 (5.8-13.9)	6.6 (3.4-11.7)
Bilirubin mg/dL (<1.2)	**0.5** (0.2-0.8)	**3,8** (0.2-28.2)	**0.8** (0.2-2.3)	**15** (4.1-19)	**0.74** (0.4-1.8)	**0.6** (0.4-1.1)	**0.7** (0.3-1.3)
mHAI (0-18)	-	8 (3-14)	7 (2-12)	9 (4-13)	-	-	-
ANA ($\leq$ 1 : 160)	**-**	**1: 1280** (1:80-1:5120)	**1: 320** (1:80-1:5120)	**1: 160** (1:80-1:5120)	**1: 320** (1:160-1:640)	**1: 5120** (1:80-1:5120)	1: 320 (1:160-1:320)
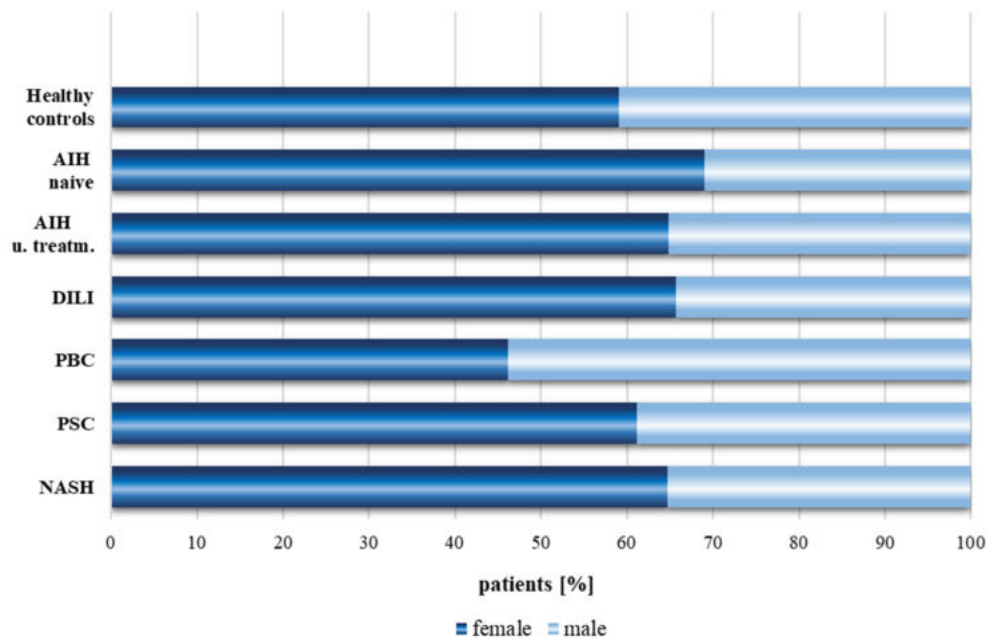
Figure 8 **Gender distribution in study groups.**

2.2.2. Isolation of human plasma

Human blood plasma was isolated for cytokine analyses. Freshly isolated human blood that was kept in three 7 mL EDTA tubes (Sarstedt) was centrifuged at 1500rpm and room-temperature (RT) for 10 min. 2 mL human blood plasma was collected into 2 mL micro cryo tubes (Sarstedt) using 1 mL pipettes (Eppendorf). Micro cryo tubes were stored at -80°C.

2.2.3   Isolation of human peripheral blood mononuclear cells

Human peripheral blood mononuclear cells (PBMCs) were isolated to examine blood lymphocytes of AIH patients in comparison to control subjects. Freshly isolated human blood was transferred into a 50 mL tube (Greiner Bio-One). By use of a 25 mL pipette RT PBS (2.7 mM KCl, 1.5 mM KH_2PO_4,137 mM NaCl, 6.5 mM Na_2HPO_4; ph 7,4) was added to the blood until a final volume of 35 mL was reached. Diluted blood was gently mixed. A fresh 50 mL tube was filled with 15 mL ficoll (GE Healthcare Life Sciences) and diluted blood was slowly layered on top of the ficoll. The solution was centrifuged at 600 xg and RT for 20 min. PBMCs were collected using a Pasteur pipette (Sarstedt) and transferred into a fresh 50 mL tube. PBS was added to isolated cells up to a final volume of 50 mL. For washing, cells in PBS were centrifuged at 400 xg and RT for 5 min. Supernatant was discarded and cell pellet was resuspended in fresh PBS. PBS was added to cells up to a final volume of 50 mL and cells were additionally centrifuged at 400 xg and RT for 5 min. After cells were resuspended in 10 mL PBS, they were counted. Cells were once again centrifuged at 400 xg and RT for 5 min.

2.2.4   Isolation of human T cells from peripheral blood mononuclear cells

T cells were isolated from PBMCs that were freshly isolated from human blood. PBMCs in PBS (2.7 mM KCl, 1.5 mM KH_2PO_4,137 mM NaCl, 6.5 mM Na_2HPO_4; ph 7,4) were counted and passed through a 30 µm nylon mesh cell strainer (Miltenyi Biotec). PBMCs were collected in a 15 mL tube (Greiner Bio-One) and were centrifuged at 300 xg and RT for 10 min. Supernatant was discarded and cell pellet was resuspended in 40 µL MACS buffer (PBS, 0.5% BSA, 2.5 mM EDTA) per 10^7 total cells. 10 µL MACS antibody biotin cocktail (Miltenyi Biotec) per 10^7 total cells were added and PBMCs incubated at 4 °C for 5 min. 30 µL MACS buffer per 10^7 total cells was given to the PBMCs as well as 20 µL MACS magnetic micro bead cocktail (Miltenyi Biotec) per 10^7 total cells. Magnetic beads and PBMCs were mixed well. PBMCs incubated at 4 °C for additional 10 min. LS column (Miltenyi Biotec) was placed into MACS® MultiStand (Miltenyi Biotec) and rinsed three times with 1 mL of MACS buffer. After incubation, cell suspension was applied onto LS column and the flow-through, which contained the unlabelled CD3$^+$ T lymphocytes was collected in a fresh 15 mL tube. LS column was washed three times with 1 mL of MACS buffer and flow-through was collected. Unlabelled CD3$^+$ T lymphocytes were counted and used for further analyses.

2.2.5 Counting cells

Cells were counted to determine cell concentrations in each volume. 90 µL of trypan blue solution (Invitrogen) was pipetted into a well of a 96-well flat plate (Sarstedt). 10 µL of cells in PBS or cell culture media was added to the well with tryptanblau and gently mixed. A cover slide (Carl Roth) was placed on a Neubauer hemocytometer (Paul Marienfeld) and 10 µL of the cell-trypan blue mixture was pipetted into the gap between cover slide and Neubauer hemocytometer. Neubauer hemocytometer was placed under the microscope (Olympus) and cells were counted. The Neubauer hemocytometer consists of nine 1 mm^2 squares and cells on two or four squares were counted to determine cell concentration:

$cell_{total}\ concentration= (cells_{counted}\ /squares_{counted}) \cdot 10 \cdot volume \cdot 10^4.$

2.2.6 Freezing peripheral blood mononuclear cells

PBMCs that were freshly isolated from human blood according to chapter 2.2.3 and were stored in liquid nitrogen. For this, supernatant of washed and counted PBMCs was discarded. Cell pellet was resuspended in 1 mL freeze medium (RPMI, 5% P/S, 10% FCS, 10% DMSO) per 10^7 total cells. Cells in freeze medium were aliquoted in micro cryo tubes (Sarstedt) and stored at -80 °C for 5 days. Afterwards, the cells were placed in liquid nitrogen (German-Cryo).

2.2.7 RNA isolation from blood peripheral T cells and whole liver tissue samples

RNA was isolated from blood peripheral T cells or whole liver tissue samples for real time polymerase chain reaction analyses. To whole liver tissue samples ($\leq$ 30 mg) or pellet of blood peripheral T cells ($\leq$ 5 $\cdot 10^6$), 350 µL lysis buffer (Macherey-Nagel) and 3.5 µL ß-mercapthoethanol (Sigma-Aldrich Chemie) was added. Whole liver tissue samples were crushed by use of pestle (Carl Roth) and peripheral blood T cells were vortexed (Heidolph Instruments). Cell lysates were transferred into NucleoSpin®Filters with collection tubes (Macherey-Nagel) and centrifuged at 11,000 xg and RT for 1 min. 350 µL of 70 % ethanol (Carl Roth) was added to homogenised lysates in collection tubes and lysates were transferred to NucleoSpin®RNA columns with collection tubes (Macherey-Nagel). Cell lysates were centrifuged at 11,000 xg and RT for 30 sec. 350 µL Membrane Desalting Buffer (MDB, Macherey-Nagel) was applied to the membranes of NucleoSpin®RNA columns. Columns were centrifuged at 11,000 xg and RT for 1 min. Membranes incubated in 95 µL rDNase (Macherey-Nagel) at RT for 15 min and washed firstly in 200 µL RAW2 (Macherey-Nagel) and secondly in 600 µL RA3 (Macherey-Nagel). Both wash steps included centrifugation at 11,000 xg and RT for 30 sec. Additionally, membranes were washed in 250 µL RA3 (Macherey-Nagel) and

centrifuged at 11,000 xg and RT for 2 min. RNA of blood peripheral T cells was eluted by adding 50 µL of RNase-free water (Macherey-Nagel) and RNA of whole liver tissue samples was eluted by adding 40 µL of RNase-free water. To complete the elution of RNA, membranes were centrifuged at 11,000 xg and RT for 1 min. RNA concentration of the samples was determined using Nanodrop™ 2000 (Thermo Fischer Scientific) and for storage, RNA samples were kept in 1.5 mL micro reagent tubes (Sarstedt) at -80 °C.

2.2.8 cDNA synthesis

RNA from sorted blood peripheral T cells or whole liver tissue samples were reverse transcribed to complementary DNA (cDNA). For each RNA sample, 2.4 µL reaction buffer, 0.96 µL deoxyribonucleotide triphosphate (dNTPs, 100 mM), 2.4 µL random primers and 1.2 µL of reverse transcriptase (50 U/µL) was applied as master mix (Applied Biosystems). 5.8 µL of master mix was added to each 14.2 µL of 500 ng RNA sample. RNA samples and reagents were placed on ice during pipetting. RNA samples were placed in PCR/Thermo Cycler peqSTAR 2x universal gradient (VWR Peqlab). The program for the thermal cycler was as followed:

	step 1	*step 2*	*step 3*	*step 4*
temperature °C	25	37	85	4
time	10 min	2 h	5 min	∞ (storage)

Concentration of cDNA was measured with Nanodrop™ 2000 (Thermo Fischer Scientific) and cDNA samples were stored at -20 °C.

2.2.9 Real-time quantitative PCR analyses

Gene expression analyses were performed on synthesised cDNA (see chapter 2.2.8) by use of real-time quantitative PCR. For this, 5 µL KAPA PROBE FAST qPCR Master Mix (KAPA Biosystems), 0.2 µL ROX fluorescein reference dye (KAPA Biosystems) and 0.5 µL probe (see table 3) were pipetted into a micro reagent tube (Sarstedt) that was placed on ice. Solutions were mixed well using vortex (Heidolph Instruments). In a 96 well qPCR plate (Applied Biosystems), 5.7 µL of the mixture was added to 4.3 µL of 2.5 µg/µL cDNA. If necessary, 20 µL of 2.5µg/µL cDNA was diluted in RNase-free water (Macherey-Nagel) in a ratio of 1:4, 1:5 or 1:6. Reagents were placed in ViiA7™ Real-Time PCR System (Applied Biosystems) and PCR program was adjusted using ViiA 7 RUO software. After initial denaturation for 20 sec at

95 °C, cycles of primer annealing at 60 °C for 20 sec and elongation at 95 °C for 1 sec followed. 40 cycles of amplification were applied. Mean relative expression of the genes of interest were normalised to that of housekeeper HPRT1 (Thermo Fisher Scientific) and calculated using the $2^{-\Delta\Delta CT}$ method.

2.2.10 Flow cytometric analyses

2.2.10.1 Staining of freshly isolated peripheral blood T cells

$CD3^+$ T cells that were freshly isolated from PBMCs (see chapter 2.2.4) were stained with flow cytometry antibodies to examine the purity of the T lymphocyte-MACS-flow-through. $1 \cdot 10^7$ cells of MACS flow through were centrifuged at 400 xg and RT for 5 min. For the life/dead staining, 1 µL Pacific Orange™ succinimidyl ester (Thermo Fisher Scientific) was added to 999 µL PBS (2.7 mM KCl, 1.5 mM KH_2PO_4, 137 mM NaCl, 6.5 mM Na_2HPO_4; ph 7,4). Cells were resuspended in 150 µL diluted Pacific Orange™ and incubated at 4 °C for 20 min. Subsequently, cells were washed in 1 mL PBS with centrifugation at 400 xg and RT for 5 min. Cell pellet was resuspended in 15 µL Fc Receptor Binding Inhibitor (eBioscience) and 85 µL FACS buffer (0.5% BSA, 0.02% NaN_3, PBS). Cells incubated at 4 °C for 20 min. In 100 µL Fc Receptor Binding Inhibitor solution, antibody cocktail (2 µL anti-CD3 PECy7, 5 µL anti-CD4 Pacific Blue, 2 µL anti-CD8 BV510, 5 µL anti-CD14 APC, 5 µL anti-CD25 AF700, 2 µL anti-CD45 BV785, 3 µL anti-CD127 PerCP Cy5.5 and 10 µL anti-FOXP3 Texas Red) was applied to the cells and cells incubated in antibody cocktail at 4 °C for 30 min. Afterwards, 1 mL PBS was added to cells for washing at 400 xg and RT for 5 min. Cell pellet was resuspended in 200 µL PBS. Cells were acquired with flow cytometer LSR II Fortessa (BD Biosciences) and analysed by use of software FlowJo (BD Biosciences).

2.2.10.2 Protein staining of CBL-B in unstimulated PBMCs

To examine the protein expression of CBL-B in PBMCs of AIH patients or control subjects, 100 µL of freshly isolated human blood was incubated in 1 mL FACS™ lysing solution (BD Biosciences) at RT for 10 min. For this, FACS™ lysing solution was diluted in distilled water at a ratio of 1:10. Afterwards, cells were centrifuged at 400 xg for 5 min and washed in 2 mL FACS buffer (0.5% BSA, 0.02% NaN_3, PBS). Cell pellet was resuspended in 100 µL IC fixation buffer (eBioscience) an incubated in the dark at RT for 20 min. 1 mL permeabilisation buffer (500 mL DPBS, 25 mL FCS, 10 g BSA, 0.5 g triton-X) was added to cells, followed by centrifugation at 400 xg for 5 min. Cell pellet was resuspended in 15 µL Fc Receptor Binding Inhibitor (eBioscience) and 85 µL FACS buffer. Then, cells incubated at 4 °C for 20 min. To

cells in Fc Receptor Binding Inhibitor solution, antibody cocktail (2 μL anti-CD3 PECy7, 5 μL anti-CD4 Pacific Blue, 3 μL anti-CD8 AF700, 5 μL anti-CD14 APC, 3 μL anti-CD19 PECy5, 5 μL anti-CD127 PerCP Cy5.5, 10 μL anti-FOXP3 Texas Red and 2 μL anti-CBL-B pure) was added and cells incubated in antibody cocktail at 4 °C for 30 min. Subsequently, cells were washed twice in 1 mL permeabilisation buffer at 400 xg for 5 min and incubated with 100 μL anti-rabbit IgG Dylight 488 (Dianova) that was diluted 1:200 in FACS buffer, at 4 °C for 30min. Cells were washed in 2 mL permeabilisation buffer at 400 xg for 5 min and resuspended 200 μL FACS buffer. Flow cytometer LSR II Fortessa (BD Biosciences) was used for acquisition of cells and analysis was performed by use of software FlowJo (BD Biosciences).

2.2.10.3   Protein staining of CBL-B, CTLA-4, ICOS and PD-1 in PBMCs

Protein expression of CBL-B, CTLA-4, ICOS and PD-1 in PBMCs of AIH patients or control subjects was determined by use of flow cytometry. For this purpose, 1 mL FACS^{TM} lysing solution (BD Biosciences) that was diluted in distilled water at a ratio of 1:10 was added to 100 μL of freshly isolated human blood and incubated at RT for 10 min. Cells were centrifuged at 400 xg for 5 min and supernatant was decanted cautiously. Cell pellet was resuspended in 500 μL of stimulation medium (RPMI, 10% FCS, 5% penicillin-streptomycin) with 2 μL purified anti-CD3 (Biolegend) and 1 μL purified anti-CD28 (Biolegend) antibodies. Cells incubated at 37°C for 4 h. After incubation, cells were centrifuged at 400 xg for 5 min and supernatant was transferred cautiously into micro reagent tubes (Sarstedt). Supernatant was stored at -80 °C. Alexa Fluor™ 750 NHS Ester (Thermo Fisher Scientific) was diluted in PBS (2.7 mM KCl, 1.5 mM KH_2PO_4,137 mM NaCl, 6.5 mM Na_2HPO_4; ph 7,4) at a ratio of 1:1000. Cell pellet was resuspended in 150 μL diluted Life/Dead APC-Cy7 (Thermo Fisher Scientific) solution and incubated at 4 °C for 20 min. Cells were washed in 1 mL PBS at 400 xg for 5 min and incubated in 100 μL IC fixation buffer (eBioscience) in the dark at RT for 20 min. 1 mL permeabilisation buffer (500 mL DPBS, 25 mL FCS, 10 g BSA, 0.5 g triton-X) was added to cells. After centrifugation at 400 xg for 5 min, cells incubated in blocking buffer (PBS, 1% BSA, 5% normal donkey serum) with antibody cocktail (2 μL anti-CD3 PECy7, 5 μL anti-CD4 Pacific Blue, 2 μL anti-CD8 BV510, 4 μL anti-CD19 AF700, 5 μL anti-CD38 BV650, 2 μL anti- CD45 BV785, 5 μL anti-CD127 PerCP Cy5.5, 10 μL anti-FOXP3 Texas Red, 2 μL anti-CBL-B pure, 5 μL anti-CTLA-4 APC, 2 μL anti-ICOS BV605, 5 μL anti-PD-1 BV711) at 4 °C for 30 min. Then, cells were washed in 1 mL permeabilisation buffer at 400 xg for 5 min and incubated in 100 μL diluted donkey anti-rabbit IgG Dylight 488 (Dianova) solution at 4 °C for 30 min. For this, secondary antibodies was diluted in PBS+1% BSA at a ratio of 1: 200. Cells

were washed in 1 mL permeabilisation buffer at 400 xg for 5 min and cell pellet was resuspended in 150 µL PBS. Cells were detected with flow cytometer LSR II Fortessa (BD Biosciences) and analysed by use of FlowJo software (BD Biosciences).

2.2.10.4   Protein staining of CBL-B, CTLA-4, ICOS and PD-1 in whole liver tissue

Protein expression of CBL-B, CTLA-4, ICOS and PD-1 was examined in whole liver tissue samples of AIH patients or control subjects. Whole liver tissue samples were biopsies that were obtained by performing mini-laparoscopy at the University Medical Centre Hamburg-Eppendorf. Freshly extracted biopsy was mashed through a 100 µm nylon mesh cell strainer (BD Biosciences) and rinsed with medium (RPMI, 10% FCS, 5% penicillin-streptomycin). Liver cells were centrifuged at 400 xg for 5 min and supernatant was removed gently by pipetting. Cell pellet was resuspended in medium with 2 µL purified anti-CD3 (Biolegend) and 1 µL purified anti-CD28 (Biolegend) antibodies. Cells incubated at 37 °C for 4 h. After incubation, the protocol was continued according to 2.2.10.3.

2.2.11 Immunohistochemical staining

2.2.11.1   Haematoxylin-Eosin (HE) staining

HE dyes were performed on formalin-fixed paraffin-embedded (FFPE) whole liver tissue samples of AIH and DILI patients to examine liver tissue structures and various cellular structures. FFPE of 2 µm human liver sections were deparaffinised in xylene (Th Geyer) for 12 min. For hydration of liver sections, slides were placed in ethanol (Carl Roth) for 16 min. For this, slides incubated in a descending order of 100%-, 90%-, 80%-, and 70%- ethanol for 4 min each. Slides were then rinsed in distilled water for 2 min and incubated in acidic hemalum solution according to Mayer (Carl Roth) for 10 min. Afterwards, slides were rinsed with tap water for 15 minutes and incubated in eosin (Carl Roth) for 1 min. After the slides were dipped in tap water, liver sections were dehydrated by use of an ascending order of 50%-, 70%-, 90%- and 100%-ethanol. In addition, slides incubated in xylene for 8 min. Sections were mounted by use of Entellan (Merck-Millipore) and cover slips (Carl Roth).

2.2.11.2   Modified histological activity index

Modified histological activity index (mHAI) according to Ishak *et al*. is a histological grading of hepatic inflammation [184, 185]. For assessment of mHAI score, liver tissue samples were stained with haematoxylin and eosin. mHAI scores of liver tissue samples were evaluated in a blinded manner by the Department of Pathology at University Medical Centre Hamburg-Eppendorf. The mHAI score according to Ishak *et al*. describes the assessment of:

A. interface hepatitis (0-4),

B. confluent necrosis (0-6),

C. Focal necrosis/apoptosis and focal inflammation (0-4)

D. portal inflammation (0-4).

2.2.11.3   RNA *in-situ* hybridisation

To examine RNA expression of *CBL-B*, *CTLA-4*, *ICOS* and *PD-1* in single cells in liver tissue sample of AIH or DILI patients, RNA *in-situ* hybridisation was performed. For this, FFPE of 2 µm liver tissue sample sections incubated in hybridisation oven (UVP Laboratory Products) at 60 °C for 1 h. Liver sections were deparaffinized by incubation in xylene (Th Geyer) for 10 min followed by 2 min in ethanol (Carl Roth). To block endogenous peroxidase activity, liver tissue slides incubated in hydrogen peroxide (Advanced Cell Diagnostics) 10 min. After rinsing the slides in distilled water, slides were gently heated in target retrieval (Advanced Cell Diagnostics) first at 360 W for 3 min and 900 W for 12 min. Then, slides were rinsed with distilled water for 30 sec and incubated in ethanol for 1-2 min. ImmEdge pen (Vector Laboratories Inc) created hydrophobic barriers circling the liver tissue sections on the slides. The next day, liver tissue slides incubated with Protease Plus (Advanced Cell Diagnostics) in Hybez oven (Advanced Cell Diagnostics) at 40 °C for 30 min. Subsequently, liver tissue slides incubated with target probes (*CBL-B*, *CTLA-4*, *ICOS*, *PD-1*; Advanced Cell Diagnostics) at 40 °C for 2 h. After protease treatment, slides incubated with amplifier solution 1-4 each at 40°C and amplifier solution 5 and 6 (Advanced Cell Diagnostics) at RT (alternating between 30 min and 15 min). For alkaline phosphatase-based detection., liver tissue slides incubated in 75 µL Fast Red solution (Advanced Cell Diagnostics) at RT for 10 min. Then, slides were washed in tap water for 5 min and incubated in acidic hemalum solution according to Mayer (Carl Roth) for 2 min. Slides were washed in tap water for 7 min and aquatex aqueus mounting medium (Merck-Millipore) sealed the stained slides. Slides stored at RT.

2.2.11.4   RNA *in-situ* hybridisation and anti-CD3 co-staining

RNA *in-situ* hybridisation with additional immunohistochemical anti-CD3 staining was performed on liver tissue sample of AIH or DILI patients to examine RNA expression of *CBL-B*, *CTLA-4*, *ICOS* and *PD-1* in liver-infiltrating CD3^{+} T lymphocytes. FFPE of 2 µm liver tissue sample sections were treated according to chapter 2.2.11.2. After alkaline phosphatase-based detection with Fast Red solution (Advanced Cell Diagnostics) and rinsing the slides with tap water for 5 min, liver tissue slides incubated in blocking buffer (PBS, 1% BSA, 5% normal goat serum) at 4 °C for 1 h. Anti-human CD3 antibodies (Thermo Fisher Scientific) were diluted in blocking buffer at a ratio of 1:20 and slides incubated in 100 µL of primary antibody solution at 4 °C overnight. Slides were washed thrice in PBS (2.7 mM KCl, 1.5 mM KH_2PO_4,137 mM NaCl, 6.5 mM Na_2HPO_4; ph 7,4) and incubated in 100 µL anti-mouse IgG horseradish peroxidase (Invitrogen) at RT for 1 h. For this, 1.5 µL anti-mouse IgG horseradish peroxidase was mixed with 1 mL PBS+1% BSA. After incubation, liver tissue slides were washed thrice in PBS and incubated in 100 µL chromogenic 3, 3'-diaminobenzidine (DAB) substrate solution (Dako) at RT for 50 sec. Immediately after, slides were washed in PBS to stop detection and incubated in 50% in acidic hemalum solution according to Mayer (Carl Roth) for 2 min. Slides were washed in tap water for 7 min and liver tissue slides were mounted using aquatex aqueus mounting medium (Merck-Millipore). Slides stored at RT.

2.2.11.5 Quantification of immunohistochemically stained liver tissues

AIH or DILI liver tissue slides that were stained by use of RNA *in-situ* hybridisation with or without additional anti-CD3 co-staining were analysed using light microscopy (Keyence). Liver-infiltrating lymphocytes expressing RNA of *CBL-B*, *CTLA-4*, *ICOS* or *PD-1* were quantified. For this, five representative images of high-power fields of hepatic portal areas and hepatic lobular areas of each liver tissue slide were taken and analysed in a blinded manner.

2.2.12 Immunofluorescence

By use of immunofluorescence on liver tissue sections of healthy control subjects, the distribution of CBL-B protein in healthy liver tissue cells was investigated. For this purpose, cryo slides of the liver tissue samples sections were created using cryostat (Thermo Fisher Scientific) and the slides stored at -80 °C. Cryo slides incubated in roti-Histofix (Carl Roth) at RT for 10 min and were washed thrice in PBS (2.7 mM KCl, 1.5 mM KH_2PO_4,137 mM NaCl, 6.5 mM Na_2HPO_4; ph 7,4) for 5 min. After washing, cryo slides incubated in aceton (Th Geyer) for 3 min and were washed thrice in PBS for 5 min. Then, cryo slides incubated in permeabilisation buffer (500 mL DPBS, 25 mL FCS, 10 g BSA, 0.5 g triton-X) for 5 min

followed by washing thrice in PBS for 5 min. To detect CBL-B protein in liver-infiltrating CD3^{+} lymphocytes, both unconjugated anti-CBL-B antibodies (Proteintech) and anti-CD3 FITC antibodies (Biolegend) were diluted in blocking buffer (PBS, 1% BSA, 5% normal goat serum) at a ratio of 1:100. Cryo slides incubated in 100 µL in antibody solution at 4 °C overnight. On the next day, cryo slides were washed thrice in PBS for 5 min followed by incubation with 100 µL secondary antibody anti-rabbit IgG PE (Invitorgen) solution for 1 h at 4 °C. For this, secondary antibody anti-rabbit IgG PE was diluted in PBS+ 1% BSA. After incubation, cryo slides were washed in thrice in PBS for 5 min and incubated in Hoechst pentahydrate (bis-benzimide) solution (Invitrogen) for 2 min to stain cell nucleic acid. Hoechst solution was a 1:20.000 mixture with PBS. Cryo slides were rinsed with PBS for 30 sec and by use of Dako fluorescent mounting medium (Dako), the cryo slides were mounted and stored at 4 °C. Stained cryo slides were analysed using fluorescence microscopy (Keyence).

2.2.13 Quantitative assessment of cytokines

2.2.13.1 Enzyme-linked Immunosorbent Assay (ELISA)

With Enzyme-linked Immunosorbent Assay the cytokine expression in human blood plasma and cell stimulation supernatant was determined. 96-well flat bottom plate (Greiner Bio-One) was washed twice with 200 µL wash buffer (PBS, 1% Tween® 20) per well and 100 µL of standard solutions (Thermo Fisher Scientific) was pipetted into the wells of column 1 and 2 on the 96-well flat bottom plate in duplicates. 30 µL plasma or stimulation supernatant (samples) were mixed with 20 µL assay buffer (PBS, 1% Tween® 20, 10% BSA) and 50 µL diluted samples were pipetted into wells of column 3-12. In addition, 50 µL of both assay buffer and biotin conjugate solution (Thermo Fisher Scientific) was added to all wells and ELISA plate incubated for 2 h with gently shaking on platform shaker (Heidolph Instruments GmbH). After incubation, ELISA plate was washed thrice with 200 µL wash buffer per well and 100 µL streptavidin-HRP solution (Thermo Fisher Scientific) was added to all wells. ELISA plate incubated for 1h with gently shaking and after incubation the plate was washed thrice with 200 µL wash buffer per well. 100 µL 3,3',5,5'-tetramethylbenzidine (TMB) substrate solution (Thermo Fisher Scientific) was given to the wells and ELISA plate incubated in the dark for 10-15 min. As the substrate solution turned blue, 100 µL of 1M Phosphoric acid stop solution was given to the wells to inhibit further reaction with TMB. ELISA plate was read by use of ELISA reader INFINITY F50 (Tecan) at 450 nm wavelength.

2.2.13.2 Multi-analyte immunoassay Legendplex™

For initial determination of cytokine of interest in human blood plasma or stimulation supernatant, multi-analyte immunoassay LEGENDplex ™ (BioLegend) was performed. For this, 12.5 µL of standard solutions (Biolegend) and 12.5 µL of Matrix B (Biolegend) were mixed and pipetted into wells of column 1 and 2 on 96-well V bottom plate (Greiner Bio-One). Also, 12.5 µL of human blood plasma or stimulation supernatant (samples) and 12.5 µL of assay buffer (PBS, 1% Tween® 20, 10% BSA) were mixed and pipetted into wells of column 3-2 on the same 96-well V bottom plate. Beads (Biolegend) that carry different APC fluorescence levels and are conjugated to analyte-specific antibody were vortexed (Heidolph Instruments GmbH) for 1 min and 12.5 µL of beads solution was added to all wells. V bottom plate incubated at 800 rpm for 2 h and after samples were centrifuged at 250 xg for 5 min, supernatant was discarded by rapid inverting the plate. Plate was washed with 150 µL wash buffer (PBS, 1% Tween® 20) per well and centrifuged at 250 xg for 5 min. 12.5 µL of biotinylated detection antibodies (Biolegend) were pipetted to all wells and samples incubated at 800 rpm for 1 h. After incubation, the supernatant was not discarded and 12,5 of PE conjugated streptavidin (Biolegend) was added to all wells. Samples incubated at 800 rpm for 30 min followed by centrifugation at 250 xg for 5 min. Supernatant was discarded and 150 µL wash buffer per well was added. Sample solutions were transferred from the wells of the 96-well V bottom plate into flow cytometry reaction tubes (Sarstedt). The fluorescence intensity of the PE signal of the different (APC) bead populations was quantified using the flow cytometer BD LSR II FACS Canto (BD Biosciences) and the concentrations of the analytes were determined using a standard curve and the data analysis software LEGENDplex ™ (Biolegend).

2.2.14 Statistical analysis

Statistical analyses were performed using GraphPad Prism® (GraphPad Software Inc). Data were analysed with Mann-Whitney U-test. For multiple comparison analyses, ANOVA test was performed. Spearman's rank correlation coefficient was applied for correlation analyses. All data are shown as median values (horizontal bars) with interquartile range (IQR). P-Values that were $p < 0.05$ (*), $p < 0.01$ (**), $p < 0.001$ (***) and $p < 0.0001$ (****) considered as significant.

3. Results

3.1 Real-time PCR screening in peripheral blood T cells and whole liver tissue samples

In order to identify altered expression of T cell co-stimulatory or inhibitory molecules that may facilitate unbalanced activation of T effector cells in AIH, we performed real-time quantitative PCR screening in peripheral blood T cells and whole liver tissues samples from AIH patients. Targets of interest were genes encoding for E3 ubiquitin ligases CBL-B, GRAIL, NEDD4 and ITCH; T cell co-receptor CTLA-4, ICOS, PD-1 and OX40; protein kinase PKCθ and TNF receptor-associated factor TRAF6. Gene expression analyses were performed according to chapter 2.2.9 and calculated using the $2^{-\Delta\Delta CT}$ method. For comparability purposes, housekeeper HPRT1 was applied and RNA expression was normalised on healthy control subjects.

Before PCR screening was performed on peripheral blood T cells, CD3$^+$ T cells were isolated from human PBMCs and purity of T cell isolation was assessed using flow cytometry. Therefore, isolated CD3$^+$ T cells were stained with fluorescence conjugated antibodies against the human proteins CD3, CD4, CD8, CD25, CD45, CD127 or FOXP3. Analysis with flow cytometry showed that 97% of the isolated cells were vital CD45$^+$CD3$^+$ T cells (*figure 9*).

Human liver tissue sample | **Human blood cells**
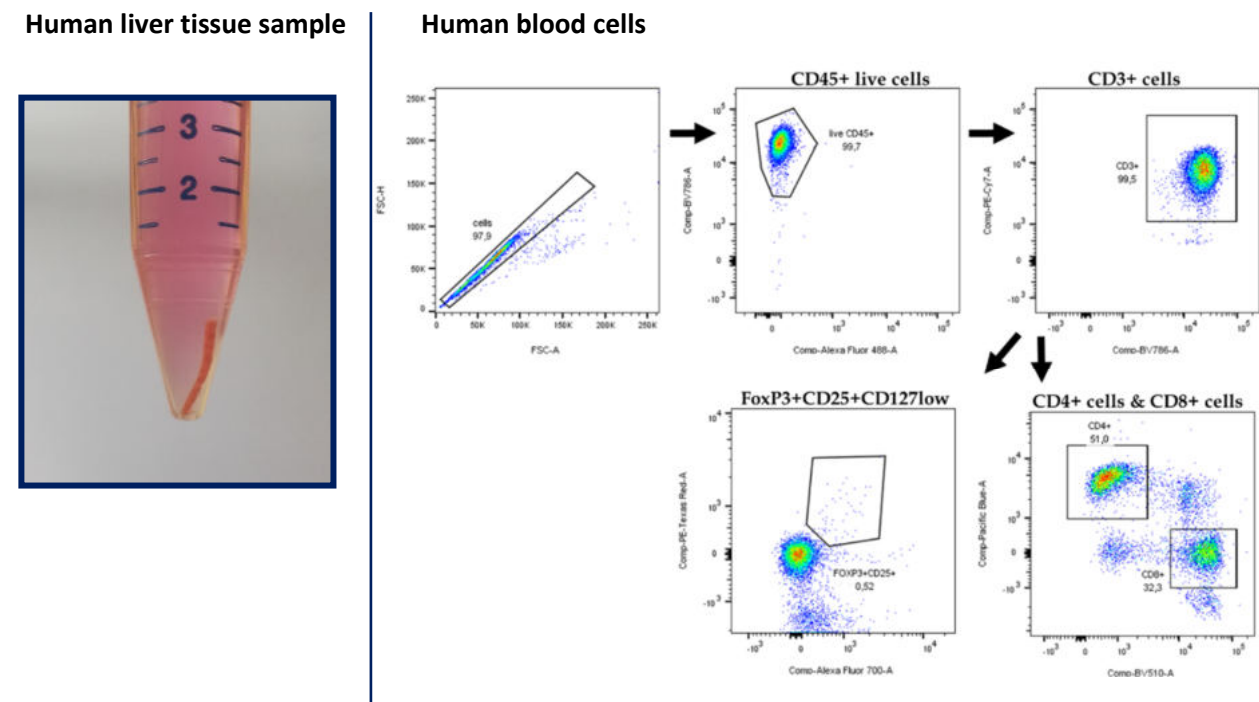
***Figure 9* Exemplary human liver tissue sample (< 30mg, 1.2 cm) from AIH patient and dot plot of isolated CD3$^+$ T cells (10^5 cells acquired) from a healthy subject.** Figures are from personal collection.

3.1.1 Elevated expression of *CBL-B* in whole liver tissue of AIH patients

Gene expression of *CBL-B*, *GRAIL*, *ITCH* and *NEDD4* was analysed in peripheral blood T cells from healthy control subjects (n= 10), treatment-naive AIH patients (n= 6), AIH patients under treatment (n= 10), DILI (n= 7), NASH (n= 6), PBC (n= 4) and PSC patients (n= 4). Relative expression levels of *CBL-B*, *GRAIL*, *ITCH* and *NEDD4* in peripheral blood T cells from patient with treatment-naive AIH were not significantly different as compared to control groups and showed comparable levels of expression (*figure 10*). However, screening of whole liver tissue samples from healthy control subjects (n= 8), treatment-naive AIH patients (n= 15), AIH patients under treatment (n= 7), DILI (n= 6), NASH (n= 8), PBC (n= 4) and PSC (n= 4) patients revealed that levels of *CBL-B* expression in liver tissue samples from treatment-naive AIH patients was significantly increased compared with healthy controls (2.2-fold expression; p= 0.008) and patients with PBC or PSC (1.8-fold expression; p= 0.046; PBC/PSC). Expression levels of *GRAIL* (3.8-fold expression; p= 0.002) and *ITCH* (2.6-fold expression; p= 0,002) were elevated in NASH patients as compared to healthy controls. However, expression levels of *GRAIL*, *ITCH* and *NEDD4* were not significantly different in liver tissue from treatment- naive AIH patients in comparison to control subjects (*figure 11*).
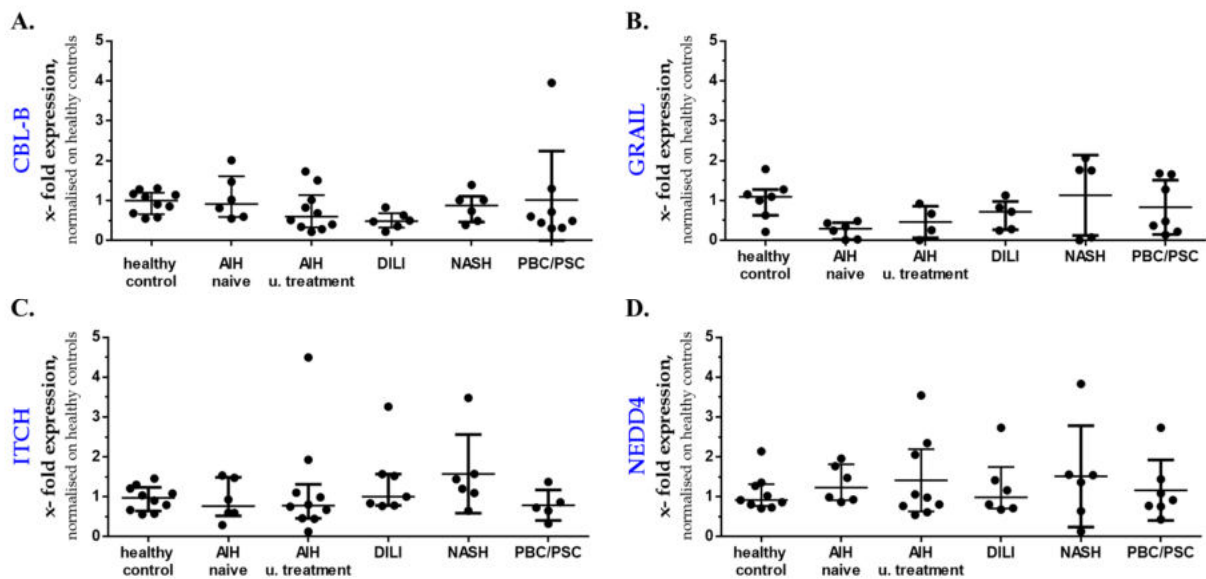
***Figure 10** Relative RNA expression of **CBL-B** (A.), **GRAIL** (B.), **ITCH** (C.) and **NEDD4** (D.) in peripheral blood T cells from healthy control subjects, treatment-naive AIH patients, AIH patients under treatment, DILI, NASH and PBC or PSC patients.*

45
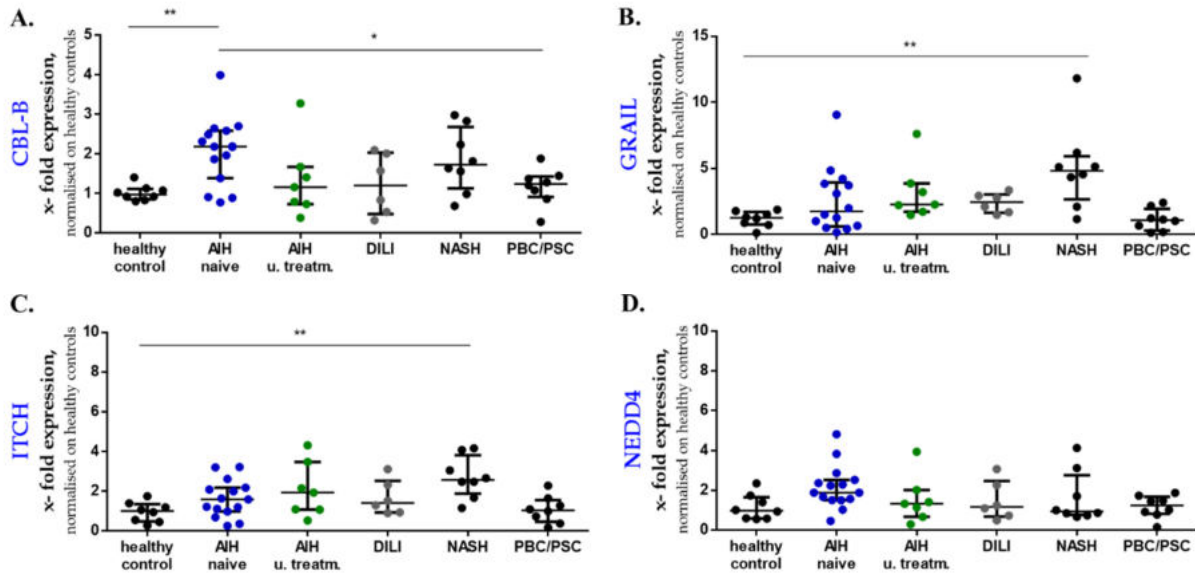
Figure 11 Relative RNA expression of *CBL-B* (A.), *GRAIL* (B.), *ITCH* (C.) and *NEDD4* (D.) in whole liver tissue samples from healthy control subjects, treatment-naive AIH patients, AIH patients under treatment, DILI, NASH and PBC or PSC patients.

Contrary to our initial expectations, real-time PCR screening revealed no considerable deficiency of *CBL-B*, *GRAIL*, *ITCH*, or *NEDD4* in peripheral blood T cells or in liver tissue samples from AIH patients. To the contrary, *CBL-B* expression in liver tissue samples from treatment-naive AIH patients was increased, unlike previous findings in Multiple sclerosis patients described by Stürner and associates [196]. Moreover, elevated expression of *CBL-B* was not seen in peripheral blood T cells of treatment-naive AIH patients or AIH patients under treatment with immunosuppressants, but in liver tissue of treatment-naive AIH patients.

3.1.2 Elevated expression of *CTLA-4*, *ICOS* and *PD-1* in liver tissue of AIH patients

Gene expression levels of *CTLA-4*, *ICOS*, *OX40* and *PD-1* were examined in peripheral blood T cells and liver tissue samples of treatment-naive AIH patients and control subjects. Expression levels of *CTLA-4*, *ICOS*, *OX40* and *PD-1* were not considerably diminished or elevated in peripheral blood T cells of treatment-naive AIH patients and control subjects (*figure 12*). Whereas, PCR screening in whole liver tissue samples showed that expression levels of *CTLA-4* was significantly up-regulated in patients with treatment-naive AIH, as compared with AIH patients under treatment (10.6-fold expression; p= 0.032), healthy control subjects (21.3-fold expression; p< 0.001), NASH (20.0-fold expression; p= 0.005) or PBC/PSC patients (10.8-fold expression; p< 0.01). Relative RNA expression levels of *ICOS* were increased in patients with treatment-naive AIH, as compared to healthy control subjects (26.7-fold expression; p= 0.001), DILI (5.8-fold expression; p= 0.031), NASH (15.9-fold expression; p= 0.003) or

PBC/PSC patients (26.8-fold expression; p= 0.002). Also, *PD-1* expression in liver tissue samples from treatment-naive AIH patients was significantly elevated in comparison to healthy control subjects (10.4-fold expression; p= 0.002) or NASH patients (5.6- fold expression; p= 0.012; *figure 13*).
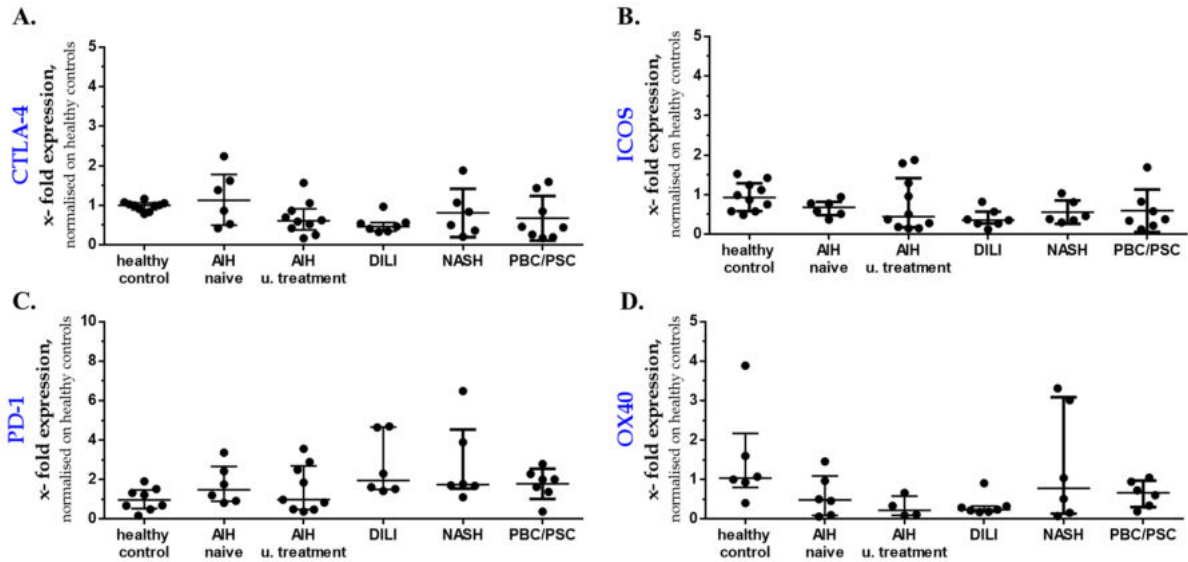
Figure 12 Relative RNA expression of *CTLA-4* (A.), *ICOS* (B.), *PD-1* (C.) and *OX40* (D.) in peripheral blood T cells from healthy control subjects (n= 10), treatment-naive AIH patients (n= 6), AIH patients under treatment (n= 10), DILI (n=7), NASH (n= 6) and PBC (n= 4) or PSC patients (n= 4).
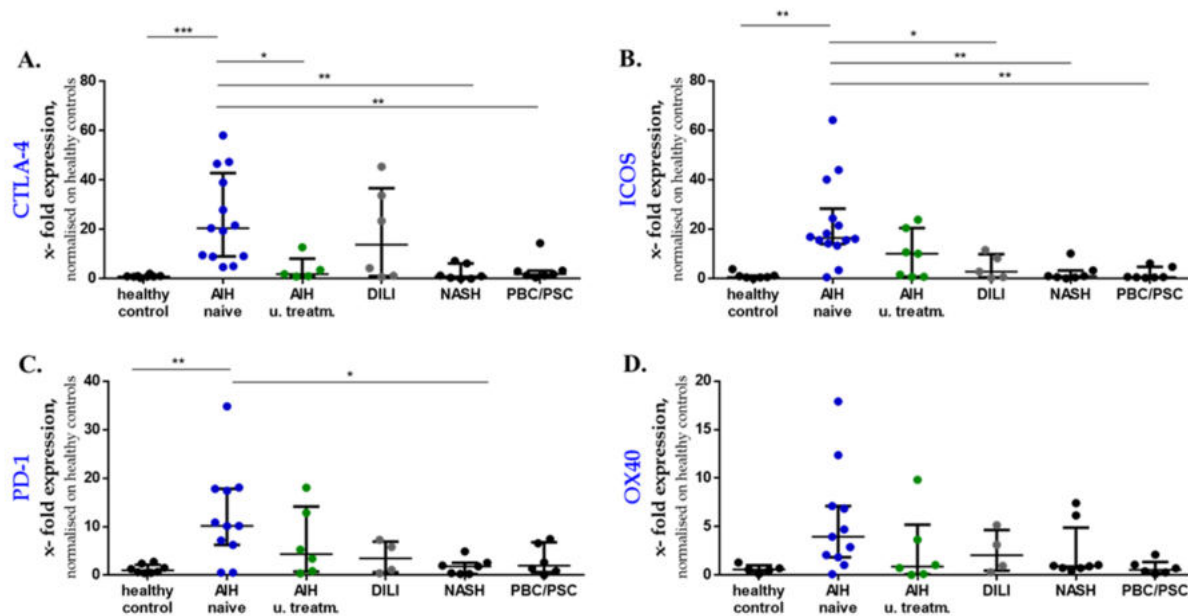
Figure 13 Relative RNA expression of *CTLA-4* (A.), *ICOS* (B.), *PD-1* (C.) and *OX40* (D.) in whole liver tissue samples from healthy control subjects (n= 8), treatment-naive AIH patients (n= 15), AIH patients under treatment (n= 7), DILI (n=6), NASH (n= 8) and PBC (n= 4) or PSC patients (n= 4).

Thus, PCR screening revealed that expression of *CTLA-4*, *PD-1* and *ICOS* was significantly elevated in liver tissue samples, but not in peripheral blood T cells of treatment-naive AIH patients compared with healthy controls. According to these results and previous findings of intrahepatic *CBL-B* expression in liver tissue samples of treatment-naive AIH patients, we considered to perform subsequent analyses based on liver tissue samples and not on peripheral blood samples.

3.1.3 Comparable *PKCθ* and *TRAF6* expression in peripheral blood T cells and whole liver tissue in AIH *versus* controls

Expression of *PKCθ* and *TRAF6* was not significantly different in peripheral blood T cells or whole liver tissue samples from AIH patients, as compared to control subjects (*figure 14, 15*). For this reason, *PKCθ* and *TRAF6* were not included in further analyses.
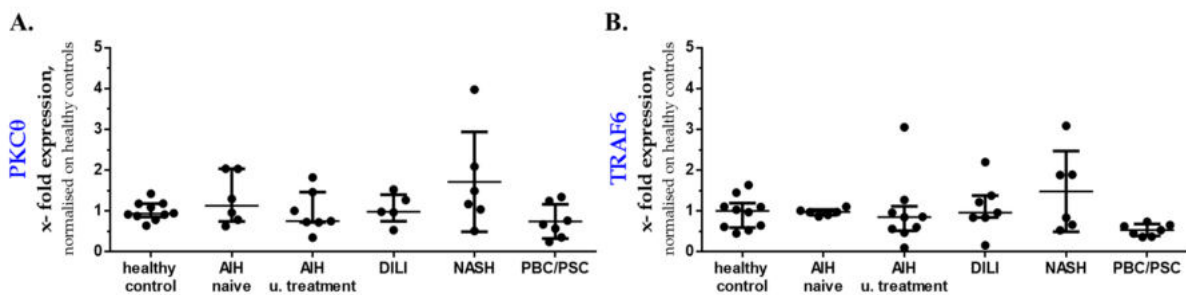
Figure 14 Relative RNA expression of *PKCθ* (A.) and *TRAF6* (B.) in peripheral blood T cells from healthy control subjects (n= 10), treatment-naive AIH patients (n= 6), AIH patients under treatment (n= 10), DILI (n=7), NASH (n= 6) and PBC (n= 4) or PSC patients (n= 4).
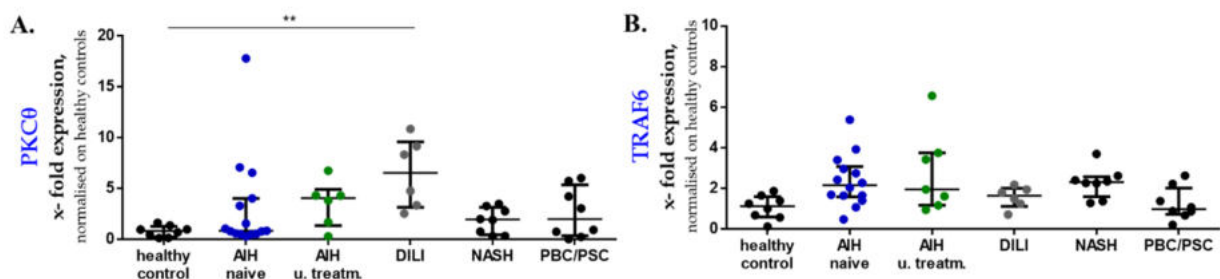
Figure 15 Relative RNA expression of *PKCθ* (A.) and *TRAF6* (B.) in whole liver tissue from healthy control subjects (n= 8), treatment-naive AIH patients (n= 15), AIH patients under treatment (n= 7), DILI (n=6), NASH (n= 8) and PBC (n= 4) or PSC patients (n= 4).

3.1.4 Intrahepatic expression of *CBL-B*, *CTLA-4*, *ICOS* and *PD-1* positively correlate with mHAI

With real-time PCR, we identified *CBL-B*, *CTLA-4*, *ICOS* and *PD-1* as relevant targets of interest for further analysis. In order to associate the identified activation regulatory molecules with disease activity and liver injury in AIH patients, gene expression levels of *CBL-B*, *CTLA-4*, *ICOS* and *PD-1* in liver tissues from AIH patients (treatment-naive or under immunosuppressive treatment; n= 22) were correlated with the modified hepatic activity index (mHAI) and with serum AST and ALT. Correlation was measured with Spearman's rank correlation coefficient R_s. We observed that intrahepatic expression levels of *CBL-B* (R_s= 0.6; p< 0.005), *CTLA-4* (R_s= 0.6; p< 0.005), *ICOS* (R_s= 0.4) and *PD-1* (R_s= 0.2) positively correlated with mHAI of AIH patients. These results suggested that with an increase of intrahepatic disease activity, levels of RNA expression of the T cell activation regulators *CBL-B*, *CTLA-4*, *ICOS* and *PD-1* were also increased in liver tissue from patients with AIH (*figure 16*).
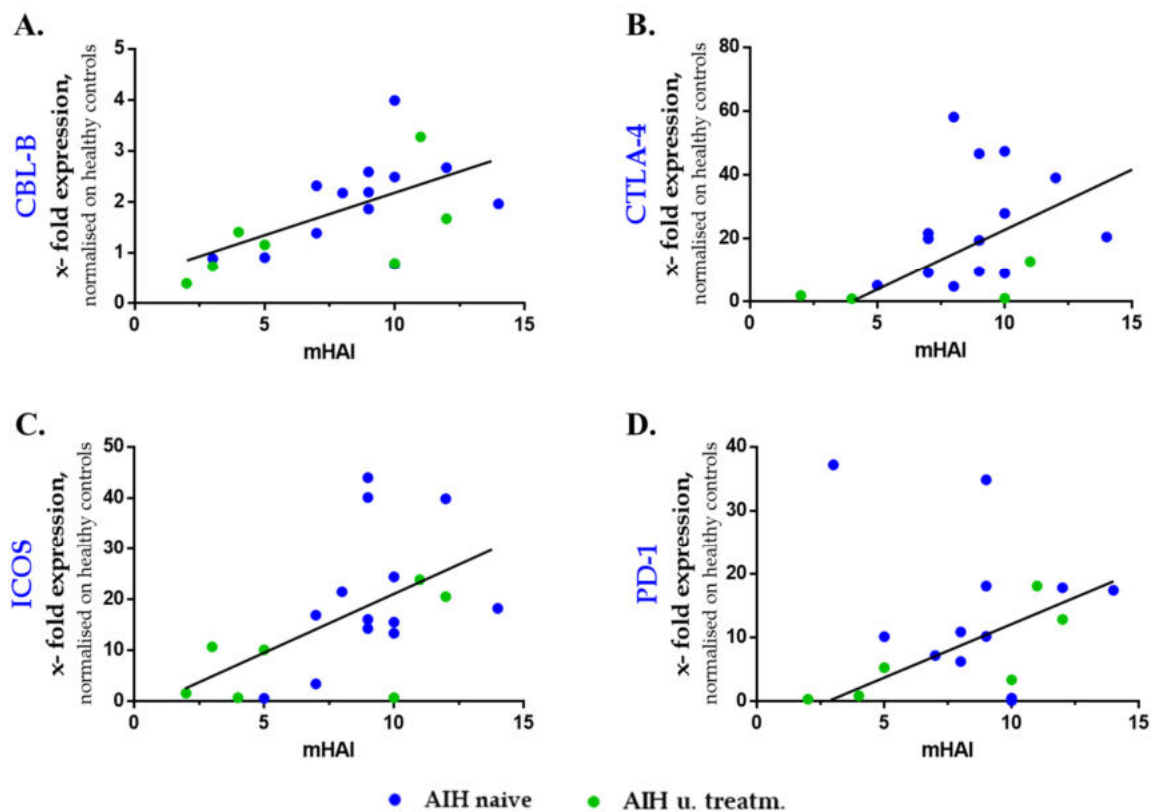
Figure 16 **Relative RNA expression of *CBL-B* (A.), *CTLA-4* (B.), *ICOS* (C.) and *PD-1* (D.) in whole liver tissue from AIH patients positively correlate with mHAI.**

3.1.5 Intrahepatic expression of *CBL-B* correlates with AST and ALT

Intrahepatic expression of *CBL-B*, *CTLA-4*, *ICOS* and *PD-1* was correlated with serum AST and ALT to determine the association between these targets with liver injury in AIH patients. Intrahepatic expression levels of *CTLA-4*, *ICOS* and *PD-1* neither correlated with AST nor with ALT. However, intrahepatic expression of *CBL-B* positively correlated with AST (R_s= 0.6; p= 0.003) and ALT (R_s= 0.6; p= 0.003; *figure 17*). Implying, that intrahepatic expression of *CBL-B* increases with liver injury and hepatic disease activity in patients with AIH.
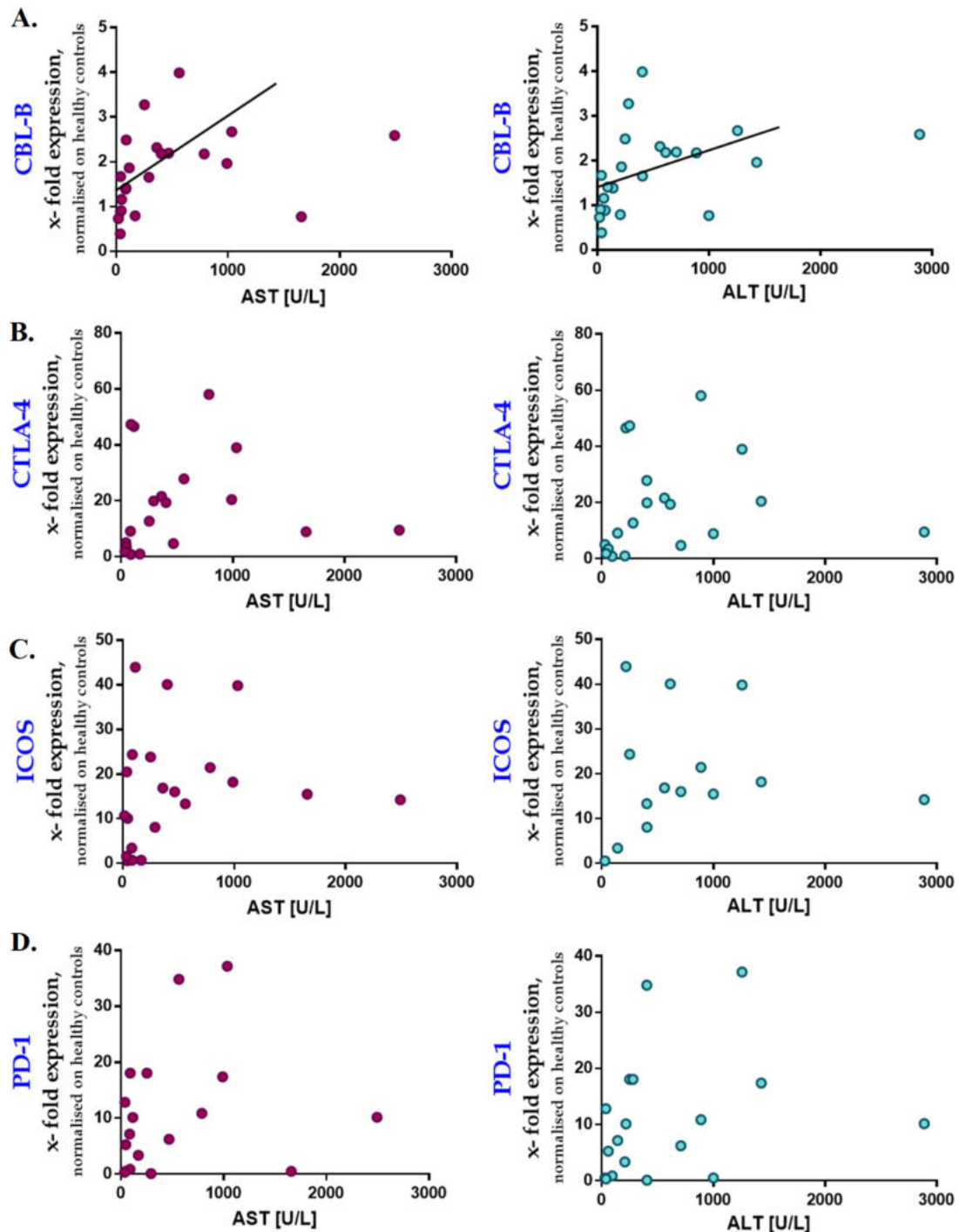
Figure 17 **Relative RNA expression of intrahepatic *CBL-B* (A.) but not of intrahepatic *CTLA-4* (B.), *ICOS*(C.) and *PD-1* (D.), positively correlated with serum AST and ALT in AIH patients.**

50

3.2   Similar expression of CD3$^+$ cells in livers of AIH or DILI patients

Real-time PCR analysis of *CBL-B*, *CTLA-4*, *ICOS* and *PD-1* expression in intrahepatic T cells from livers of AIH patients would require isolation of vital T cells from liver tissue samples. However, due to size and amount of the liver biopsy (<30 mg, 0.7- 1.5 cm; one punch), it is so far not possible to isolate CD3$^+$ T cells from liver biopsy samples from AIH patients in sufficient quantity. For this reason, RNA expression of *CBL-B*, *CTLA-4*, ICOS and *PD-1* was determined by liver immunohistochemical staining in subsequent analyses. For these analyses, a DILI cohort served as control group. DILI causes non-autoimmune liver injury and patients with DILI exhibit similar clinical and histological appearances as AIH patients (*figure 18*). Before performing immunohistochemical staining, we examined whether the expression of T cells in liver samples of DILI patients did not significantly differ from that in liver samples of treatment-naive AIH patients.
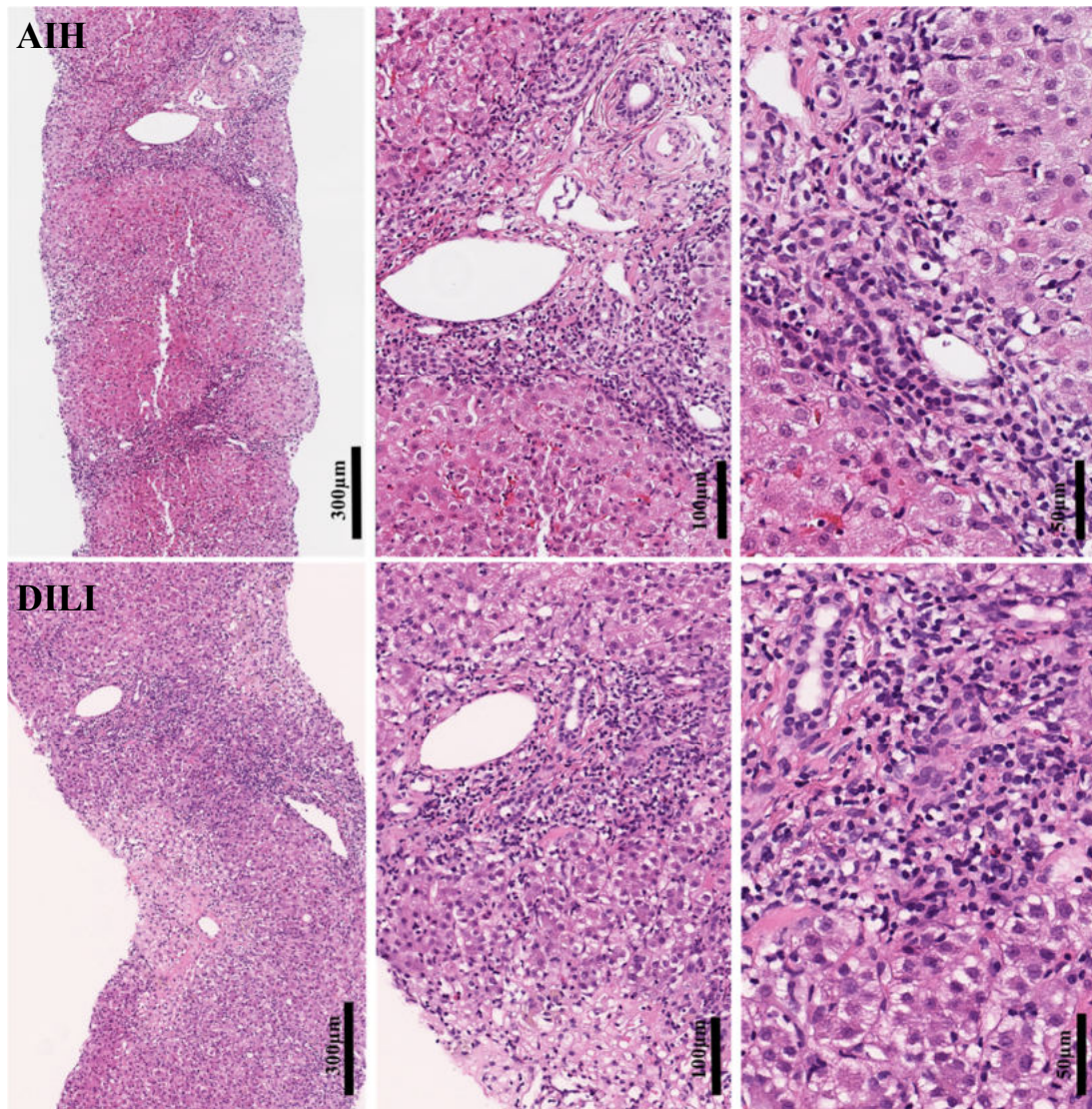
Figure 18 **HE staining of liver tissue samples from DILI and AIH patient.** Figures are from personal collection.

3.2.1 RNA expression of *CD3*, *CD4* and *CD8* in DILI and AIH whole liver tissues

In order to compare the levels of *CD3*, *CD4* and *CD8* RNA expression in AIH or DILI liver tissues, real-time PCR analysis was performed using liver tissue samples from treatment-naive AIH patients (n= 10), DILI patients (n= 6) and healthy controls (n= 6). PCR screening showed that relative RNA expression levels of *CD3* in samples of DILI (21.7-fold expression; p=0.032) or treatment-naive AIH patients (21.3-fold expression; p= 0.006) were significantly increased as compared to healthy controls. However, *CD3* expression did not significantly differ between DILI and treatment-naive AIH patients. Moreover, RNA expression of *CD4* or *CD8* was not significantly different between DILI and treatment-naive patients, although expression of *CD4* (4.2-fold expression; p= 0.048) and *CD8* (22.5-fold expression; p= 0.016) was significantly increased in treatment-naive AIH in comparison to healthy controls. Thus, the PCR results supported the assumption that expression levels of CD3$^+$ cells in livers of DILI and AIH patients were comparable and not significantly different (*figure 19*).
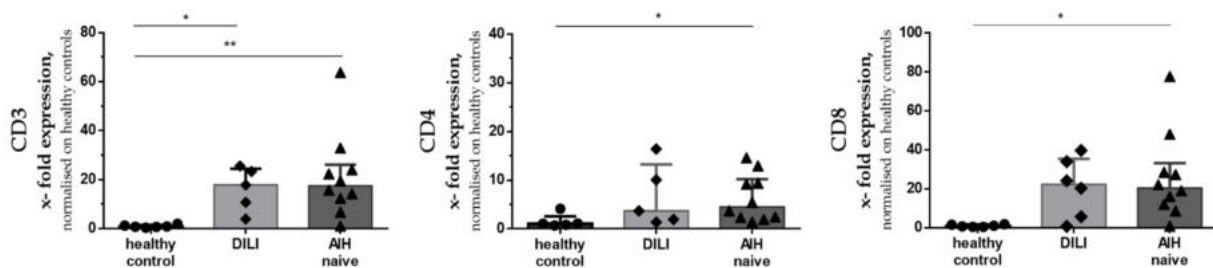
Figure 19 Relative RNA expression of *CD3*, *CD4* and *CD8* in liver tissue samples of healthy controls, DILI or treatment-naive AIH patients.

3.2.2 Expression of CD3$^+$ cells in hepatic portal areas of DILI and AIH patients

For further analysis of T cell numbers in liver portal areas in DILI or AIH liver tissues, CD3$^+$ cells were immunohistochemically stained with anti-human CD3 antibodies (see chapter 2.2.11.4). For quantification, five representative high-power field images of hepatic portal areas of each liver tissue slide were analysed in a blinded manner. The immunohistochemical staining showed that the numbers of CD3$^+$ cells of liver-infiltrating lymphocytes in portal areas was not significantly different in liver tissue samples from AIH patients (treatment-naive or patients under treatment; n= 10) as compared to DILI patients (n= 8; *figure 20*). Thus, T cell infiltration of portal areas was similar in AIH and DILI patients.
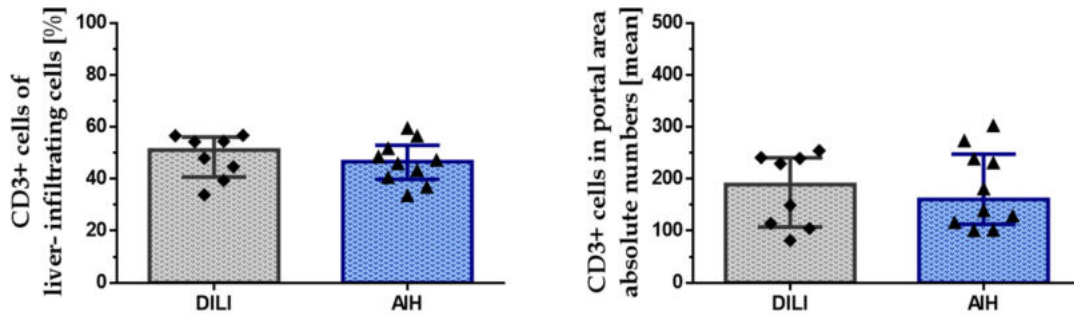
Figure 20 **Similar numbers CD3⁺ T cells in hepatic portal areas in liver tissue samples of DILI and AIH patients.**

3.2.3 Detection of intrahepatic CD3⁺ cells using flow cytometry

Intrahepatic CD3⁺ T cells in liver tissue samples of treatment-naive AIH patients or DILI patients were assessed by flow cytometry. Therefore, intrahepatic T cells were stained with antibodies according to chapter 2.2.10.3. Flow cytometric analysis showed that the size of vital intrahepatic CD45⁺CD3⁺ cell population was similar in treatment-naive AIH patients and DILI patients (*figure 21*).
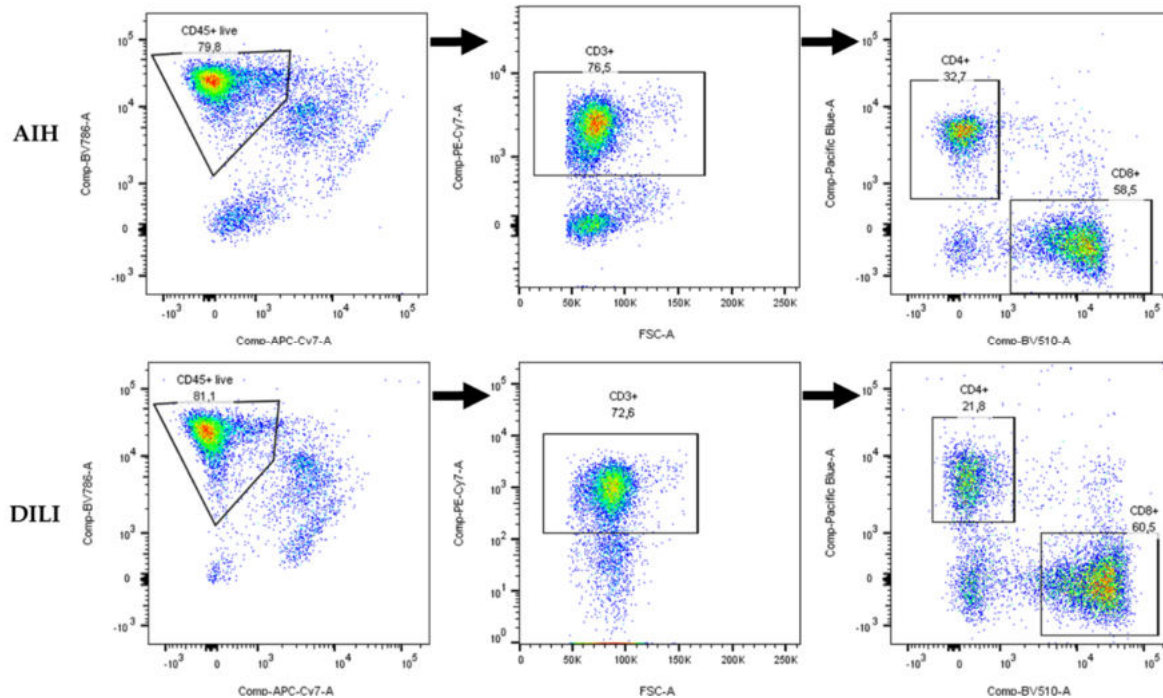
Figure 21 **Flow cytometry staining of CD45⁺CD3⁺ T cells in liver tissue sample of DILI patient and treatment-naive AIH patient.**

3.3 Elevated expression of *CBL-B*, *CTLA-4*, *ICOS* and *PD-1* in liver-infiltrating cells in AIH patients

PCR screening results showed that the expression of *CBL-B*, *CTLA-4*, *ICOS* and *PD-1* was increased in whole liver tissue samples from treatment-naive AIH patients, as compared to controls. Because the PCR screening did not provide information on the hepatic location where the targets of interest were mainly expressed, RNA *in-situ* hybridisation was performed on liver tissues from treatment-naive AIH (n= 12) and DILI (n= 12) patients according to chapter 2.2.11.3 (*figure 22*). Expression of the targets of interest in hepatic portal areas were quantified according to chapter 2.2.11.5. In liver tissues from treatment-naive AIH patients, 46.9% of the liver-infiltrating cells expressed *CBL-B* in hepatic portal areas, whereas in DILI patients, only 17.3% of the liver-infiltrating cells expressed *CBL-B* (p< 0.001). *CTLA-4* was expressed by 27.3% of the liver-infiltrating cells in hepatic portal areas of treatment-naive AIH patients, which is increased compared to only 16.7% of liver-infiltrating cells in DILI patients (p= 0.007). 22.9% of the liver- infiltrating cells expressed *ICOS* in the hepatic portal areas of treatment-naive AIH patients in comparison to only 11.1% of the liver-infiltrating cells in DILI patients (p= 0.013). Moreover, *PD-1* was expressed by 23.8% of liver-infiltrating cells in hepatic portal areas of treatment-naive AIH patients, as compared to only 12.1% of liver-infiltrating cells in DILI patients (p= 0.001; *figure 23*).
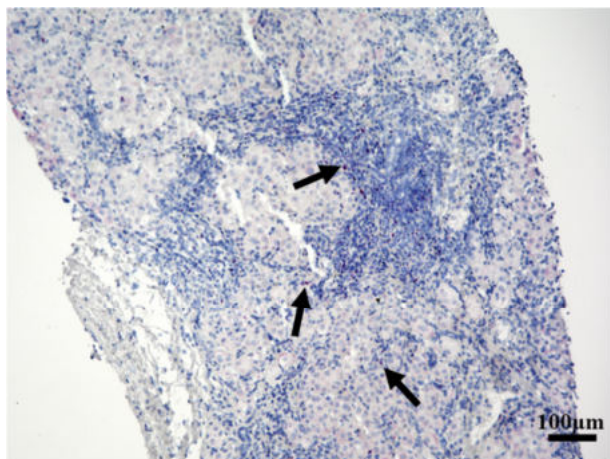
Figure 22 CTLA-4 expression in liver-infiltrating lymphocytes in liver from AIH patient. RNA expression of *CTLA-4* (red dots) on AIH liver tissue sample was stained using RNA *in-situ* hybridisation. Black arrows show exemplary *CTLA-4* staining.
Figure is from personal collection.
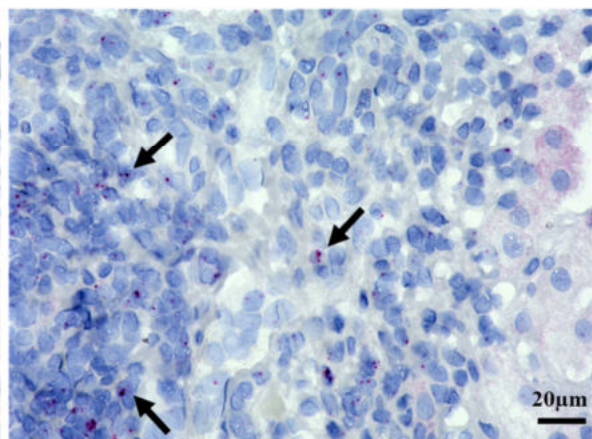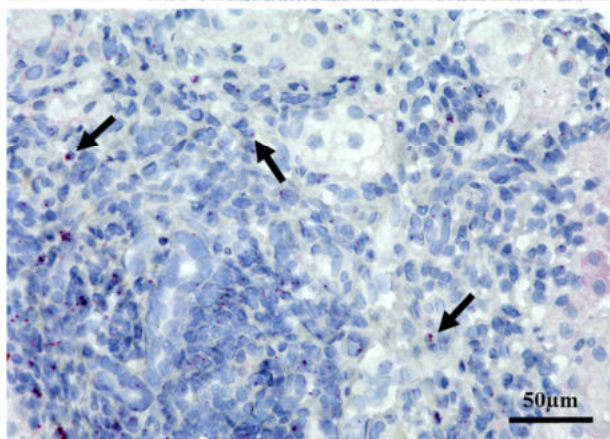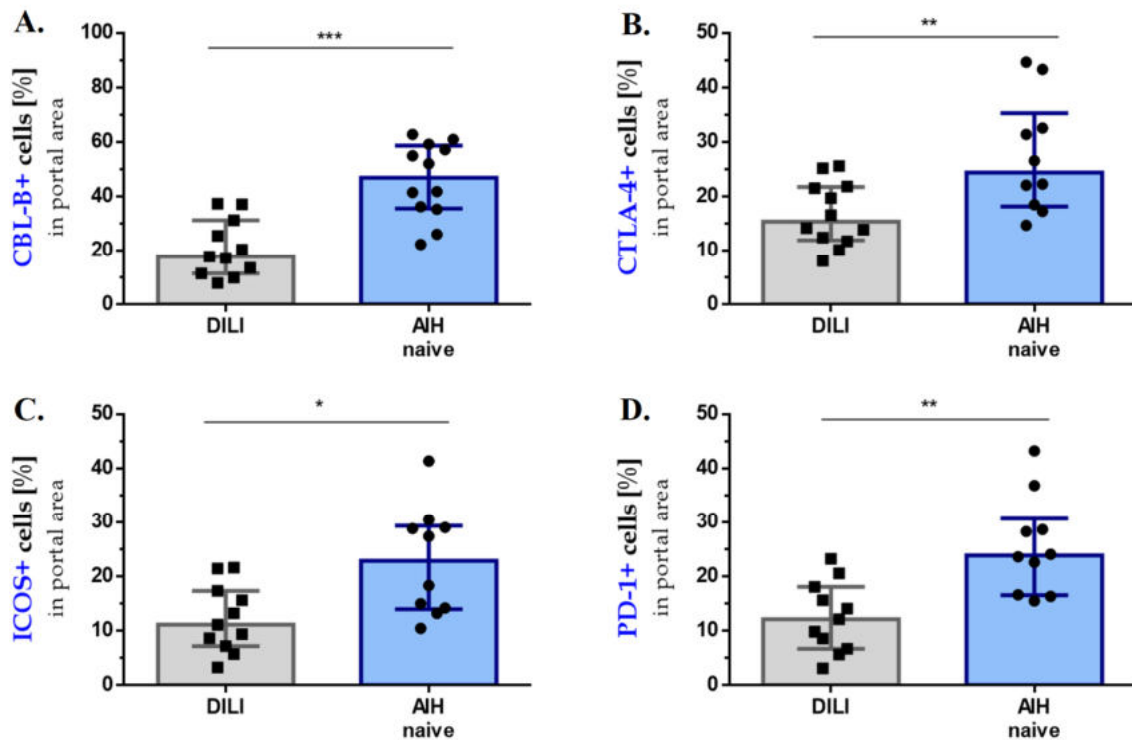
Figure 23 RNA expression of *CBL-B* (A.), *CTLA-4* (B.), *ICOS* (C.) and *PD-1* (D.) in liver-infiltrating cells in hepatic portal areas of treatment-naive AIH patients or DILI patients. RNA expression of *CBL-B*, *CTLA-4*, *ICOS* and *PD-1* detected in liver tissues using RNA *in-situ* hybridisation.

RNA expression of targets of interest was also examined in the liver lobes of treatment-naive AIH patients (n= 7) and DILI patients (n= 5; *figure 24*). The percentage of cells that expressed *CBL-B*, *CTLA-4*, *ICOS* or *PD-1* in hepatic lobules did not significantly differ between liver tissue samples from treatment-naive AIH patients or from DILI patients (*figure 25*). These results suggested that the liver-infiltrating cells in hepatic portal areas and not cells in the hepatic lobules, might account for the different levels of *CBL-B*, *CTLA-4*, *ICOS* and *PD-1* expression found in AIH livers, as compared to DILI livers.
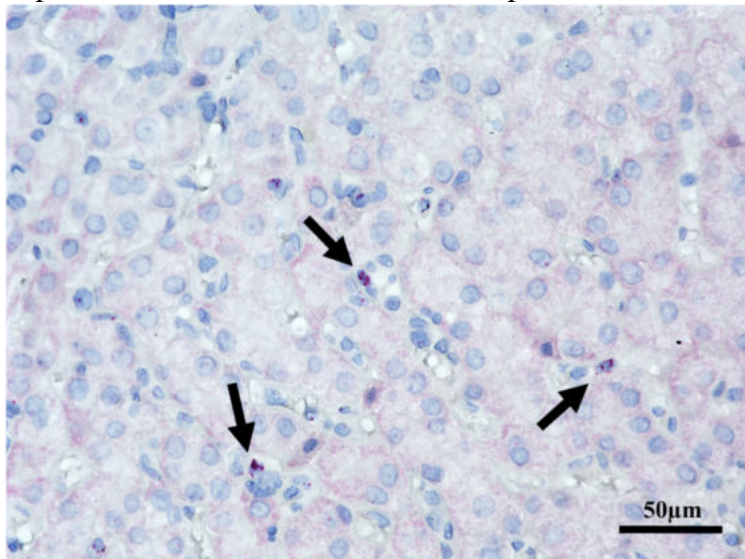
Figure 24 CTLA-4 **expression in the liver lobes of AIH patient.** RNA expression of *CTLA-4* (red dots) on AIH liver tissue sample was stained using RNA *in-situ* hybridisation. Black arrows show exemplary *CTLA-4* staining. Figure is from personal collection.
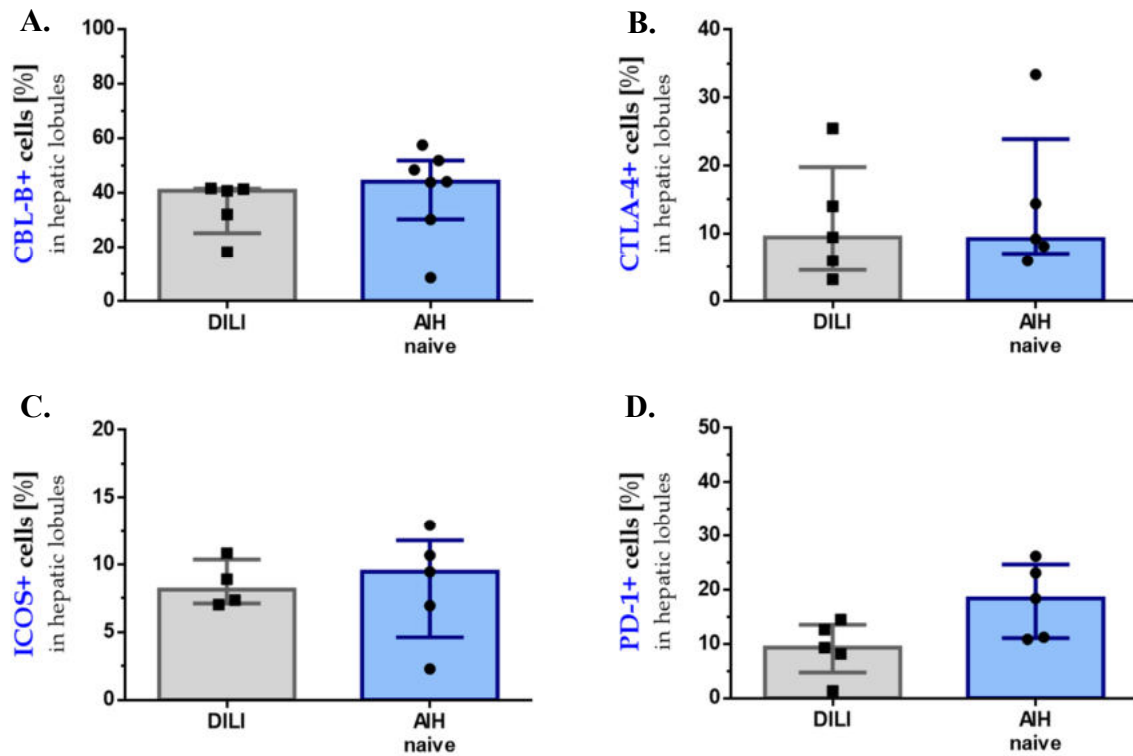
Figure 25 RNA expression of ***CBL-B*** (A.), ***CTLA-4*** (B.), ***ICOS*** (C.) and ***PD-1*** (D.) in cells in liver lobes of treatment-naive AIH or DILI patients. RNA expression of *CBL-B*, *CTLA-4*, *ICOS* and *PD-1* was detected by use of RNA *in-situ* hybridisation on liver tissue slides.

3.3.1 Elevated expression of *CBL-B*, *CTLA-4*, *ICOS* and *PD-1* in liver-infiltrating T cells in AIH

To quantify the expression of *CBL-B*, *CTLA-4*, *ICOS* and *PD-1* in liver-infiltrating CD3$^+$ cells, RNA *in-situ* hybridisation was combined with anti-CD3 co-staining and applied to liver tissue slides according to chapter 2.2.11.4 (*figure 26*). For this purpose, the expression of the targets of interest was quantified in intrahepatic T cells in hepatic portal areas from treatment-naive AIH patients (n= 6), AIH patients under immunosuppressive treatment (n= 4) and DILI patients (n= 7). In hepatic portal areas of treatment-naive AIH patients, 44.1% of the liver-infiltrating CD3$^+$ cells were *CBL-B* positive, as compared to only 19.9% of the CD3$^+$ cells in DILI patients (p= 0.01) and 27.0% of the CD3$^+$ cells in AIH patients under treatment (p= 0.039). With respect to *CTLA-4* expression, 30.4% of the CD3$^+$ cells were *CTLA-4* positive in treatment-naive AIH, as compared to only 20.2% in DILI patients (p= 0.006) and 9.2% in AIH patients under treatment (p< 0.0001; p= 0.004). Moreover, 27.4% of the liver-infiltrating CD3$^+$ cells were positive for *ICOS* in treatment-naive AIH patients, compared with 16.7% of the CD3$^+$ cells in DILI patients (p= 0.045) and 13.3% in AIH patients under treatment (p= 0.029). In addition,

30.0% of the CD3⁺ cells were *PD-1* positive in comparison with 11.3% in DILI patients (p= 0.008) and 13.7% in AIH patients under treatment (p= 0.019; *figure 27*). These results confirmed the findings of the gene expression analyses regarding the *CBL-B*, *CTLA-4*, *ICOS* and *PD-1* expression in liver tissues of treatment-naive AIH patients.
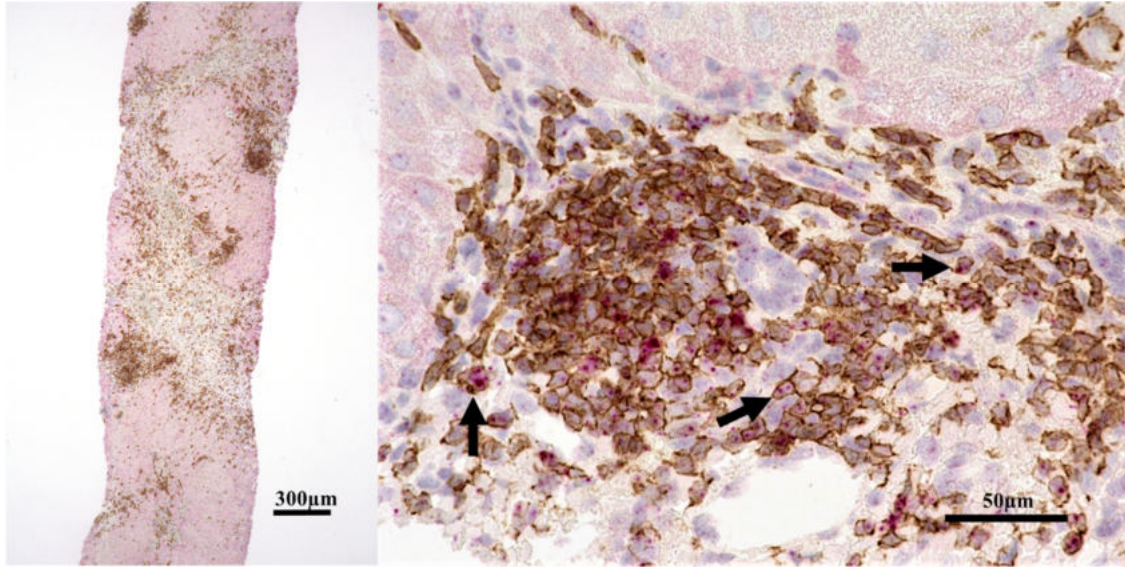
Figure 26 CTLA-4 **expression in liver–infiltrating T cells in hepatic portal area of AIH patient.** RNA expression of *CTLA-4* (red dots) in AIH liver tissue sample was stained using RNA *in-situ* hybridisation. Additional anti-CD3 co-staining was applied to detect CD3⁺ cells (brown). Black arrows show exemplary T cells that express *CTLA-4*. Figure is from personal collection.
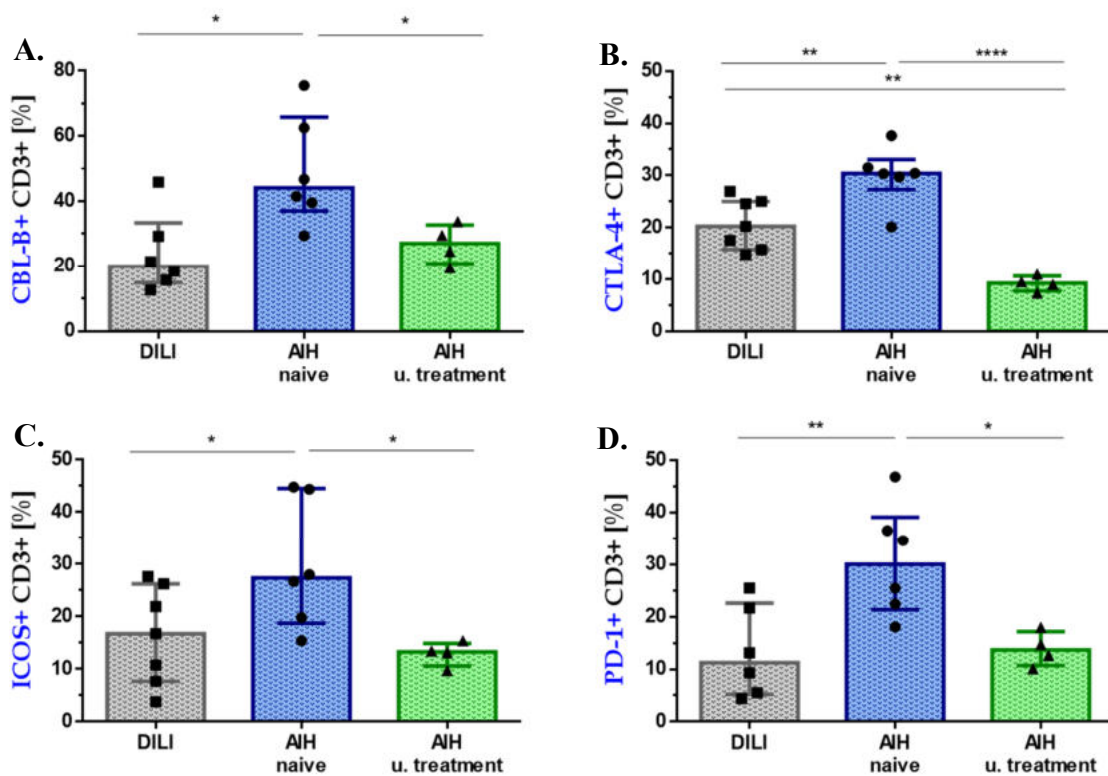
Figure 27 **RNA expression of *CBL-B* (A.), *CTLA-4* (B.), *ICOS* (C.) and *PD-1* (D.) in liver-infiltrating CD3⁺ T cells in hepatic portal areas from treatment-naive AIH patients, DILI patients or AIH patients under treatment.** RNA expression of *CBL-B*, *CTLA-4*, *ICOS* and *PD-1* by use of RNA *in-situ* hybridisation with additional anti-CD3 co-staining.
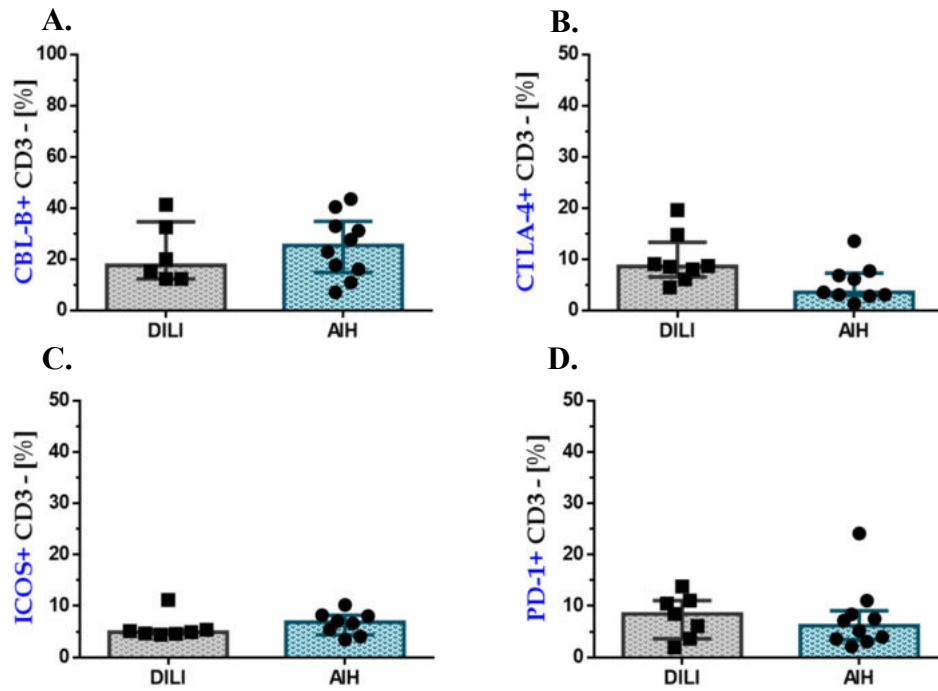
Figure 28 RNA expression of *CBL-B* (A.), *CTLA-4* (B.), *ICOS* (C.) and *PD-1* (D.) in liver-infiltrating CD3⁻cells in hepatic portal areas from AIH patients (treatment-naive and patients under treatment) or DILI patients.

Having analysed the liver-infiltrating $CD3^+$ cells, we then analysed the liver-infiltrating $CD3^-$ cells. For this purpose, hepatic portal areas in livers from DILI patients (n=7) and AIH patients (treatment-naive or under treatment; n= 10) were analysed. The expression of *CBL-B*, *CTLA-4*, *ICOS* or *PD-1* by liver-infiltrating $CD3^-$ cells in AIH livers was low. Moreover, the percentage of liver-infiltrating $CD3^-$ cells that were positive for *CBL-B*, *CTLA-4*, *ICOS* or *PD-1* was similar in AIH and DILI patients (*figure 28*). These results suggested that liver-infiltrating $CD3^+$ cells in hepatic portal areas might account for the elevated RNA expression of *CBL-B*, *CTLA-4*, *ICOS* and *PD-1* detected in whole liver tissue samples from treatment-naive AIH patients. Furthermore, expression of *CBL-B* (R_s= 0.6) or *CTLA-4* (R_s= 0.5) in liver-infiltrating $CD3^+$ T cells positively correlated with disease activity expressed as mHAI (*figure 29*).
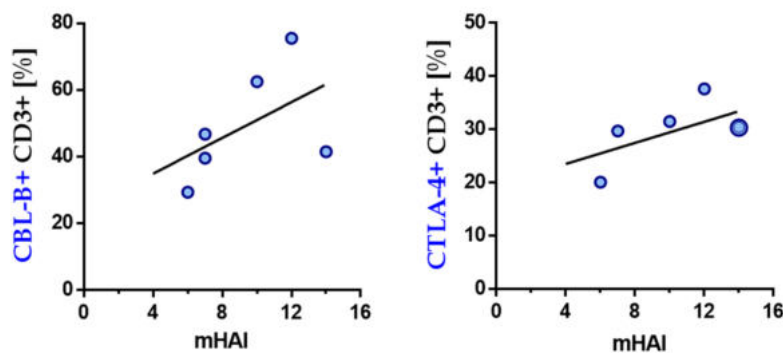
Figure 29 CBL-B and ***CTLA-4*** **expression in liver-infiltrating T cells in hepatic portal areas of livers from treatment-naive AIH patients (n=6) correlated with mHAI**.

58

3.4   Elevated expression of protein CBL-B, CTLA-4, ICOS and PD-1 in liver-infiltrating T cells in AIH patients as compared to healthy controls

As we found that liver-infiltrating T cells of treatment-naive AIH patients expressed increased levels of *CBL-B*, *CTLA-4*, *ICOS* and *PD-1*, we examined whether the RNA findings are confirmed at the protein level. CBL-B protein expression was qualitatively assessed in intrahepatic T cells from healthy controls by use of immunofluorescence. Healthy intrahepatic T cells were found to express CBL-B protein, however fluorescence intensity was low in T cells as compared to surrounding CD3$^-$ cells (*figure 30*). To confirm this finding, we analysed CBL-B protein expression in intrahepatic CD4$^+$ or CD8$^+$ T cells from treatment-naive AIH patients (n= 5) or from healthy control subjects (n= 7) with flow cytometry according to chapter 2.2.10.4. Furthermore, we assessed CBL-B protein expression in response to T cell stimulation with anti-CD3 and anti-CD28 antibodies, as was previously published by Li and associates [133].
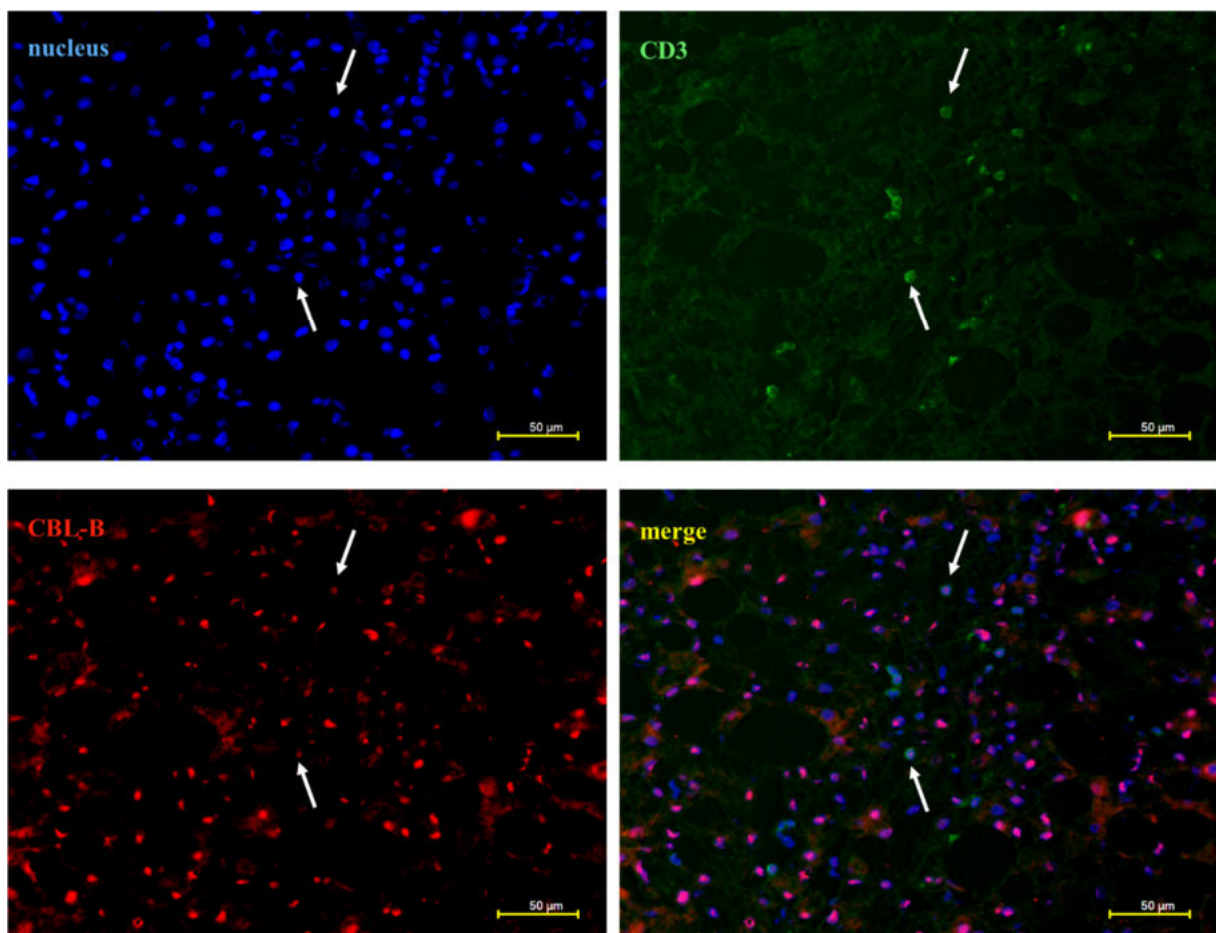
***Figure 30* Protein expression of CBL-B in liver tissue sample of healthy control subject.** Nuclei (blue; upper left) in Hoechst dye stain, CD3$^+$ cells (green; upper right) in AF488 stain, protein CBL-B (red; lower left) in PE stain and merged image (lower right). White arrows show exemplary CD3$^+$ cells. Figures are from personal collection.

In healthy control subjects, CBL-B was detected in 26.7% of the intrahepatic CD4^{+} T cells before stimulation, but after stimulation, was reduced to only 10.2% of the intrahepatic CD4^{+} T cells (p= 0.002). Likewise, 18.1% of the intrahepatic CD8^{+} T cells in healthy subjects expressed CBL-B protein before stimulation, compared to only 9.0% of the intrahepatic CD8^{+} T cells after stimulation (p= 0.007). Thus, in accordance with Li and co-workers [133], CBL-B protein expression was significantly decreased in healthy intrahepatic CD4^{+} or CD8^{+} T cells after stimulation with anti-CD3 and anti-CD28 antibodies (*figure 31*).
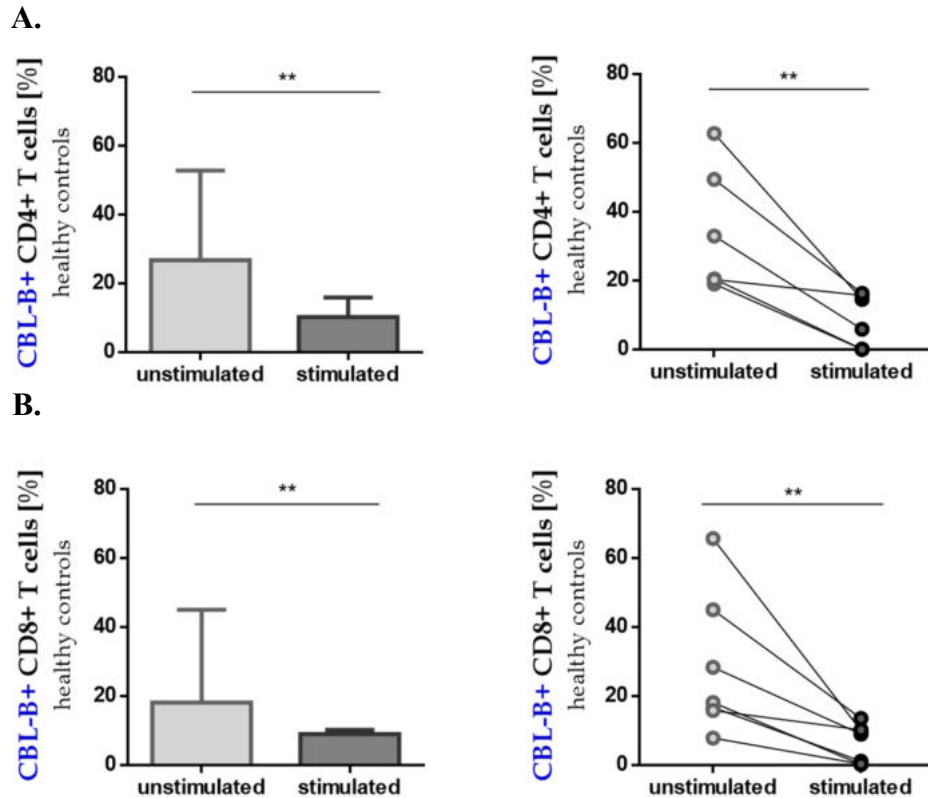
Figure 31 **CBL-B protein expression by intrahepatic CD4^{+} (A.) or CD8^{+} (B.) T cells from livers of healthy control subjects, before and after anti-CD3/CD28 stimulation for 4 h.**

In treatment-naive AIH patients, no staining could be performed prior to stimulation due to limited sample size of the liver tissue. However, after stimulation with anti-CD3 and anti-CD28 antibodies, 75.3% of the intrahepatic CD4^{+} T cells from treatment-naive AIH patients showed high CBL-B expression, in contrast to only 10.2% of the intrahepatic CD4^{+} T cells from healthy control subjects (p= 0.004). Accordingly, CBL-B was detected in 81.8% of the intrahepatic CD8^{+} T cells from treatment-naive AIH patients in response to stimulation, in contrast to only 9.0% of the CD8^{+} T cells from healthy control subjects (p= 0.003).

Moreover, mean fluorescence intensity (MFI) of intrahepatic CD4^{+} T cells expressing CBL-B protein was significantly increased in treatment-naive AIH patients, as compared to healthy

controls (6867 vs. 1480; p= 0.01). Likewise, MFI of CBL-B expression in intrahepatic $CD8^+$ T cells from treatment-naive AIH patients was significantly elevated, as compared to healthy controls (7243 vs 1347; p= 0.03). These results indicated that, in contrast to healthy intrahepatic T cells, CBL-B protein expression was not reduced in intrahepatic T cells in treatment-naive AIH patients after stimulation with anti-CD3/CD28 antibodies (*figure 32*).
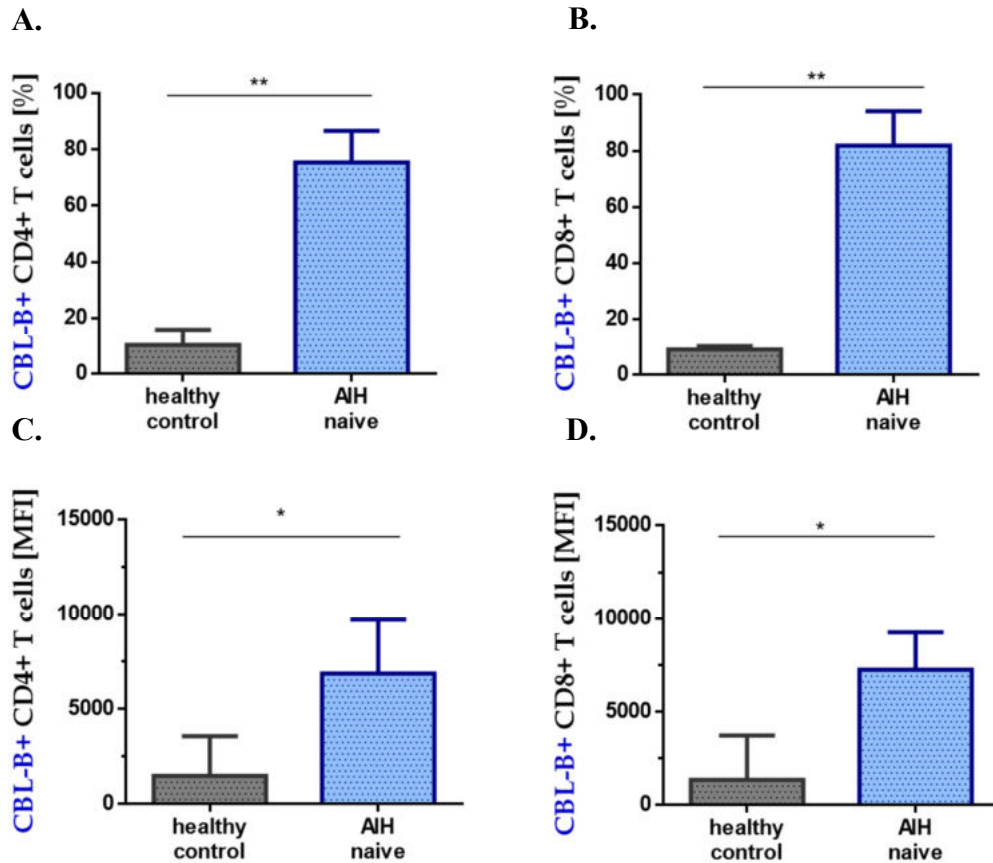
Figure 32 **After anti-CD3/CD28 stimulation for 4 h, CBL-B protein expression is not reduced in intrahepatic CD4$^+$ or CD8$^+$ T cells from treatment-naive AIH patients.** CD4$^+$ (A.) and CD8$^+$ T cells (B.) from treatment-naive AIH patients were compared to healthy controls. Mean fluorescence intensity (MFI) of CD4$^+$ or CD8$^+$ T cells expressing CBL-B was determined (C., D.).

With flow cytometry, protein expression of CTLA-4, ICOS and PD-1 was also examined in intrahepatic CD4$^+$ or CD8$^+$ T cells from patients with treatment-naive AIH in comparison to intrahepatic T cells from healthy controls. 29.4% of the intrahepatic CD4$^+$ T cells from treatment-naive AIH expressed CTLA-4, as compared to 10.2% of healthy CD4$^+$ T cells (p= 0.048). In addition, 13.3% of the intrahepatic CD4$^+$ T cells from treatment-naive AIH patients expressed ICOS, as compared to 3.7% of healthy CD4$^+$ T cells. Whereas PD-1 expression in intrahepatic CD4$^+$ T cells from treatment-naive AIH patients or healthy controls was not significantly different (17.2% vs. 10.2%; *figure 33*), a difference in PD-1 expression was found

in intrahepatic CD8^{+} T cells (41.5% in treatment-naive AIH vs. 4.9% in healthy control subjects; p= 0.001). Furthermore, 30.8% of the intrahepatic CD8^{+} T cells from treatment-naive AIH patients expressed CTLA-4 in comparison to 0.8% of healthy CD8^{+} T cells (p= 0.005). However, ICOS expression in intrahepatic CD4^{+} T cells from treatment-naive AIH patients or healthy controls was not significantly different (5.3% vs. 4.3%; *figure 34*). These results revealed that the intrahepatic T cells from treatment-naive AIH patients responded to stimulation with an increase in numbers of CTLA-4^{+}CD4^{+}, ICOS^{+}CD4^{+} T cells and CTLA-4^{+}CD8^{+}, PD-1^{+}CD8^{+} T cells, as compared to healthy controls.
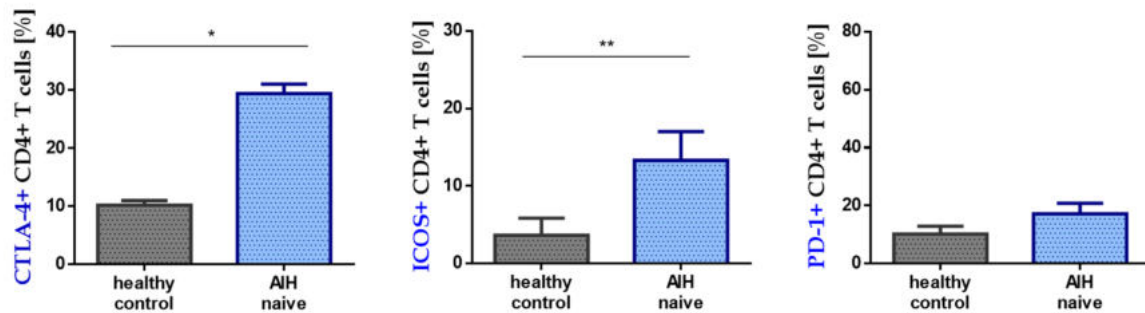
Figure 33 **Protein expression of CTLA-4, ICOS and PD-1 in liver-infiltrating CD4^{+} T cells from treatment-naive AIH patients or healthy controls after anti-CD3/CD28 stimulation for 4 h.**
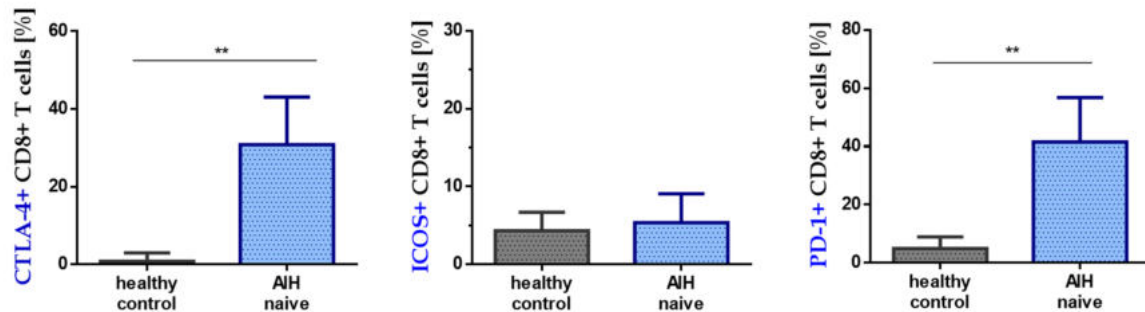
Figure 34 **Protein expression of CTLA-4, ICOS and PD-1 in liver- infiltrating CD8^{+} T cells from treatment-naive AIH patients or healthy controls after anti-CD3/CD28 stimulation for 4 h.**

To learn whether these findings were non-specifically related to liver inflammation or a specific feature of AIH, flow cytometry was also performed on liver tissue samples of NASH (n= 4) and DILI patients (n= 2). However, as there were only 2 DILI patients, the p value should be taken with caution. Nevertheless, there was a clear trend. CBL-B protein expression in intrahepatic T cells from NASH or DILI patients was compared after stimulation to that in intrahepatic T cells from treatment-naive AIH patients. CBL-B was expressed by 9.1% of the intrahepatic CD4^{+} T cells in NASH (p< 0.0001) and by 5.4% in DILI (p< 0,0001), as compared

to 75. 3% in treatment-naive AIH patients. Moreover, 12.6% of intrahepatic CD8^{+} T cells in NASH (p< 0.0001) and 4.4% in DILI (p< 0,0001) were positive for CBL-B expression, as compared to 80.4% in treatment-naive AIH (*figure 35*). These results showed that protein expression of CBL-B in intrahepatic T cells of NASH or DILI patients was low after stimulation, whereas protein expression levels of CBL-B remained high in intrahepatic T cells of treatment-naive AIH patients.
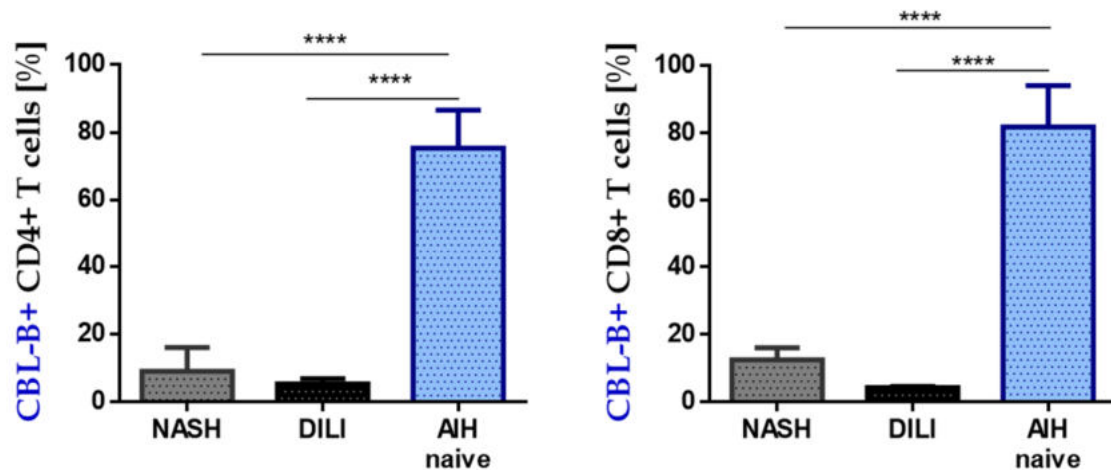
Figure 35 **Protein expression of CBL-B in liver- infiltrating CD4^{+} T cells from treatment-naive AIH patients, NASH or DILI after anti-CD3/CD28 stimulation for 4 h.**

Protein expression of CTLA-4, ICOS and PD-1 was also examined in liver-infiltrating T cells from NASH or DILI patients. Expression levels of ICOS or PD-1 in intrahepatic CD4^{+} T cells was similar and not significantly different between NASH, DILI or treatment- naive AIH patients. However, 29.4% of the intrahepatic CD4^{+} T cells expressed CTLA-4 in treatment-naive AIH patients, which was elevated as compared to 14.9% in DILI patients and significantly increased as compared to 7.6% in NASH patients (p= 0.021; *figure 36*). Moreover, 30.8% of the intrahepatic CD8^{+} T cells in treatment-naive AIH, expressed CTLA-4 as compared to 2.7% in NASH patients (p= 0.044) and 12.1% in DILI patients (not significant). Furthermore, in treatment-naive AIH patients, 41.5% of the intrahepatic CD8^{+} T cells were positive for PD-1, as compared to 7.7% in NASH (p= 0.031) and 19.1% in DILI (not significant). The percentage of intrahepatic CD8^{+} T cells that expressed ICOS was below 10% and did not significantly differ between the study groups. These results indicated that intrahepatic CTLA-4^{+}CD4^{+} T cells, CTLA-4^{+}CD8^{+} and PD-1^{+}CD8^{+}T cells might be enriched in livers of treatment-naive AIH patients. Upon stimulation, ICOS^{+}CD4^{+} T cells of liver tissues from treatment-naive AIH patients were increased compared to those from healthy controls but not considerably different compared to ICOS^{+}CD4^{+} T cells of DILI or NASH patients (*figure 37*).
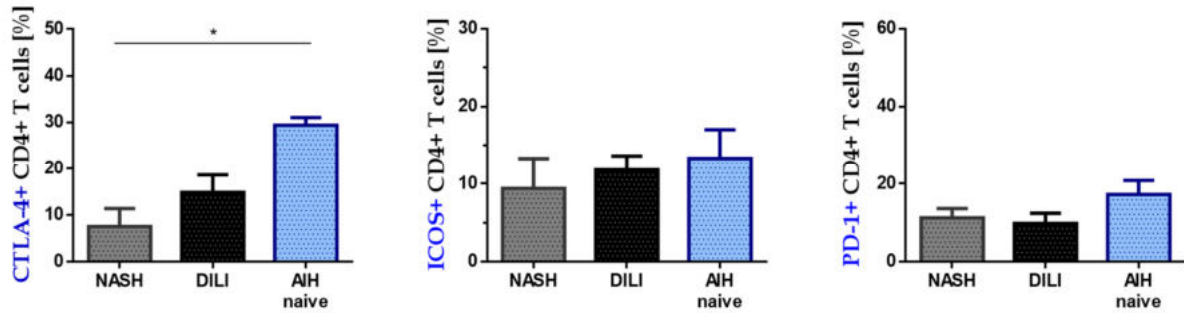
Figure 36 Protein expression of CTLA-4, ICOS and PD-1 in liver-infiltrating CD4$^+$ T cells from treatment- naive AIH patients, NASH or DILI patients after anti-CD3/CD28 stimulation for 4 h.
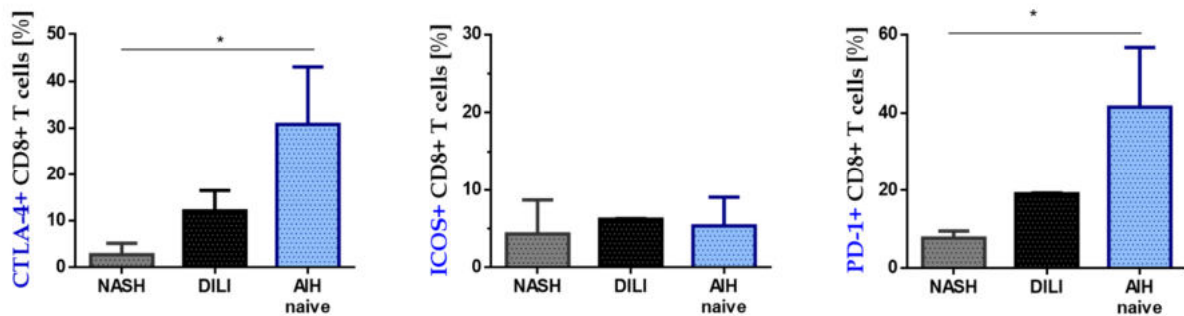
Figure 37 Protein expression of CTLA-4, ICOS and PD-1 in liver-infiltrating CD8$^+$ T cells from treatment- naive AIH patients, NASH or DILI patients after anti-CD3/CD28 stimulation for 4 h.

Hence, we identified that intrahepatic T cells of treatment-naive AIH patients, in contrast to controls, maintained high levels of CBL-B after stimulation. Moreover, the proportion of CTLA-4- or PD-1- expressing cells was increased among liver-infiltrating T cells of treatment-naive AIH patients.

Next, we analysed intrahepatic CD4$^+$ or CD8$^+$ T cells that expressed high or low levels of CBL-B (CBL-B^{hi} or CBL-B^{low}) with respect to expression of CTLA-4, ICOS and PD-1. We examined whether CBL-B^{hi} or CBL-B^{low} T cells in the respective patient groups, differ with regard to the expression of CTLA-4, ICOS, PD-1 or co-expression of PD-1 and CTLA-4 (PD-1/CTLA-4). In treatment-naive AIH, the percentage of CBL-B^{hi}CD4$^+$ T cells that also expressed CTLA-4 were significantly increased after stimulation, as compared to healthy controls (22.6% vs. 0%; p< 0.0001) or NASH patients (26% vs. 5.5%; p= 0.0004). In contrast, intrahepatic CBL-B^{low}CD4$^+$ T cells expressed similarly low CTLA-4 levels in all patient groups. Moreover, expression of PD-1, ICOS or co-expression of PD-1/CTLA-4 by CBL-B^{hi}CD4$^+$ or CBL-B^{low}CD4$^+$ T cells was not significantly different in treatment-naive AIH patients, as compared to control groups (*figure 38*). Thus, a greater proportion of intrahepatic CBL-B^{hi}CD4$^+$ T cells also expressed CTLA-4 in treatment-naive AIH, as compared to CBL-B^{hi}CD4$^+$ T cells of control groups.
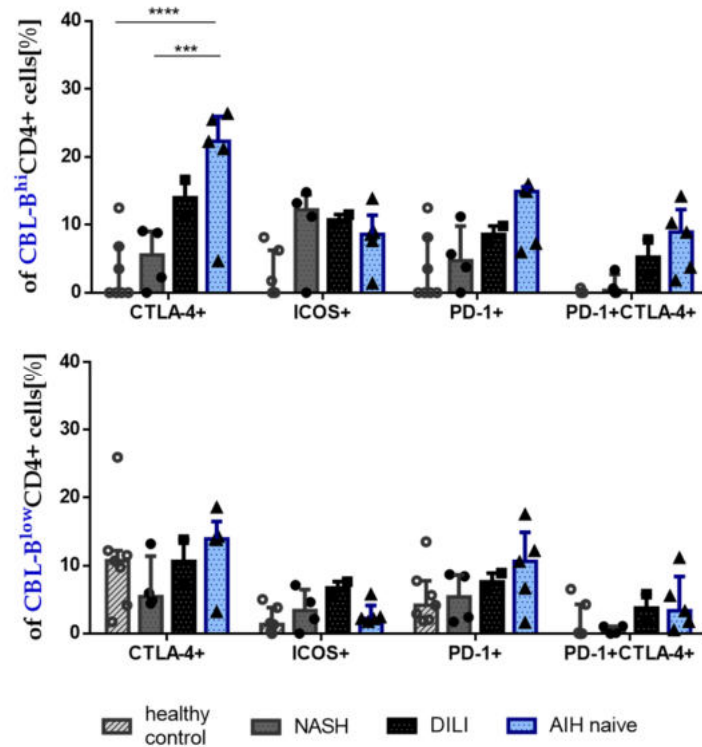
Figure 38 **Protein expression of CTLA-4, ICOS and PD-1 in liver-infiltrating CBL-B^{hi} or CBL-B^{low} CD4$^+$ T cells from treatment-naive AIH patients, healthy controls, NASH or DILI patients after anti-CD3/CD28 stimulation for 4 h.**

We detected that in treatment-naive AIH, the percentage of CBL-B^{hi} CD8$^+$ T cells that also expressed CTLA-4 was significantly increased, as compared to healthy controls (35.8% vs. 0%; p< 0.0001) and NASH (35.8% vs. 0%; p< 0.0001). Furthermore, expression of PD-1 by CBL-B^{hi}CD8$^+$ T cells from treatment-naive AIH patients, was elevated as compared to healthy controls (42.8% vs. 4.1%; p< 0.0001) and NASH patients (42.8% vs. 11.4%; p< 0.001). Moreover, the percentage of CBL-B^{hi}CD8$^+$ T cells that also co-expressed PD-1/CTLA-4 was significantly increased in treatment-naive AIH, as compared to healthy controls (31.9% vs. 0%; p< 0.0001), NASH (31.9% vs. 0%; p< 0.0001) or DILI (31.9% vs. 4.5%; p= 0.0076).

Furthermore, expression of CTLA-4 by CBL-B^{low}CD8$^+$ T cells was increased in treatment-naive AIH, as compared to healthy controls (22.8% vs. 0.8%; p< 0.0001) and NASH (22.8% vs. 1.0%; p< 0.0001). Furthermore, PD-1 expression in CBL-B^{low}CD8$^+$ T cells from treatment-naive AIH patients was significantly increased, as compared to healthy controls (30.7% vs. 6.3%; p< 0.0001), NASH (30.7% vs. 5.7%; p< 0.0001) or DILI patients (30.7% vs. 12.3% p< 0.02). Moreover, the percentage of CBL-B^{low}CD8$^+$ T cells that also co-expressed PD-1/CTLA-4 in treatment-naive AIH, were significantly elevated as compared to healthy controls (13.5% vs. 0.1%; p= 0.001) and NASH patients (13.5% vs. 0.6%; p= 0.005). However, ICOS

expression by CBL-B^hiCD8^+ or CBL-B^lowCD8^+ T cells was not significantly different in treatment-naive AIH patients, as compared to control groups (*figure 39*). Thus, a greater proportion of intrahepatic CBL-B^hiCD8^+ T cells or CBL-B^lowCD8^+ T cells also expressed CTLA-4, PD-1 or co-expressed PD-1/CTLA-4 in treatment-naive AIH, as compared to control groups. Moreover, we noticed that CBL-B^lowCD8^+ T cells had a lower expression of CTLA-4 (35.8% CBL-B^hiCD8^+ T cells vs. 22.8% CBL-B^lowCD8^+), PD-1 (42.8% CBL-B^hiCD8^+ T cells vs. 30.7% CBL-B^lowCD8^+) and co-expression of PD-1/CTLA-4 (31.9% CBL-B^hiCD8^+ T cells vs. 13.5% CBL-B^lowCD8^+), as compared to CBL-B^hiCD8^+ T cells. These results suggested that expression of CBL-B is associated with CTLA-4 and PD-1 expression.
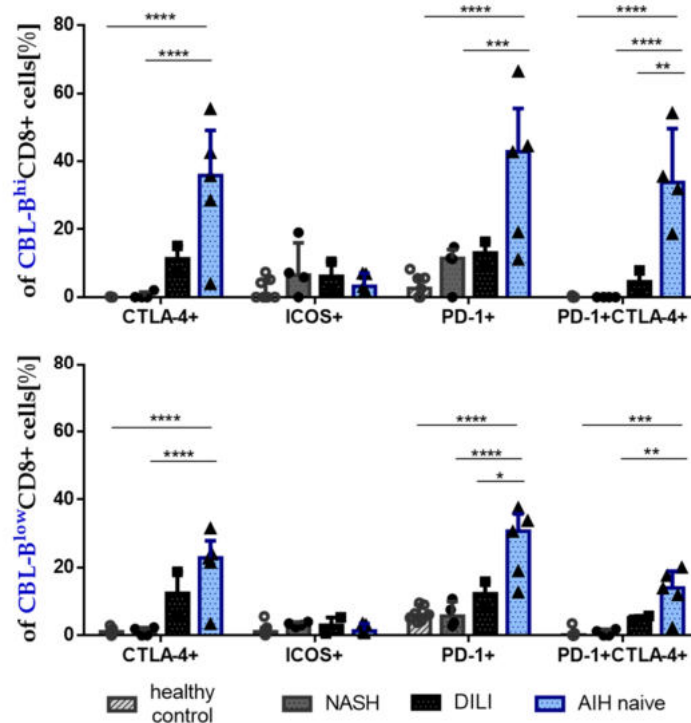
Figure 39 **Protein expression of CTLA-4, ICOS and PD-1 in liver- infiltrating CBL-B^hi or CBL-B^low CD8^+ T cells from treatment-naive AIH patients, healthy controls, NASH or DILI patients after anti-CD3/CD28 stimulation for 4 h.**

3.4.1 Peripheral blood T cells did not exhibit elevated levels of CBL-B, CTLA-4, PD-1 and ICOS in AIH

Having analysed CBL-B protein expression by liver-infiltrating CD3^{+} cells, we then analysed fresh peripheral blood T cells using flow cytometry. For this, CBL-B expression in peripheral blood CD4^{+} or CD8^{+} T cells of healthy control subjects (n= 8) was examined before and after stimulation with anti-CD3/CD28 antibodies. In healthy subjects, CBL-B expression was detected in 51.1% of the peripheral blood CD4^{+} T cells, but after stimulation, CBL-B expression was detected in only 0.3% of the peripheral blood CD4^{+} T cells (p= 0.002). Likewise, 42.3% of the peripheral blood CD8^{+} T cells in the healthy subjects expressed CBL-B protein before stimulation and after stimulation, only 0.2% of the peripheral blood CD8^{+} T cells (p= 0.002) expressed CBL-B (*figure 40*).

Furthermore, we analysed CBL-B expression in unstimulated peripheral blood T cells from AIH patients and control subjects to examine whether CBL-B expression was significantly different, as compared to control groups in absence of stimulation. For this we tested treatment-naive AIH patients (n= 3), patients under treatment with active AIH (n= 4; AST/ALT≥ 100, IgG> 16g/L) or inactive AIH (n= 7; AST/ALT≤ 100), AIH patients with liver cirrhosis (n= 5), healthy control subjects (n= 9), PSC (n= 10) and PBC (n= 6) patients. As assumed, in absence of stimulation, protein expression levels of CBL-B in peripheral blood CD4^{+} or CD8^{+} T cells did not significantly differ between healthy control subjects, treatment-naive AIH patients, AIH patients under treatment (active or inactive), AIH patients with liver cirrhosis, PSC and PBC patients (*figure 41*).
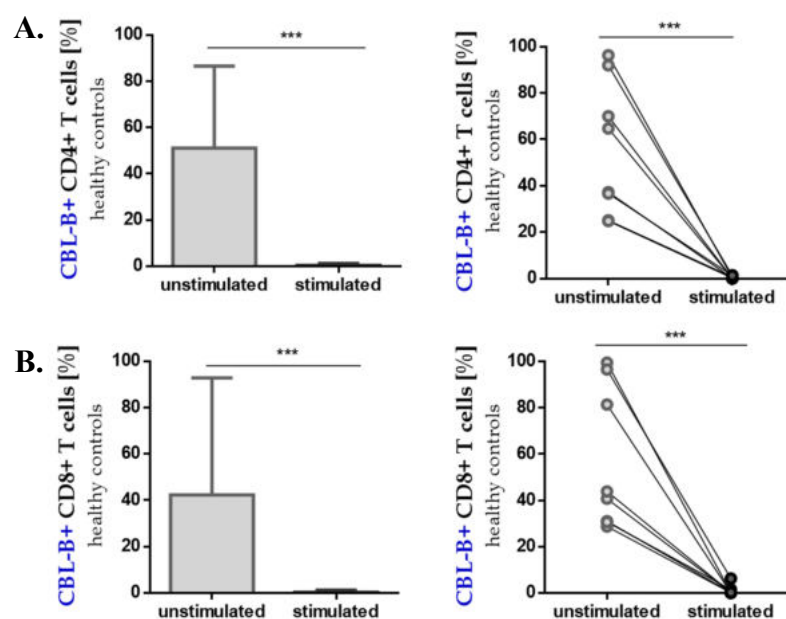
Figure 40 **CBL-B protein expression in unstimulated and stimulated peripheral blood CD4^{+} (A.) or CD8^{+} T cells (B.).** Peripheral blood T cells were from healthy control subjects. Stimulation was with anti-CD3/CD28 for 4 h.
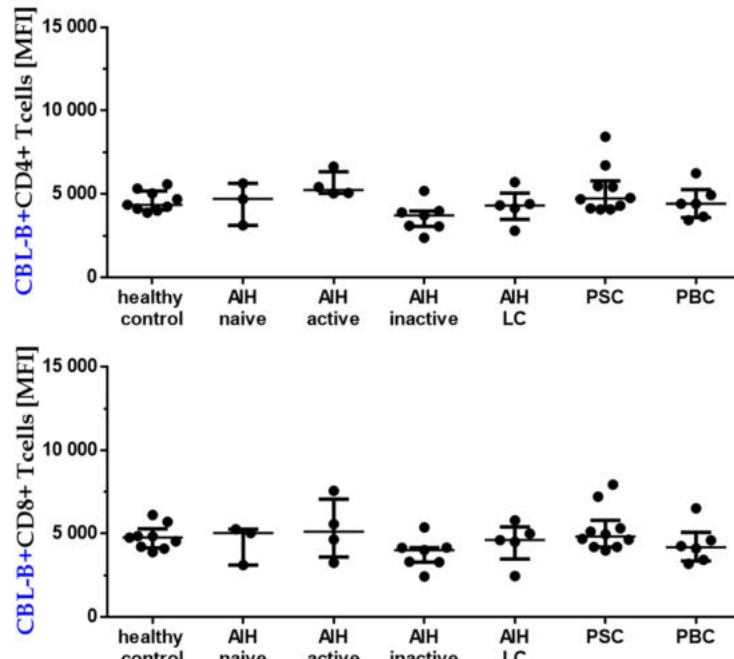
***Figure 41* CBL-B protein expression (mean fluorescence intensity) in unstimulated peripheral blood CD4⁺ or CD8⁺ T cells.** Peripheral blood T cells were from healthy control subjects, treatment- naive AIH patients, AIH patients under treatment (active or inactive), AIH patients with liver cirrhosis (LC), PSC and PBC patients.

Moreover, we examined CBL-B expression as well as CTLA-4, PD-1 and ICOS expression in peripheral blood T cells of treatment-naive AIH patients (n= 3), healthy control subjects (n= 9) or DILI patients (n= 4) after stimulation with anti-CD3/CD28 antibodies. After stimulation, levels of CBL-B expression in peripheral blood CD4⁺ or CD8⁺ T cells was not significantly different in treatment-naive AIH, as compared to healthy controls and DILI (*figure 42*). Furthermore, unlike intrahepatic T cells in treatment-naive AIH patients, the percentage of peripheral blood CD4⁺ or CD8⁺ T cells that expressed CTLA-4, ICOS or PD-1 in treatment-naive AIH, was similar as compared to healthy controls and DILI (*figure 43, 44*).

Based on the RNA screening results, we assumed that the analysis of the activation regulators CBL-B, CTLA-4, ICOS and PD-1 in peripheral blood T cells was not indicative of the intrahepatic T cell regulation in AIH. These results indicated that CBL-B protein expression in peripheral blood T cells of treatment-naive AIH patients was similar to that of healthy control subjects, whereas intrahepatic T cells of treatment-naive AIH patients exhibited an aberrant CBL-B protein expression pattern. Furthermore, the elevation in CTLA-4 and PD-1 expression after T cell stimulation was confined to intrahepatic T cells of treatment-naive AIH patients.
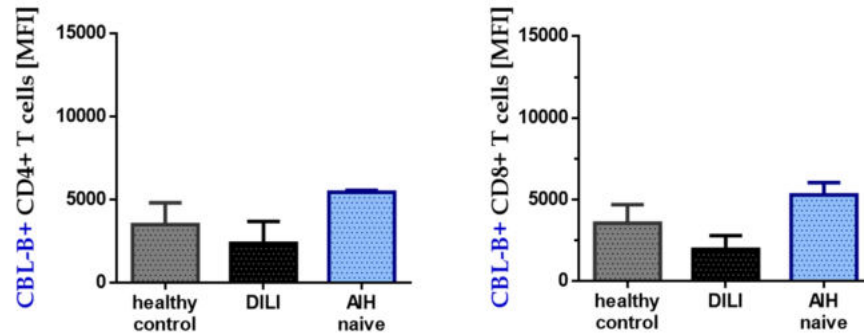
Figure 42 **CBL-B protein expression (mean fluorescence intensity) in peripheral blood CD4$^+$ or CD8$^+$ T cells of healthy control subjects, treatment-naive AIH patients and DILI patients after anti-CD3/CD28 treatment for 4 h.**
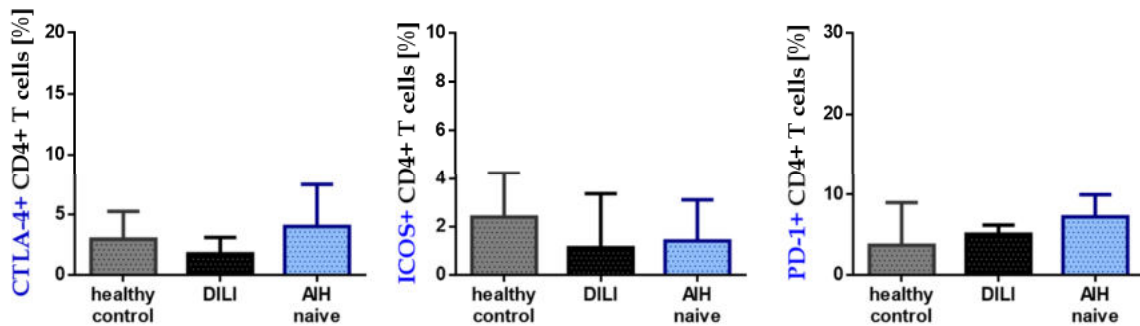
Figure 43 **CTLA-4, ICOS and PD-1 protein expression by peripheral blood CD4$^+$ T cells of healthy control subjects, treatment-naive AIH patients and DILI patients after anti-CD3/CD28 treatment for 4 h.**
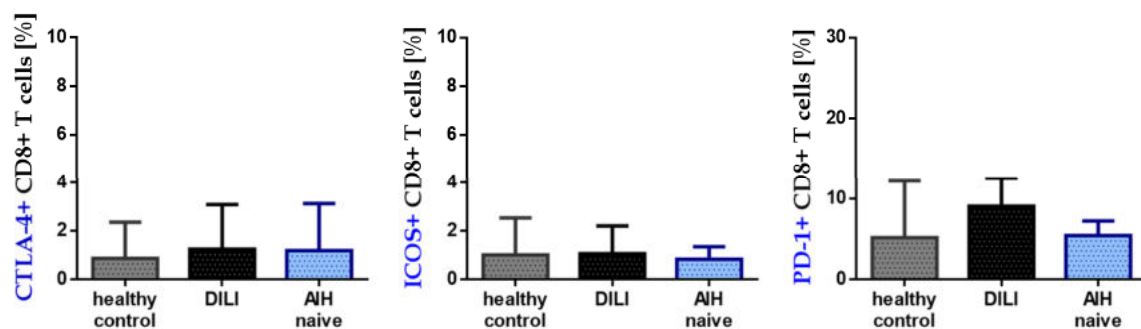
Figure 44 **CTLA-4, ICOS and PD-1 protein expression by peripheral blood CD8$^+$ T cells of healthy control subjects, treatment-naive AIH patients and DILI patients after anti-CD3/CD28 treatment for 4 h.**

3.5 Preliminary analysis of secretory cytokines of intrahepatic T cells in AIH

3.5.1 Intrahepatic expression of pro- inflammatory cytokines TNFα and IFNγ

The unusual expression pattern of T cell activation regulators in AIH could affect the secretion of cytokines by intrahepatic T cells. For this reason, typical pro-inflammatory cytokines produced by T cells, TNFα (or TNF) and IFNγ were examined in liver tissue samples from treatment-naive AIH patients, healthy controls and DILI patients. By use of real-time PCR, we detected that as compared to intrahepatic *TNF* expression in healthy controls, expression levels in liver tissue samples from treatment-naive AIH was significantly increased (14.7-fold expression; $p < 0.01$). Moreover, *TNF* expression in liver tissue samples from DILI patients were slightly up-regulated as compared to healthy controls (10.6-fold expression; not significant). However, intrahepatic expression of *TNF* was not significantly different between DILI and treatment-naive AIH patients. Furthermore, intrahepatic expression of *IFNγ* was slightly elevated in liver tissue samples of DILI (5.4-fold expression; not significant) and treatment-naive AIH patients (5.6-fold expression; not significant) as compared to healthy controls (*figure 45*). However, intrahepatic expression of *IFNγ* in liver tissue samples of treatment-naive AIH patients was similar as to DILI patients (5.6- vs 5.4-fold expression). This indicated that levels of *TNF* and *IFNγ* expression in liver tissue samples of treatment-naive AIH and DILI patients were not particularly different but deviated from normal expression levels.
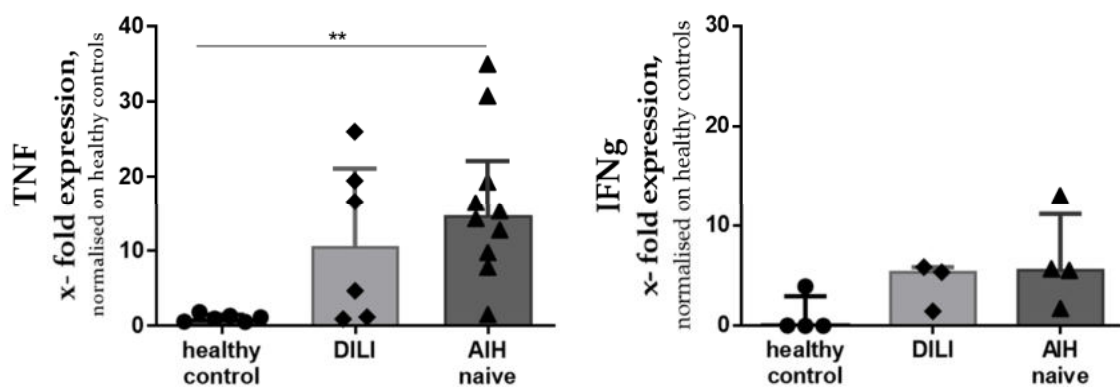
Figure 45 **Relative RNA expression of intrahepatic *TNF* or *IFNγ* in whole liver tissue samples.** *TNF* expression was detected in liver tissue sample from 6 healthy controls, 6 DILI and 10 patients with treatment- naive AIH patients. *IFN* expression in whole liver tissue was determined in 4 healthy controls, 3 DILI patients and 4 patients with treatment- naive AIH patients.

3.5.2 Expression of cytokines in stimulation supernatant

In the supernatants of the stimulation approaches of the previous analyses with intrahepatic T cells, the cytokines were determined to get a first impression whether there are differences in cytokine expression. However, it should be noted that cell mixtures are present in the stimulation approaches. Thus, the cytokine expression in the supernatant cannot be correlated with the CBL-B, CTLA-4, or PD-1 expression by the intrahepatic T cells. We examined TNF, IFNγ, IL-2, IL-6, IL-10, IL-13, IL-17A, IL-21 and TGFβ using enzyme linked immunosorbent assay (ELISA) and ELISA based multi-analyte immunoassay according to chapters 2.2.13.1 and 2.2.13.2. We tested healthy control subjects (n=3), patients with treatment-naive AIH (n= 5) and DILI patients (n= 2). After stimulation, similar quantities in pg/mL of IL-2, IL-13, IL-17A, IL-21 and TGFβ was determined in supernatant media of intrahepatic cells from healthy control subjects, treatment- naive AIH and DILI patients. However, TNF was slightly increased in supernatant of intrahepatic cells from DILI patients (26.6 pg/mL) or from treatment-naive AIH patients (26.8 pg/mL), as compared to healthy controls (9.3 pg/mL; not significant). Moreover, IFNγ was slightly elevated in supernatant of intrahepatic cells from treatment-naive AIH patients (2.2 pg/mL; not significant), as compared to healthy controls (1.2 pg/mL) or DILI patients (1.2 pg/mL). IL-6 secretion by intrahepatic cells derived from treatment-naive AIH (10.9 pg/mL) or DILI patients (10.4 pg/mL) was slightly elevated, as compared to healthy controls (3.1 pg/mL; not significant). Furthermore, IL-10 in supernatant media of intrahepatic cells from treatment-naive AIH patients (7.7 pg/mL; not significant) was slightly increased, as compared to healthy controls (4.6 pg/mL) and DILI patients (4.6 pg/mL; *figure 46, 47, 48*). Therefore, no striking secretory cytokine profile was detected in the supernatant after stimulation. However, detailed analyses of cytokine expression by intrahepatic T cells requires flow cytometric analyses after PMA/Ionomycin stimulation and Brefaldin A supplement.
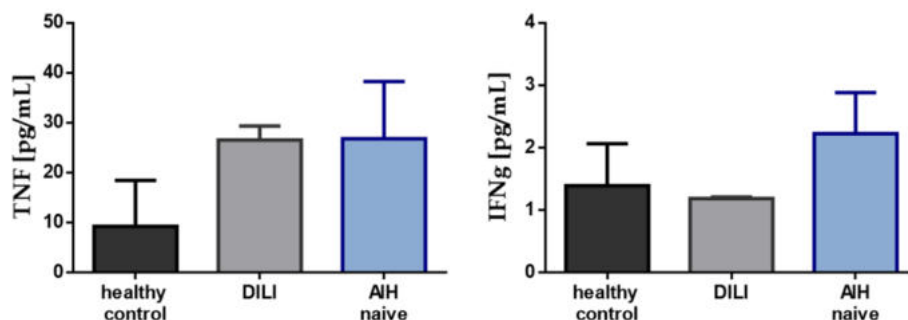
Figure 46 Secretion of TNF and IFNγ by intrahepatic cells from healthy control subjects, DILI patients and treatment-naive AIH patients after stimulation with anti-CD3/CD28. for 4 h.
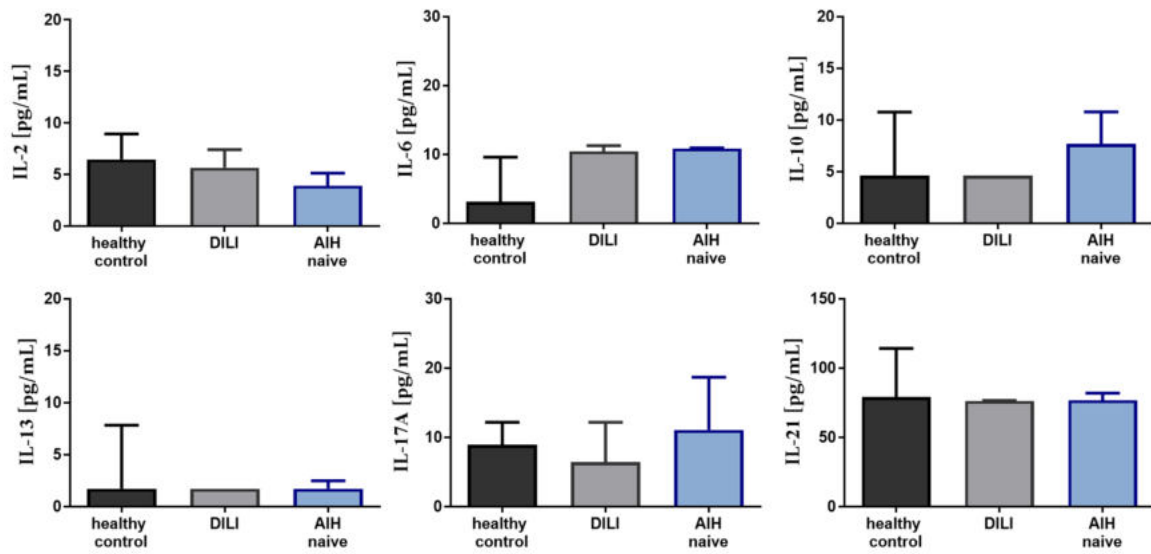
Figure 47 **Secretion of interleukins by intrahepatic cells from healthy control subjects, DILI patients and treatment- naive AIH patients after stimulation with anti-CD3/CD28 for 4 h.**
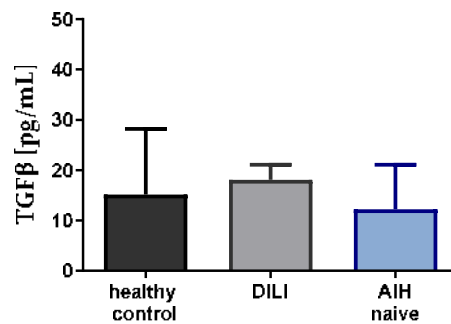
Figure 49 **Secretion of TGFβ by intrahepatic cells from healthy control subjects, DILI patients and treatment-naive AIH patients after stimulation with anti-CD3/CD28 for 4 h.**

4. Discussion

Autoimmune hepatitis (AIH) is a chronic inflammatory liver disease, which leads to liver fibrosis and severe liver damage. Only lifelong treatment with immunosuppressive drugs can prevent progression to liver cirrhosis and liver failure in AIH. The pathogenesis of AIH is unknow, however, activated T effector cells seem to play a key role in mediating hepatic inflammation. The activation threshold of T effector cells can be regulated by various molecules. Regulatory molecules of T cell activation may be altered in expression and thus, facilitate uncontrolled immune responses by T effector cells in patients with AIH. Therefore, the aim of this study was to investigate the expression of intrinsic regulatory molecules of T cell activation in peripheral blood and intrahepatic T effector cells of AIH patients. Furthermore, the aberrant expression of T cell activation regulatory molecules detected by this study, were analysed in their context to histological disease activity as well as to possible effects on T cell cytokine secretion. For this purpose, gene expression analyses were performed by use of quantitative real-time PCR and RNA *in-situ* hybridisation, and protein expression analyses were conducted using immunofluorescence and flow cytometry; cytokine release in culture media was measured by use of ELISA and ELISA based multi-analyte immunoassay. For these analyses, human liver tissue samples and human peripheral blood samples from AIH patients, healthy control subjects, DILI, NASH, PBC and PSC patients were tested.

4.1 T effector cells in AIH

In AIH, CD4^{+} T helper (Th) cells and cytotoxic CD8^{+} T cells (CTLs) formed the predominant population within the lymphocytic liver-infiltration. Moreover, Th cells and CTLs increased with histological disease severity [197]. It was postulated that the immune response in AIH was initiated upon recognition of self-antigenic peptides by TCR of uncommitted T cells [198, 199], thereby, CD4^{+} T cells become activated and differentiate into Th cell subsets, such as Th1, Th2 or Th17 cells, and CD8^{+} T cells mainly differentiate into CTLs upon activation. Th1 cells mainly secrete pro-inflammatory cytokines, like IFNγ and TNFα, which stimulate CTLs, recruit inflammatory macrophages and enhance MHC class I and II expression on hepatocytes, thereby they maintain inflammation [2, 197]. Furthermore, activated Th2 cells help autoantibody production by activated B cells, and activated CTLs augment liver damage through secretion of cytotoxic proteins [200]. It was suggested that liver-resident APCs, including liver sinusoidal endothelial cells and Kupffer cells, present hepato-specific self-antigen to both CD4^{+} and CD8^{+} T effector cells, hence, activated CD4^{+} and CD8^{+} T effector cells might obviate trafficking to the regional lymph nodes and breach self-tolerance [199, 201, 202]. However, the mechanisms

involved in the loss of self-tolerance in AIH remain uncertain [3, 204]. Furthermore, it is believed that the impairment of extrinsic or intrinsic immune regulation of activated T effector cells is partly responsible for the breakdown of self-tolerance to autoimmune liver antigens. Key to extrinsic immune regulation of T effector cells are Tregs [200]. Tregs which can develop in the thymus (thymus-derived Tregs, tTregs) or originate in the periphery (peripheral Tregs, pTregs), can suppress activated T effector cells in a cell-cell dependent or independent manner [205, 206]. Previous studies investigated quantities and functional capacities of Tregs in AIH, suggesting that Tregs were unable to exert inhibiting effects on pathogenic activities of autoreactive T effector cells. [207, 208]. However, as some studies confirmed both deficiency in number and function of Tregs in AIH patients [209, 210, 211], others failed to verify these findings [197, 23]. Moreover, Tregs were found to be increased in patients with active AIH, as compared to those in AIH patients who were in remission [23]. While extrinsic immune regulation might not be impaired in AIH, impairment of intrinsic immune regulation by regulatory molecules of T cell activation might lead to unresponsiveness to extrinsic immune regulation and consequent autoimmune liver damage. However, previous studies have not yet examined intrinsic immune regulatory molecules of T effector cells.

In this study, we identified altered gene expression of T cell activation regulators CBL-B, CTLA-4, ICOS and PD-1 in intrahepatic T effector cells of treatment-naive AIH patients, but not in peripheral blood T cells. Moreover, intrahepatic *CBL-B* expression positively correlated with histological disease activity in AIH patients. Furthermore, intrahepatic T cells expressing *CBL-B* or *CTLA-4* were directly associated with hepatic inflammatory activity in treatment-naive AIH. In addition, intrahepatic $ICOS^+CD4^+$ T helper cells as well as $CTLA4^+CD8^+$ and $PD1^+CD8^+$ T cells of treatment-naive AIH patients were enriched upon stimulation with anti-CD3 and anti-CD28 antibodies. Furthermore, CBL-B protein expression was increased in intrahepatic T cells of treatment-naive AIH patients. These findings indicated an aberrant expression of intrinsic regulatory molecules of T cell activation in AIH.

4.2   CBL-B expression in active AIH

CBL-B is an E3 ubiquitin ligase of the RING finger-type family that targets various molecules for posttranslational modification or proteasomal degradation. CBL-B is believed to play a role in the induction of T cell anergy [212, 213, 214], a peripheral T cell tolerance mechanism to regulate self-reactive T cells in peripheral homeostasis. The majority of autoreactive T cells are eliminated by negative selection during T cell maturation in the thymus. However, some self-reactive T cells are not eliminated in the thymus, requiring control by peripheral tolerance

mechanisms, including deletion of self-reactive T cells through apoptosis, intrinsic inactivation of self-reactive T cell functions (anergy) or suppression by Tregs [215, 216, 217]. It was reported that the induction of T cell anergy by TCR stimulation in the absence of CD28 co-stimulation is associated with the up-regulation of CBL-B, which seems to be caused by calcium ion (Ca^{2+}) influx and activation of NFAT in the absence of concomitant activation of transcription factor AP1 [218, 219]. As a consequence, the Zinc finger transcription factors Egr-2 and Egr-3 are activated, leading to up-regulation of CBL-B [220]. CBL-B is also known to negatively regulate T cell activation by interfering and prohibiting TCR and co-receptor CD28 induced signalling pathways [164]. Thereby, CBL-B negatively regulate signalling proteins, such as ZAP70, PI3K and PLC-γ1 [166, 221]. Moreover, it was reported that CBL-B can modulate Vav-1, thereby, inhibiting TCR clustering and T cell proliferation [222].

Murine studies showed that ablation of CBL-B in T cells facilitated lymphocytic infiltration of multiple organs linked to highly reactive T cells [165, 223, 224] and *CBL-B* deficient T cells could escape immune regulation through loss of self-tolerance and sensitivity to Tregs and TGFβ [225, 226]. Notwithstanding these findings in mice, the human data shown here indicated that peripheral blood T cells featured *CBL-B* and inflamed livers of treatment-naive AIH patients exhibited elevated levels of *CBL-B* expression. However, AIH patients owned autoreactive T effector cells, which maintained hepatic inflammation and liver injury [194, 197]. Thus, the high reactivity of the T effector cells in AIH could not be accounted by CBL-B up-regulation but instead, *CBL-B* up-regulation might be a form of counter-regulation to compensate for insufficient CBL-B function.

We observed that the majority of peripheral blood CD4^{+} or CD8^{+} T cells in healthy subjects expressed CBL-B protein before stimulation; after stimulation, however, CBL-B expression was significantly reduced. Likewise, CBL-B protein expression was also detected in liver-infiltrating CD4^{+} or CD8^{+} T cells of healthy control subjects before stimulation, and significantly reduced CBL-B expression was found after stimulation. Thus, CBL-B protein expression in CD4^{+} or CD8^{+} T cells was reduced as a consequence of T cell stimulation. Consistent with previous mouse studies, our human data showed high CBL-B protein expression in peripheral blood T cells [221]. Moreover, our data was in accordance with the findings of Zhang and associates [227], who studied CBL-B ubiquitination in unstimulated or stimulated splenic T cells of wildtype (wt) BALB/c mice by use of immunoprecipitation and Western blot. They observed that CBL-B was associated with ubiquitin molecules after anti-CD3 antibodies stimulation alone, however, stimulation with anti-CD3 and anti-CD28 antibodies significantly increased ubiquitination of CBL-B in T cells. Thus, CBL-B protein

degradation was increased after T cell-specific stimulation with anti-CD3 and anti-CD28 antibodies in mice. Accordingly, the T cells from healthy individuals studied here showed a similar CBL-B degradation after stimulation with anti-CD3 and anti-CD28 antibodies. Moreover, after T cell-specific stimulation with anti-CD3 and anti-CD28 antibodies, peripheral blood T cells from treatment-naive AIH patients showed a similarly low CBL-B protein expression as that of healthy T cells. However, intrahepatic T cells from treatment-naive AIH patients maintained high levels of CBL-B protein expression after stimulation, which was consistent with our findings in gene expression analyses. Thus, our data suggested that the degradation of CBL-B protein expression in intrahepatic T cells of treatment-naive AIH patients was disturbed.

CBL-B is targeted for degradation by protein kinase C (PKCθ) and neural precursor cell expressed developmentally down-regulated protein 4 (NEDD4). In response to CD28 co-stimulation, PKCθ inactivates CBL-B through phosphorylation and thereby, promotes its degradation [228]. NEDD4 is an E3 ubiquitin ligase of the HECT-type family, which targets CBL-B protein for polyubiquitination and subsequent degradation [174]. Moreover, Gruber and associates discussed that PKCθ phosphorylated CBL-B upon TCR and CD28 stimulation, and thereby, facilitated CBL-B ubiquitination by NEDD4 [176]. One could thus hypothesise that the disturbed degradation of CBL-B in intrahepatic T cells of AIH patients might be linked to decreased expression of *PKCθ* or *NEDD4*. Thus, both genes that encode for either PKCθ or NEDD4 were included in the gene expression analyses in this study. However, expression levels of *PKCθ* and *NEDD4* in liver tissue samples of treatment-naive AIH patients and patients under immunosuppressive treatment were not considerably different as compared to healthy controls and other control subjects. Hence, our data indicated that reduced intrahepatic expression of *PKCθ* or *NEDD4* was not responsible for disturbed CBL-B degradation in treatment-naive AIH patients. This finding suggests that a mechanism distinct from *PKCθ* or *NEDD4* was responsible for the maintenance of high CBL-B levels by activated intrahepatic T cells of treatment-naive AIH patients. Possibly, CBL-B maintenance could be a cellular adaptation to the inflammatory hepatic environment in order to enhance the intrinsic inhibitory regulation of autoreactive T cells.

Increased expression of CBL-B protein by T effector cells was previously reported in self-antigen-induced anergic CD4$^+$ T cells of wt mice [229]. This was consistent with studies that found increased levels of CBL-B expression in anergic mouse T cells [220, 223]. Furthermore, it was reported that increased levels of CBL-B protein expression were found in peripheral blood mononuclear cells (PBMCs) of patients with human immunodeficiency virus (HIV)-

infection, and PBMCs were detected to be deficient in proliferation in HIV patients. It was discussed whether elevated levels of CBL-B were partly responsible for unresponsiveness of HIV-infected CD4$^+$ and CD8$^+$ T cells, and whether CBL-B might account for reduced cellular proliferation [219, 230]. In other infections with chronic immune activation, such as helminth infections, increased CBL-B expression was associated with T-cell hypo-responsiveness in chronically infected patients [231]. In accordance to these studies, our data showed high levels of CBL-B protein expression by intrahepatic T cells in active AIH; a liver disorder with chronic immune activation. However, contradicting to these previous studies, patients with active AIH possessed highly proliferative, intrahepatic T cells with pathogenic autoreactivity [194, 197]. Moreover, this suggested that intrahepatic T cells in active AIH were not anergic, despite increased levels of CBL-B protein expression. Consequently, CBL-B was impaired in intrahepatic T cells from active AIH patients and therefore, further investigation of CBL-B and its interference in intracellular signalling within intrahepatic T cells from active AIH patients is necessary.

4.3   CTLA-4, PD-1 and their association with CBL-B in active AIH

Both CTLA-4 and PD-1 encode for inhibitory T cell co-receptors, which by ligation with appropriate ligands induce downstream signalling that leads to an increase of the T cell activation threshold. Upon TCR stimulation, nuclear factor of activated T cells (NFAT2) induces PD-1 expression [145, 146, 232, 233]. In T cells other than Tregs, CTLA-4 protein expression is induced in response to TCR and CD28 co-stimulation [128]. In this study, we showed that intrahepatic expression of *CTLA-4* or *PD-1* was elevated in treatment-naive AIH patients; moreover, T cells from treatment-naive AIH patients responded to T cell stimulation with an increase in numbers of CTLA-4$^+$CD4$^+$ T cells, CTLA-4$^+$CD8$^+$ and PD-1$^+$CD8$^+$ T cells. Our data was in accordance with Oikawa and associates, who reported that PD-1 expressing T cells were accumulated within the portal tracts in patients with AIH [234]. Moreover, the group of Agina investigated hepatic expression of PD-1 in children with AIH in comparison with HCV-infected children, and they detected that the intrahepatic expression of PD-1 protein was significantly increased in paediatric AIH patients as compared to HCV-infected individuals [235]. In addition, our data was consistent with the findings of Kassel *et al.*, who observed that PD-1 expression on intrahepatic lymphocytes positively correlated with hepatic inflammation in AIH patients [236]. In this respect, we assumed that PD-1$^+$CD8$^+$ T effector cells contributed to the hepatocellular damage in active AIH patients and therefore, these cells were highly autoreactive in AIH. Kassel *et al*. also detected that hepatocytes highly expressed MHC class I

molecules (HLA-A/B/C) and PD-1 ligand (PD-L1) in active AIH patients. They suggested that increased expression of MHC class I molecules and PD-L1 by hepatocytes could be mainly due to the ongoing hepatic inflammation and exposure to inflammatory cytokines secreted by T effector cells, Kupffer cells and liver sinusoidal endothelial cells (LSECs) [236]. In accordance with Kassel *et al.* and other previous findings [237], we considered that the PD-1 signalling pathway was disturbed in active AIH patients, because we assumed that PD-1/ PD-L1 ligation should have actually lead to the suppression of activated PD-1$^+$CD8$^+$ T effector cells; however, this was not the case. Therefore, it is possible that the loss of intrinsic co-inhibitory regulation contributed to the pathogenic autoreactivity of intrahepatic CD8$^+$ T cells.

Previous studies showed that in patients with acute viral hepatitis infection, elevated expression of CTLA-4 and PD-1 associated with dysfunctional virus-specific T cells. Moreover, human hepatitis B or C (HBV or HCV)-specific T cells expressed elevated levels of CTLA-4 and PD-1, and were functionally impaired [238, 239, 240, 241, 242, 243]. Furthermore, expression of CTLA-4 and PD-1 by intrahepatic HCV or HBV-specific T cells was found to be increased as compared to that in circulating T cells; in addition, CTLA-4 and PD-1 expression positively correlated with impaired intrahepatic T cells [244, 245]. Therefore, it was suggested that in active HCV- or HBV-infected patients, viral-specific T cells were functionally exhausted as they showed up-regulated CTLA-4 and PD-1 expression [244, 245]. It is known that during chronic infections, such as HBV or HCV, T cells are consistently stimulated because of persistent antigen exposure. In such setting, T cells become exhausted and accordingly up-regulate co-inhibitory receptors, like CTLA-4 and PD-1. T cell exhaustion results in a dysfunctional state of T cells with inadequate effector functions [246, 247, 248].

In active AIH, intrahepatic T cells are not likely to exhibit an exhausted phenotype since they show hyper-reactivity and mediate hepatic inflammation and damage [217]. Thus, we suggested that intrahepatic CTLA-4$^+$CD4$^+$ T cells, CTLA-4$^+$CD8$^+$ and PD-1$^+$CD8$^+$ T cells were activated, but not exhausted in patients with active AIH. Accordingly, the work of Petrelli *et al.* evaluated the presence of PD-1$^+$CD8$^+$ T cells in synovial fluid of patients with juvenile idiopathic arthritis (JIA), a chronic inflammatory disease [249]. They detected that highly activated PD-1$^+$CD8$^+$ T cells were proliferative and enriched at the site of inflammation in JIA patients. Moreover, based on gene expression profiling (gene set enrichment analysis, GSEA) and functional studies, they identified PD-1$^+$CD8$^+$ T cells as functional effector cells with no exhaustion profile in JIA. Therefore, we assumed that enhanced expression of *CTLA-4* and *PD-1* by intrahepatic T cells from treatment-naive AIH patients could result from continual T cell

stimulation. Nevertheless, elevated expression of CTLA-4 or PD-1 by intrahepatic T cells could be a counter-regulation to compensate for CTLA-4 or PD-1 dysfunction.

The work of Li and colleagues reported that CBL-B and CTLA-4 protein expression was associated [133]. The authors investigated CBL-B expression in T cells of wt BALB/c mice, CD28 knockout (KO) or CTLA-4 KO mice after stimulation with anti-CD3 antibodies and B7-1Ig. They showed that TCR stimulation and CD28 co-stimulation induced the degradation of CBL-B in wt T cells; however, CTLA-4 expression and its ligation with B7 promoted re-expression of CBL-B protein. Moreover, the expression of CBL-B was diminished in T cells of CTLA-4 KO [133]. Furthermore, Leng *et al*. found that T cells in chronically immune-activated individuals associated with increased levels of CTLA-4 and CBL-B. The group also proposed that increased CTLA-4 expression probably induced high levels of CBL-B expression [250]. In addition, previous studies investigated the association of PD-1 with CBL-B and they observed that interaction between PD-1 and PD-L1 induced the up-regulation of CBL-B expression in murine T cells [250, 251, 252].

Thus, it was previously described that the interaction of CTLA-4 and PD-1 were involved in the up-regulation of CBL-B expression in T cells. Accordingly, our human data shown here suggested that increased CBL-B expression might be associated with elevated CTLA-4 or PD-1 expression in intrahepatic T cells of treatment-naive AIH patients. Therefore, we suspected that the aberrant expression of CTLA-4, PD-1 and CBL-B in active AIH were interrelated. However, whether the aberrant expression of CBL-B, CTLA-4 and PD-1 in intrahepatic T cells is cause or consequence of AIH pathogenesis needed further investigation.

4.4   ICOS

ICOS is a T cell co-stimulatory receptor, which is induced upon T cell activation and it is expressed mainly on T helper cells. Previous studies with *in-vivo* mouse models showed that ICOS is involved in the immune response of different T helper cell subsets, in particular Th1 and Th2 cells, against various infections, such as *Mycobacterium tuberculosis or Chlamydia muridarum* infection [121]. Thus, ICOS plays a relevant role in Th cell activation. Moreover, the work of Löhning *et al*. described that ICOS expression in secondary lymphoid tissue was mainly restricted to inflammatory CD4$^+$ T effector cells [253]. Furthermore, previous studies in mice suggested that elevated *ICOS* gene expression in T cells and failure to degrade *ICOS* expression promoted the development of autoimmune phenotypes [254, 255]. In this study, we found that in response to T cell-specific stimulation, intrahepatic ICOS$^+$CD4$^+$ T cells from treatment-naive AIH patients were increased as compared to those from healthy controls, which

was in accordance with previous findings. However, in comparison to other liver diseases, such as DILI and NASH, the expression of ICOS protein by intrahepatic CD4$^+$ T cells was not significantly different. Thus, it seemed that ICOS$^+$CD4$^+$ T effector cells were activated Th cells that contributed to the intrahepatic inflammation in active AIH. However, we assumed that the increased numbers of ICOS$^+$CD4$^+$ T effector cells were not disease-specific but rather an indication of ongoing inflammation in treatment-naive AIH patients.

4.5   Cytokine expression in AIH

Cytokine secretion by inflammatory lymphocytes, in particular liver-infiltrating T effector cells may contribute to the disease pathogenesis of AIH by perpetuating inflammation. Early studies showed that the serum levels of IFNγ, TNFα, IL-1β and IL-6 were increased in patients with chronic hepatitis [256]. Moreover, serum levels of IFNγ, TNFα, IL-6 and IL-8 were elevated in children with AIH [257]. Furthermore, increased production of IFNγ, TNFα, IL-6 and IL-8 was detected in the microenvironment of diseased livers [258, 259]. A recent study reported that the frequency of TNFα-expressing CD4$^+$ T cells was increased in liver and blood of AIH patients; furthermore, TNFα$^+$CD4$^+$ T cells expressed IFNγ [260]. Moreover, anti-TNFα agents were used for treatment of patients with AIH, Crohn's disease and ulcerative colitis to reduced damaging inflammatory immune responses [261, 262]. However, treatment with TNFα-antagonists has also been associated with liver injury [263]. Behfarjam *et al*. observed that the gene expression of *interleukin-17A* (*IL-17A*), *interleukin-22* (*IL-22*) and *retinoic acid receptor-related orphan receptors gamma* (*RORγt*) in PBMCs of AIH patients was increased as compared to healthy control subjects [264]. Moreover, Zhao and associates detected that the serum levels of IL-17 and IL-23 were increased in AIH patients in comparison to chronic HBV-infected patients or healthy control subjects [265]. They also showed that numbers of IL-17$^+$ cells were elevated in livers from AIH patients as compared to HBV patients and healthy controls. RORγt is the master transcription factor for Th17 cells, which produce IL-17 and IL-22, and IL-23 promote the maintenance of Th17 cells [266, 267, 268]. Therefore, it was proposed that Th17-related cytokines might play an essential role in the pathogenesis of AIH. Moreover, Th17 cells have been associated with other autoimmune liver disease, including PBC [269]. However, IL-17 can be produced by non-T cells, including natural killer (NK) cells [270].

Consistent with previous studies, our human data showed that intrahepatic expression of *TNFα* was increased in livers from treatment-naive AIH patients as compared to healthy control subjects; however, it was similar to that in livers of DILI patients. Likewise, intrahepatic expression of *IFNγ* was elevated in both treatment-naive AIH patients or DILI patients, as

compared to healthy controls. In addition, our preliminary analyses with Enzyme-linked immunosorbent assay (ELISA) showed that after T cell-specific stimulation, the expression of TNFα, IFNγ, IL-6 or IL-10 was not significantly different, but slightly up-regulated in supernatant of intrahepatic T cells from treatment-naive AIH, as compared to healthy controls. Thus, we suggested that the cytokine expression of TNFα and IFNγ could not be considered as AIH disease-specific but might be related to liver injury. Thus, it remains to be determined whether AIH is linked to a distinct cytokine pattern or a distinct T helper cell response. However, it should be considered that other inflammatory cells, distinct from T cells, can also produce considerable amounts of cytokines, making it difficult to link serum cytokine levels to distinct cytokine-producing cells.

4.6   Future prospects

I.   *Cytokine expression by intrahepatic T cells in AIH*

It is of great interest to further characterise AIH T cells with respect to intracellular cytokine production and intrinsic activation regulators by use of multi-colour flow cytometry. By the currently available flow cytometers, we are limited in the number of parameters that can be simultaneously detected. Recently developed instruments will allow for concomitant detection of several parameters in the near future. By doing so, we will be able to verify that intrahepatic T cells of treatment-naive AIH patients express pro-inflammatory cytokines despite impaired expression of CBL-B. Furthermore, by extending the staining panel with antibodies against T cell proteins that are related to T cell exhaustion such as CD39, we can examine and possibly prove that intrahepatic PD-1$^+$ or CTLA-4$^+$ T cells of treatment-naive AIH patients are not exhausted and produce cytokines. In addition, assessing the cytokine production and transcription factors in intrahepatic T cells could facilitate the identification of CD4$^+$ and CD8$^+$ T cell subtypes.

II.   *Functional analysis with anti-PD-1 and anti-CTLA-4*

We would like to examine the functional association of CBL-B, CTLA-4 and PD-1 protein expression in intrahepatic T cells of treatment-naive AIH patients. In this study, we suggested that increased CBL-B expression in intrahepatic T cells of treatment-naive AIH patients might associate with enhanced CTLA-4 and PD-1. By use of anti-PD-1 with or without anti-CTLA-4 in stimulation approaches, we can further analyse whether increase of CBL-B expression is uncoupled from CTLA-4 and PD-1 interacting with their ligands. For this purpose, we can use multi-colour flow cytometry.

*III.	Limitations for future projects*

In this study, we applied human blood cells and human liver tissue samples from AIH, DILI, NASH, PBC and PSC patients. Future analyses would also base on human liver tissue samples of AIH, DILI, NASH, PBC and PSC patients, which are a limiting factor to this project. The limitations are not only that the biopsy samples of untreated patients are rare, but also that the numbers of liver-infiltrating cells that can be obtained from a biopsy are few. Another limitation, as mentioned above, is the access to multi-colour flow cytometer that supports staining panels of more than fourteen fluorescent staining dyes in one panel.

5.   Summary

Autoimmune hepatitis (AIH) is a chronic inflammatory liver disease with unknown aetiology and pathogenesis. Highly activated T effector cells seem to play a central role in the immunopathogenesis of AIH by mediating the inflammatory immune responses in the liver. In this study, we hypothesise that altered expression of T cell co-stimulation or co-inhibition may account for the disproportionate T cell activation in AIH, leading to improper monitored T cell immune responses. The aim of this study was to analyse various intrinsic regulatory molecules of T cell activation in peripheral blood and in livers of patients with AIH. For this purpose, we investigated expression levels of CBL-B, CTLA-4, GRAIL, ICOS, ITCH, NEDD4, OX40, PD-1, PKCθ and TRAF6 in liver and blood of treatment-naive AIH patients (n= 42) and AIH patients under immunosuppressive treatment (n= 37) in comparison with healthy controls (n= 44), patients with other autoimmune-mediated liver diseases such as PBC (n= 13) or PSC (n=18), and with patients with non-autoimmune liver disorders such as DILI (n= 35) or NASH (n= 17). By use of quantitative real-time PCR screening, we identified that expression of *CTLA-4*, *PD-1* and *ICOS* were significantly increased in liver tissue samples of treatment-naive AIH patients in comparison with control groups. Moreover, intrahepatic expression of *CBL-B, PD-1* and *CTLA-4* in AIH patients correlated positively with the modified hepatic activity index (mHAI) of these patients, suggesting that with an increase of intrahepatic disease activity, expression levels of *CBL-B*, *CTLA-4*, *ICOS* and *PD-1* were also increased. Furthermore, intrahepatic expression of *CBL-B* positively correlated with serum levels of aspartate- or alanine-aminotransferase (AST or ALT), indicating that intrahepatic expression of *CBL-B* increases with liver injury and hepatic disease activity in patients with AIH. In contrast, *CTLA-4*, *PD-1* and *ICOS* expression in peripheral blood T cells of treatment-naive AIH patients was similar to that in control groups. With RNA *in-situ* hybridisation we confirmed the findings of the gene expression analyses. Moreover, we identified that liver-infiltrating T cells and not CD3$^-$ cells in hepatic portal areas of treatment-naive AIH patients, showed increased expression levels of *CBL-B*, *CTLA-4*, *ICOS* and *PD-1* as compared to those of DILI patients and AIH patients under treatment. Furthermore, expression of *CBL-B* or *CTLA-4* in liver-infiltrating T cells of treatment-naive AIH patients positively correlated with disease activity expressed as mHAI. Flow cytometric analyses revealed that in contrast to intrahepatic T cells of healthy controls, NASH or DILI patients, the normally occurring reduction of CBL-B protein expression after anti-CD3/CD28 stimulation was not reduced in intrahepatic T cells of treatment-naive AIH patients. Moreover, intrahepatic T cells from treatment-naive AIH patients responded to stimulation with an increase in numbers of CTLA-4$^+$CD4$^+$ T cells, CTLA-4$^+$CD8$^+$

and PD-1$^+$CD8$^+$ T cells, as compared to healthy controls, DILI or NASH patients. Intrahepatic ICOS$^+$CD4$^+$ T cells of treatment-naive AIH patients were increased compared to those from healthy controls but not considerably different compared to DILI or NASH patients. We also showed that expression of CTLA-4 and PD-1 by CBL-B^{hi} T cells of treatment-naive AIH patients significantly differed as compared to control groups. To conclude, we identified aberrant expression of co-inhibitory T cell activation regulators CBL-B, CTLA-4 and PD-1 in intrahepatic but not in peripheral blood T effector cells in active AIH. Whether this is a counter-regulation against the increased activation of the intrahepatic T cells and to what extent this altered expression affects the intracellular cytokine production of the intrahepatic T cells, has to be further investigated. However, these molecules are potential biomarkers of disease activity and worthwhile objects of further study.

(German/Deutsch)

Die Autoimmune Hepatitis (AIH) ist eine chronisch entzündliche Lebererkrankung mit unbekannter Ätiologie und Pathogenese. Hochaktivierte T-Effektorzellen scheinen eine zentrale Rolle in der Immunpathogenese der AIH zu spielen, indem sie die Entzündung in der Leber vorantreiben. Unsere Hypothese ist, dass eine veränderte T-Zell Co-Stimulation oder Co-Inhibition für die überproportionale T-Zell-Aktivierung bei AIH verantwortlich ist und dies zu einer gestörten T-Zell-Immunantwort in AIH führt. Ziel dieser Arbeit war es, verschiedene intrinsische regulatorische Moleküle der T-Zell-Aktivierung im peripheren Blut und in der Leber von atienten mit AIH zu analysieren. Zu diesem Zweck untersuchten wir CBL-B, CTLA-4, GRAIL, ICOS, ITCH, NEDD4, OX40, PD-1, PKCθ und TRAF6 in Leber und Blut von noch unbehandelten AIH-Patienten (n= 42) und AIH-Patienten unter immunsuppressiver Behandlung (n= 37) im Vergleich zu gesunden Kontrollen (n= 44), Patienten mit anderen autoimmunvermittelten Lebererkrankungen, wie PBC (n= 13) oder PSC (n=18) und Patienten mit nicht-autoimmunen Lebererkrankungen, wie DILI (n= 35) oder NASH (n= 17). Mithilfe des quantitativen Echtzeit-PCR-Screenings konnten wir feststellen, dass die Expression von *CTLA-4*, *PD-1* und *ICOS* in Lebergewebeproben von unbehandelten AIH-Patienten im Vergleich zu Kontrollgruppen signifikant erhöht war. Darüber hinaus korrelierte die intrahepatische Expression von *CBL-B*, *PD-1* und *CTLA-4* bei AIH-Patienten positiv mit dem modifizierten Leberaktivitätsindex (mHAI) dieser Patienten, was darauf hindeutet, dass mit einer Zunahme der intrahepatischen Krankheitsaktivität auch die Expressionsniveaus von *CBL-B*, *CTLA-4*, *ICOS* und *PD-1* anstiegen. Des Weiteren korrelierte die intrahepatische Expression von *CBL-B* positiv mit den Serumwerten der Aspartat- oder Alanin-aminotransferase (AST oder ALT), was darauf hinweist, dass die intrahepatische Expression von *CBL-B* mit der Leberschädigung bei AIH Patienten zunimmt. Im Gegensatz dazu war die Expression von *CTLA-4*, *PD-1* und *ICOS* in peripheren Blut-T-Zellen von unbehandelten AIH-Patienten, derjenigen der Kontrollgruppen ähnlich. Mit der RNA-*in-situ*-Hybridisierung haben wir die Ergebnisse der Genexpressionsanalysen bestätigt. Zusätzlich haben wir festgestellt, dass die Leber-infiltrierenden T-Zellen und nicht die CD3⁻ Zellen, in hepatischen Portalfeldern von unbehandelten AIH-Patienten eine erhöhte Expression von *CBL-B*, *CTLA-4*, *ICOS* und *PD-1* im Vergleich zu DILI-Patienten und AIH-Patienten in Behandlung zeigten. Darüber hinaus korrelierte die Expression von *CBL-B* oder *CTLA-4* in Leber-infiltrierenden T-Zellen von unbehandelten AIH-Patienten positiv mit der histologischen Krankheitsaktivität (mHAI). Durchflusszytometrische Analysen ergaben, dass die CBL-B-Proteinexpression bei

intrahepatischen T-Zellen von unbehandelten AIH-Patienten nach anti-CD3/CD28-Stimulation nicht reduziert wurde, im Gegensatz zu gesunden Kontrollen, NASH- oder DILI-Patienten, bei denen die Stimulation eine deutliche Reduktion der CBL-B-Proteinexpression bewirkte. Des Weiteren reagierten intrahepatische T-Zellen von unbehandelten AIH-Patienten auf die Stimulation mit einer Zunahme von CTLA-4$^+$CD4$^+$ T-Zellen, CTLA-4$^+$CD8$^+$ und PD-1$^+$CD8$^+$ T-Zellen im Vergleich zu gesunden Kontrollen, DILI- oder NASH-Patienten. Intrahepatische ICOS$^+$CD4$^+$ T-Zellen von unbehandelten AIH-Patienten waren im Vergleich zu denen aus gesunden Kontrollen erhöht, unterschieden sich jedoch nicht wesentlich von denjenigen bei DILI- oder NASH-Patienten. Wir zeigten auch, dass sich die Expression von CTLA-4 und PD-1 durch CBL-B^{hi} T-Zellen von unbehandelten AIH-Patienten im Vergleich zu Kontrollgruppen signifikant unterscheidet. Zusammenfassend konnte eine abweichende Expression der intrinsischen T-Zell-Aktivierungsregulatoren CBL-B, CTLA-4 und PD-1 in intrahepatischen, jedoch nicht in peripheren Blut-T-Effektorzellen in aktiven AIH festgestellt werden. Ob dies eine Gegenregulation zur erhöhten Aktivierung der intrahepatischen T-Zellen war und inwieweit diese veränderte Expression die intrazelluläre Zytokinproduktion der intrahepatischen T-Zellen beeinflusste, muss weiter untersucht werden. Diese Moleküle eignen sich jedoch als potentielle Biomarker der Krankheitsaktivität und sollten Objekt weiterführender Studien sein.

6.   Appendix

6.1   References

1. **Krawitt EL**. Clinical features and management of autoimmune hepatitis. World J Gastroenterol, June 2008; 14(21): 3301–3305. DOI: 10.3748/wjg.14.3301.

2. **Mieli-Vergani G**, Vergani D, Czaja AJ, Manns MP, Krawitt EL, Vierling JM, Lohse AW, Montano-Loza AJ. Autoimmune hepatitis. Nature Reviews Disease Primers, 2018; 4: 18017

3. **Longhi MS**, Ma Y, Mieli-Vergani G, Vergani D. Aetiopathogenesis of autoimmune hepatitis. J Autoimmun, February 2010; 34: 7-14. DOI:10.1016/j.jaut.2009.08.010.

4. **Suzuki A**, Brunt EM, Kleiner DE, Miquel R, Smyrk TC, Andrade RJ, Lucena MI, Castiella A, Lindor K, Björnsson. The use of liver biopsy evaluation in discrimination of idiopathic autoimmune hepatitis vs. drug-induced liver injury. Hepatology, September 2011; 54(3): 931–939. DOI: 10.1002/hep.24481.

5. **Czaja AJ**, Bianchi FB, Carpenter HA, Krawitt EL, Lohse AW, Manns MP, McFarlane IG, Mieli-Vergani G, Toda G, Vergani D, Vierling J, Zeniya M. Treatment challenges and investigational opportunities in autoimmune hepatitis. Hepatology, January 2005; 41(1): 207-15. DOI: 10.1002/hep.20539

6. **Miyake Y**, Iwasaki Y, Sakaguchi K, Shiratori Y. Aliment Pharmacol Ther, Auguast 2006; 24(3):519-23. Clinical features of Japanese male patients with type 1 autoimmune hepatitis. DOI: 10.1111/j.1365-2036.2006.03013.x

7. **Al-Chalabi T**, Boccato S, Portmann BC, Mcfarlane IG, Heneghan MA. Autoimmune hepatitis (AIH) in the elderly: a systematic retrospective analysis of a large group of consecutive patients with definite AIH followed at a tertiary referral centre. J Hepatol, 2006; 45(4): 575–583

8. **Alvarez F**, Berg, Bianchi FB, Bianchi L, Burroughs AK, Cancado EL, Chapman RW, Cooksley WGE, Czaja AJ, Desmet VJ, Donaldson PT, Eddleston ALWF, Fainboim L, Heathcote, Homberg JC, Hoofnagle JH, Kakumu S, Krawitt EL, Mackay IR, MacSween RNM, Maddrey WC, Manns MP, McFarlane IG. Journal of Hepatology, November 1999; 31(5):929–938. DOI:.org/10.1016/S0168-8278(99)80297-9

9. **Oo YH**, Hubscher SG, Adams DH. Autoimmune hepatitis: new paradigms in the pathogenesis, diagnosis, and management. Hepatol Int, June 2010; 4(2): 475–493. DOI: 10.1007/s12072-010-9183-5

10. **Targan SR**, Landers C, Vidrich A, Czaja AJ. High-titer antineutrophil cytoplasmic antibodies in type-1 autoimmune hepatitis. Gastroenterology, April 1995; 108(4):1159-66. DOI: 10.1016/0016-5085(95)90215-5

11. **Roozendaal C**, de Jong MA, van den Berg AP, van Wijk RT, Limburg PC, Kallenberg CG. Clinical significance of anti-neutrophil cytoplasmic antibodies (ANCA) in autoimmune liver diseases. J Hepatol, May 2000;32(5):734-41. DOI: 10.1016/s0168-8278(00)80241-x

12. **Bridoux-Henno L**, Maggiore G, Johanet C, Fabre M, Vajro P, Dommergues JP, Reinert P, Bernard O. Features and outcome of autoimmune hepatitis type 2 presenting with isolated positivity for anti-liver cytosol antibody. Clin Gastroenterol Hepatol, 2004;2(9): 825–830. DOI: 10.1016/s0168-8278(99)80297-9

13. **Wies I**, Brunner S, Henninger J, Herkel J, Kanzler S, Meyer zum Buschenfelde KH, Lohse AW. Identification of target antigen for SLA/LP autoantibodies in autoimmune hepatitis. Lancet. 2000;355(9214):1510–1515. DOI: 10.1016/s0140-6736(00)02166-8

14. **Ichai P**, Duclos-Vallée JC, Guettier C, Hamida SB, Antonini T, Delvart V, Saliba F, Azoulay D, Castaing D, Samuel D. Usefulness of corticosteroids for the treatment of severe and fulminant forms of autoimmune hepatitis. Liver transplantation March 2007; 13:996-1003. DOI: 10.1002/lt.21036

15. **Nikias GA**, Batts KP, Czaja AJ J. The nature and prognostic implications of autoimmune hepatitis with an acute presentation. Hepatology, November 1994; 21(5): 866-71. DOI: 10.1016/s0168-8278(94)80251-3.

16. **Johnson PJ**, McFarlane IG, Williams R. Azathioprine for long-term maintenance of remission in autoimmune hepatitis. N Engl J Med, October 1995; 12,333(15):958-63. DOI: 10.1056/NEJM199510123331502

17. **Weiler-Normann C**, Schramm C, Quaas A, Wiegard C, Glaubke C, Pannicke N, Möller S, Lohse AW. Infliximab as a rescue treatment in difficult-to-treat autoimmune hepatitis. Journal of Hepatology, March 2013; 58(3):529-34. DOI: 10.1016/j.jhep.2012.11.010.

18. **Beretta-Piccoli BT**, Mieli-Vergani G, Vergani D. Autoimmune hepatitis: Standard treatment and systematic review of alternative treatments. World J Gastroenterol, September 2017; 23(33): 6030–6048. DOI: 10.3748/wjg.v23.i33.6030

19. **de Boer YS**, van Gerven NM, Zwiers A, Verwer BJ, van Hoek B, van Erpecum KJ, Beuers U, van Buuren HR, Drenth JP, den Ouden JW, Verdonk RC, Koek GH, Brouwer JT, Guichelaar MM, Vrolijk JM, Kraal G, Mulder CJ, van Nieuwkerk CM, Fischer J, Berg T, Stickel F, Sarrazin C, Schramm C, Lohse AW, Weiler-Normann C, Lerch MM, Nauck M, Völzke H, Homuth G, Bloemena E, Verspaget HW, Kumar V, Zhernakova A, Wijmenga C, Franke L, Bouma G. Gastroenterology, August 2014; 147(2): 443-52.e5
DOI: 10.1053/j.gastro.2014.04.022

20. **Donaldson PT**, Doherty DG, Hayllar KM, McFarlane IG, Johnson, R. Williams JC. Susceptibility to autoimmune chronic active hepatitis: human leukocyte antigens DR4 and A1-B8-DR3 are independent risk factors. Hepatology, 1991: 13(4): 701-6

21. **Djilali-Saiah I**, Renous R, Caillat-Zucman S, Debray D, Alvarez F. Linkage disequilibrium between HLA class II region and autoimmune hepatitis in pediatric patients. J Hepatol, June 2004; 40(6): 904-9.

22. **Al-Chalabi T**, Boccato S, Portmann BC, McFarlane IG, Heneghan MA. Autoimmune hepatitis (AIH) in the elderly: a systematic retrospective analysis of a large group of consecutive patients with definite AIH followed at a tertiary referral centre. Journal of Hepatology, October 2006; 45(4):575-8

23. **Peiseler M**, **Sebode M**, Franke B, Wortmann F, Schwinge D, Quaas A, Baron U, Olek S, Wiegard C, Lohse AW, Weiler-Normann C, Schramm C, Herkel J. FOXP3+ regulatory T cells in autoimmune hepatitis are fully functional and not reduced in frequency. Journal of Hepatology, July 2012; 57(1): 125-32. DOI: 10.1016/j.jhep.2012.02.029

24. **Tsuneyama K**, Baba H, Morimoto Y, Tsunematsu T, Ogawa H. Primary Biliary Cholangitis: Its Pathological Characteristics and Immunopathological Mechanisms. The Journal of Medical Investion, 2017; 64 (1.2): 7-13. DOI:10.2152/jmi.64.7

25. **Lee J**, Belanger A, Doucette JT, Stanca C, Friedman S, Bach N. Transplantation Trends in Primary Biliary Cirrhosis. Clinical gastroenterology and hepatology, November 2017; 2007; 5: 1313–1315

26. **Jepsen P**, Gronbaek L, Vilstrup H. Worldwide incidence of autoimmune liver disease. Digestive Diseases, December 2015; 33: 2–12. DOI: 10.1159/000440705

27. **Bowlus CL**, Gershwin ME. The Diagnosis of Primary Biliary Cirrhosis. Autoimmun Reviews, April 2014; 13(0): 441–444. DOI: 10.1016/j.autrev.2014.01.041

28. **Lindor KD**, Gershwin ME, Poupon R, Kaplan M, Bergasa NV, Heathcote EJ. Primary biliary cirrhosis Hepatology, American Association for Study of Liver Diseases, July 2009; 50(1): 291-308. DOI: 10.1002/hep.22906.

29. **Tanaka A**, Leung PSC, Gershwin ME. Environmental basis of primary biliary cholangitis. Experimental Biology and Medicine (Maywood), January 2018; 243(2): 184–189. DOI: 10.1177/1535370217748893

30. **Sasaki M**, Nakanuma Y. Biliary Epithelial Apoptosis, Autophagy, and Senescence in Primary Biliary Cirrhosis. Hepatitis Research and Treatment. November 2010; 2010: 205128. DOI: 10.1155/2010/205128

31. **Gershwin ME**, Mackay IR, Sturgess A, Coppel RL. Identification and specificity of a cDNA encoding the 70 kd mitochondrial antigen recognized in primary biliary cirrhosis. Journal of Immunology, May 1987;138(10):3525-31

32. **Jones D**. Pathogenesis of Primary Biliary Cirrhosis. Gut, November 2007; 56(11): 1615–1624. DOI: 10.1136/gut.2007.122150

33. **European Association for the Study of the Liver**. EASL Clinical Practice Guidelines: The diagnosis and management of patients with primary biliary cholangitis. Journal of Hepatology 2017; 67: 145–172

34. **Rong G**, Zhong R, Lleo A, Leung PS, Bowlus CL, Yang GX, Yang CY, Coppel RL, Ansari AA, Cuebas DA, Worman HJ, Invernizzi P, Gores GJ, Norman G, He XS, Gershwin ME. Epithelial cell specificity and apotope recognition by serum autoantibodies in primary biliary cirrhosis. Hepatology, 2011; 54: 196–203. DOI: 10.1002/hep.24355

35. **Lleo A**, Bowlus CL, Yang GX, Invernizzi P, Podda M, Van de Water J, Ansari AA, Coppel RL, Worman HJ, Gores GJ, Gershwin ME. Biliary apotopes and anti-mitochondrial antibodies activate innate immune responses in primary biliary cirrhosis. Hepatology, September 2010; 52(3): 987-98. DOI: 10.1002/hep.23783.

36. **Rodrigues PM**, Perugorria MJ, Santos-Laso A, Bujanda L, Beuers U, Banales JM. Primary biliary cholangitis: A tale of epigenetically-induced secretory failure? Journal of Hepatology, December 2018; 69(6): 1371-1383. DOI: 10.1016/j.jhep.2018.08.020

37. **Medina JF**. Role of the anion exchanger 2 in the pathogenesis and treatment of primary biliary cirrhosis. Digestive Diseases, 2011; 29(1): 103-12. DOI: 10.1159/000324144

38. **Arenas F**, Hervías I, Sáez E, Melero S, Prieto J, Parés A, Medina JF. Promoter hypermethylation of the AE2/SLC4A2 gene in PBC. Journal of Hepatology, September 2019; 1(3): 145-153. DOI: 10.1016/j.jhepr.2019.05.006

39. **Prieto J**, Qian C, García N, Díez J, Medina JF. Abnormal expression of anion exchanger genes in primary biliary cirrhosis. Gastroenterology, August 1993; 105(2): 572-8. DOI: 10.1016/0016-5085(93)90735-u

40. **Poupon R**. Evidence-based treatment of primary biliary cirrhosis. Digestive Diseases, 2014; 32(5):626-30. DOI: 10.1159/000360516

41. **Dyson JK**, Beuers U, Jones DEJ, Lohse AW, Hudson M. Primary sclerosing cholangitis. Lancet, June 2018; 23; 391 (10139): 2547-2559. DOI: 10.1016/S0140-6736(18)30300-3

42. **Hirschfield GM**, Karlsen TH, Lindor KD, Adams DH. Primary sclerosing cholangitis. Lancet, November 2013; 9; 382 (9904):1587-99. DOI: 10.1016/S0140-6736(13)60096-3

43. **Karlsen TH**, Folseraas T, Thorburn D, Vesterhus M. Primary sclerosing cholangitis– a comprehensive review. Journal of Hepatology, July 2017; 67: 1298–1323

44. **Penz-Österreicher M**, Österreicher CH, Trauner M. Fibrosis in Autoimmune and Cholestatic Liver Disease. Best Practice and Research, Clinical Gastroenterology, April 2011; 25(2-4): 245–258. DOI: 10.1016/j.bpg.2011.02.001

45. **MacCarty RL**, LaRusso NF, Wiesner RH, Ludwig J. Primary sclerosing cholangitis: findings on cholangiography and pancreatography. Radiology, October 1983; 149(1): 39-44. DOI: 10.1148/radiology.149.1.6412283

46. **Mulder AH**, Horst G, Haagsma EB, Limburg PC, Kleibeuker JH, Kallenberg CG. Prevalence and characterization of neutrophil cytoplasmic antibodies in autoimmune liver diseases. Hepatology, March 1993; 17(3): 411-7.

47. **Angulo P**, Peter JB, Gershwin ME, DeSotel CK, Shoenfeld Y, Ahmed AE, Lindor KD. Serum autoantibodies in patients with primary sclerosing cholangitis. Journal of Hepatology, February 2000; 32(2): 182-7

48. **Björnsson E,** Boberg KM, Cullen S, Fleming K, Clausen OP, Fausa O, Schrumpf E, Chapman RW. Patients with small duct primary sclerosing cholangitis have a favourable long term prognosis. Gut, November 2002; 51(5): 731-5

49. **Tischendorf JJ**, Hecker H, Krüger M, Manns MP, Meier PN. Characterization, outcome, and prognosis in 273 patients with primary sclerosing cholangitis: A single center study. American Journal of Gastroenterology, 2007; 102: 107-114. DOI: 10.1111/j.1572-0241.2006.00872.x

50. **Bambha K,** Kim WR, Talwalkar J, Torgerson H, Benson JT, Therneau TM, Loftus EV, Yawn BP, Dickson ER, Melton LJ. Incidence, clinical spectrum, and outcomes of primary sclerosing cholangitis in a United States community. Gastroenterology 2003; 125: 1364-1369. DOI: 10.1016/ j.gastro.2003.07.011

51. **Melum E**, Franke A, Schramm C, Weismüller TJ, Gotthardt DN, Offner FA, Juran BD, Laerdahl JK, Labi V, Björnsson E, Weersma RK, Henckaerts L, Teufel A, Rust C, Ellinghaus E, Balschun T, Boberg KM, Ellinghaus D, Bergquist A, Sauer P, Ryu E, Hov JR, Wedemeyer J, Lindkvist B, Wittig M, Porte RJ, Holm K, Gieger C, Wichmann HE, Stokkers P, Ponsioen CY, Runz H, Stiehl A, Wijmenga C, Sterneck M, Vermeire S, Beuers U, Villunger A, Schrumpf E, Lazaridis KN, Manns MP, Schreiber S, Karlsen TH. Genome-wide association analysis in primary sclerosing cholangitis identifies two non-HLA susceptibility loci. Nature Genetics, January 2011; 43(1): 17-9. DOI: 10.1038/ng.728

52. **Liu JZ**, Hov JR, Folseraas T, Ellinghaus E, Rushbrook SM, Doncheva NT, Andreassen OA, Weersma RK, Weismüller TJ, Eksteen B, Invernizzi P, Hirschfield GM, Gotthardt DN, Pares A, Ellinghaus D, Shah T, Juran BD, Milkiewicz P, Rust C, Schramm C, Müller T, Srivastava

B, Dalekos G, Nöthen MM, Herms S, Winkelmann J, Mitrovic M, Braun F, Ponsioen CY, Croucher PJ, Sterneck M, Teufel A, Mason AL, Saarela J, Leppa V, Dorfman R, Alvaro D, Floreani A, Onengut-Gumuscu S, Rich SS, Thompson WK *et al.* Dense genotyping of immune-related disease regions identifies nine new risk loci for primary sclerosing cholangitis; International IBD Genetics Consortium. Nature Genetics, June 2013; 45(6): 670-5. DOI: 10.1038/ng.2616

53. **Liwinski T**, Zenouzi R, John C, Ehlken, Rühlemann MC, Bang C, Growth S, Lieb W, M Kantowski, Andersen N, Schachschal G, Karlsen TH, Hov JT, Rösch T, Lohse AW, Heeren J, Franke A, Schramm C. Alterations of the bile microbiome in primary sclerosing cholangitis. Gut, January 2019; 0: 1–8. DOI: 10. 1136/ gutjnl- 2019- 318416

54. **Pereira P**, Aho V, Arola J, Boyd S, Jokelainen K, Paulin L, Auvinen P, Färkkilä M. Bile microbiota in primary sclerosing cholangitis: Impact on disease progression and development of biliary dysplasia. PLoS One, August 2017; 10; 12(8): e0182924. DOI: 10.1371/journal.pone.0182924

55. **Gidwaney NG**, Pawa S, Das KM. Pathogenesis and clinical spectrum of primary sclerosing cholangitis. World J Gastroenterol, April 2017: 14; 23(14): 2459-2469. DOI: 10.3748/wjg.v23.i14.2459

56. **Williamson KD**, Chapman RW. Primary Sclerosing Cholangitis. Digestive Diseases, 2014; 32: 438–445. DOI: 10.1159/000358150

57. **Boonstra K**, Weersma RK, van Erpecum KJ, Rauws EA, Spanier BW, Poen AC, van Nieuwkerk KM, Drenth JP, Witteman BJ, Tuynman HA, Naber AH, Kingma PJ, van Buuren HR, van Hoek B, Vleggaar FP, van Geloven N, Beuers U, Ponsioen CY; EpiPSCPBC Study Group. Population-based epidemiology, malignancy risk, and outcome of primary sclerosing cholangitis. Hepatology, December 2013; 58(6): 2045-55. DOI: 10.1002/hep.26565.

58. **Croome KP**, Gores GJ, Rosen CB. Shackelford's Surgery of the Alimentary Tract, Elsevier, 2019; 2(8): 1378-1385. DOI: 10.1016/C2015-1-00854-7

59. **Sebode M**, Schulz L, Lohse AW. „Autoimmune(-Like)" Drug and Herb Induced Liver Injury: New Insights into Molecular Pathogenesis. International Journal of Molecular Sciences, September 2017; 18, 1954

60. **Kaplowitz N**. Idiosyncratic drug hepatotoxicity. Nature Reviews, Drug Discovery, 2005; 4: 489–499. DOI: 10.1038/nrd1750

61. **Denk, H**. Drug-induced liver injury. Verhandlungen der Deutschen Gesellschaft für Pathologie2002, 86, 120–125.

62. **Teschke R**, Schulze J, Axel Eickhoff A, Danan G. Drug Induced Liver Injury: Can Biomarkers Assist RUCAM in Causality Assessment? International Journal of Molecular Sciences, April 2017; 18, 803. DOI: 10.3390/ijms1804080

63. **European Association for the Study of the Liver**. EASL Clinical Practice Guidelines: Drug-induced liver injury. Journal of Hepatology, 2019. DOI: 10.1016/j.jhep.2019.02.014

64. **Larson AM**, Polson J, Fontana RJ, Davern TJ, Lalani E, Hynan LS, Reisch JS, Schiødt FV, Ostapowicz G, Shakil AO, Lee WM; Acute Liver Failure Study Group. Acetaminophen-induced acute liver failure: results of a United States multicenter, prospective study. Hepatology, December 2005; 42(6): 1364-72. DOI: 10.1002/hep.20948

65. **Senior JR**. Drug hepatotoxicity from a regulatory perspective. Clinics in Liver Disease, August 2007; 11(3): 507-24, vi, DOI: 10.1016/j.cld.2007.06.002

66. **Danan G**, Benichou C. Causality assessment of adverse reactions to drugs—I. A novel method based on the conclusions of international consensus meetings: application to drug-induced liver injuries. Journal of clinical Epidemiol, November 1993; 46: 1323–1330. DOI: 10.1016/0895-4356(93)90101-6

67. **Lucena MI**, Andrade RJ, Kaplowitz N, García-Cortes M, Fernández MC, Romero-Gomez M, Bruguera M, Hallal H, Robles-Diaz M, Rodriguez-González JF, Navarro JM, Salmeron J, Martinez-Odriozola P, Pérez-Alvarez R, Borraz Y, Hidalgo R; Spanish Group for the Study of Drug-Induced Liver Disease. Phenotypic characterization of idiosyncratic drug-induced liver injury: the influence of age and sex. Hepatology, June 2009; 49(6): 2001-9. DOI: 10.1002/hep.22895

68. **Danan G**, Teschke R. RUCAM in Drug and Herb Induced Liver Injury: The Update. International Journal of Molecular Sciences, December 2015; 24; 17(1). DOI: 10.3390/ijms17010014

69. **Rockey DC**, Seeff LB, Rochon J, Freston J, Chalasani N, Bonacini M, Fontana RJ, Hayashi PH; US Drug-Induced Liver Injury Network. Causality assessment in drug-induced liver injury using a structured expert opinion process: comparison to the Roussel-Uclaf causality assessment method. Hepatology, June 2010; 51: 2117-26. DOI: 10.1002/hep.23577

70. **Chalasani NP**, Hayashi PH, Bonkovsky HL, Navarro VJ, Lee WM, Fontana RJ; Practice Parameters Committee of the American College of Gastroenterology. ACG Clinical Guideline: the diagnosis and management of idiosyncratic drug-induced liver injury. American Journal of Gastroenterology, July 2014; 109(7): 950-66. DOI: 10.1038/ajg.2014.131

71. **Kullak-Ublick GA**, Andrade RJ, Merz M, End P, Benesic A, Gerbes AL, Aithal GP. Drug-induced liver injury: recent advances in diagnosis and risk assessment. Gut 2017; 66: 1154–1164. DOI: 10.1136/gutjnl-2016-313369

72. **David S**, Hamilton JP. Drug-induced Liver Injury.US Gastroenterology and Hepatology Reviews, January 2010; 6: 73-80

73. **Andrade RJ**, Robles M, Fernández-Castañer A, López-Ortega S, López-Vega MC, Lucena MI. Assessment of drug-induced hepatotoxicity in clinical practice: a challenge for gastroenterologists. World Journal of Gastroenterology, January 2007; 13(3): 329-40. DOI: 10.3748/wjg.v13.i3.329

74. **Cirulli ET**, Nicoletti P, Abramson K, Andrade RJ, Bjornsson ES, Chalasani N, Fontana RJ, Hallberg P, Li YJ, Lucena MI, Long N, Molokhia M, Nelson MR, Odin JA, Pirmohamed M, Rafnar T, Serrano J, Stefánsson K, Stolz A, Daly AK, Aithal GP, Watkins PB; Drug-Induced Liver Injury Network (DILIN) investigators; International DILI consortium (iDILIC). A Missense Variant in PTPN22 is a Risk Factor for Drug-induced Liver Injury. Gastroenterology, May 2019; 156(6): 1707-1716.e2.   DOI: 10.1053/j.gastro.2019.01.034

75. **Stanford SM**, Bottini N. PTPN22: the archetypal non-HLA autoimmunity gene. Nature Reviews Rheumatology, October 2014; 10: 602-11. DOI: 10.1038/nrrheum.2014.109

76. **Huang YS**. Genetic polymorphisms of drug-metabolizing enzymes and the susceptibility to antituberculosis drug-induced liver injury. Expert Opinion on Drug Metabolism and Toxicology, February 2007; 3:1–8. DOI: 10.1517/17425255.3.1.1

77. **Tarantino G**, Di Minno MN, Capone D. Drug-induced liver injury: is it somehow foreseeable? World Journal of Gastroenterology, June 2009; 15(23): 2817-33. DOI: 10.3748/wjg.15.2817

78. **Arab JP**, Arrese M, Trauner M. Recent Insights into the Pathogenesis of Nonalcoholic Fatty Liver Disease. Annual Reviews Pathology Mechchanisms in disease, 2018; 13:321–50 DOI: 10.1146/annurev-pathol-020117-043617

79. **Chalasani N**, Younossi Z, Lavine JE, Diehl AM, Brunt EM, Cusi K, Charlton M, Sanyal AJ. The diagnosis and management of non-alcoholic fatty liver disease: practice Guideline by the American Association for the Study of Liver Diseases, American College of Gastroenterology, and the American Gastroenterological Association. Hepatology, June 2012; 55(6):2005-23. DOI: 10.1002/hep.25762.

80. **Friedman SL**, Neuschwander-Tetri BA, Rinella M, Sanyal JA. Mechanisms of NAFLD development and therapeutic strategies. Nature medicine review article, July 2018. 24: 908–922. DOI: .org/10.1038/s41591-018-0104-9

81. **Softic S**, Cohen DE, Kahn CR. Role of Dietary Fructose and Hepatic De Novo Lipogenesis in Fatty Liver Disease. Digestive diseases and sciences, May 2016; 61(5): 1282-93. DOI: 10.1007/s10620-016-4054-0.

82. **Gaggini M**, Morelli M, Buzzigoli E, DeFronzo RA, Bugianesi E, Gastaldelli A. Non-Alcoholic Fatty Liver Disease (NAFLD) and Its Connection with Insulin Resistance, Dyslipidemia, Atherosclerosis and Coronary Heart Disease. Nutrients, May 2013; 5(5): 1544–1560. DOI: 10.3390/nu5051544

83. **Anstee QM**, Targher G, Day CP. Progression of NAFLD to diabetes mellitus, cardiovascular disease or cirrhosis. Nat Rev Gastroenterol Hepatol, 2013: 10:330–44. DOI: 10.1038/nrgastro.2013.41

84. **Romeo S**, Kozlitina J, Xing C, Pertsemlidis A, Cox D, Pennacchio LA, Boerwinkle E, Cohen JC, Hobbs HH. Genetic variation in PNPLA3 confers susceptibility to nonalcoholic fatty liver disease. Nature Genetics, December 2008; 40(12):1461-5. DOI: 10.1038/ng.257

85. **Magee N**, Zou A, Zhang Y. Pathogenesis of nonalcoholic steatohepatitis: interactions between liver parenchymal and nonparenchymal cells. BioMed Research International, 2016: 2016:5170402. DOI: 10.1155/2016/5170402

86. **Wang L**, Athinarayanan S, Jiang G, Chalasani N, Zhang M, Liu W. Fatty acid desaturase 1 gene polymorphisms control human hepatic lipid composition. Hepatology, January 2015; 61(1):119-28. DOI: 10.1002/hep.27373

87. **Promrat K**, Kleiner DE, Niemeier HM, Jackvony E, Kearns M, Wands JR, Fava JL, Wing RR. Randomized controlled trial testing the effects of weight loss on nonalcoholic steatohepatitis. Hepatology, January 2010; 51(1):121-9. DOI: 10.1002/hep.23276

88. **Day CP**, James OF. Steatohepatitis: a tale of two "hits"? Gastroenterology, April 1998 Apr;114(4):842-5.

89. **Brunt EM**, Wong VW, Nobili V, Day CP, Sookoian S, Maher JJ, Bugianesi E, Sirlin CB, Neuschwander-Tetri BA, Rinella ME. Nonalcoholic fatty liver disease. Nature Reviews Disease Primers, December 2015; 17;1:15080. DOI: 10.1038/nrdp.2015.80.

90. **Kawano Y**, Cohen DE. Me chanisms of hepatic triglyceride accumulation in non-alcoholic fatty liver disease. Journal of Gastroenterology, April 2013; 48(4):434-41. DOI: 10.1007/s00535-013-0758-5

91. **Neuschwander-Tetri BA**. Hepatic lipotoxicity and the pathogenesis of nonalcoholic steatohepatitis: the central role of nontriglyceride fatty acid metabolites. Hepatology, August 2010; ;52(2): 774-88. DOI: 10.1002/hep.23719

92. **Cusi, K**. Role of obesity and lipotoxicity in the development of nonalcoholic steatohepatitis: pathophysiology and clinical implications. Gastroenterology, April 2012; 142(4):711-725.e6. DOI: 10.1053/j.gastro.2012.02.003

93. **Boursier J**, Mueller O, Barret M, Machado M, Fizanne L, Araujo-Perez F, Guy CD, Seed PC, Rawls JF, David LA, Hunault G, Oberti F, Calès P, Diehl AM. The severity of nonalcoholic fatty liver disease is associated with gut dysbiosis and shift in the metabolic function of the gut microbiota. Hepatology, March 2016; 63(3): 764-75. DOI: 10.1002/hep.28356

94. **Parham P**. The immune system. Garland Science, Taylor and Francis Group LLC, 2015. 4: 124- 140

95. **Cruse JM**, Lewis RE, Wang H. Immunology Guidebook. Elsevier, 2004; 267-276

96. **Shoenfeld Y**, Meroni PL, Gershwin ME. Autoantibodies (Third Edition): Pages 829-855, 2014

97. **Courtney AH**, Lo WL, Weiss A. TCR Signaling: Mechanisms of Initiation and Propagation. Trends in Biochemical Sciences, February 2018; 43(2): 108-123. DOI: 10.1016/j.tibs.2017.11.008

98. **Rich RR**, Fleisher TA, Shearer TW, Schroeder HW, Frew AJ, Wey CW. Clinical Immunology Principles and Practice Book. Elsevier Ltd 5th Edition 2019

99. **Beyersdorf N**, Kerkau T, Hünig T. CD28 co-stimulation in T-cell homeostasis: a recent perspective. Immunotargets Therapy, May 2015; 4: 111–122. DOI: 10.2147/ITT.S61647

100. **Curtsinger JM**, Mescher MF. Inflammatory Cytokines as a Third Signal for T Cell Activation. Current Opinion in Immunology, June 2010; 22(3): 333–340. DOI: 10.1016/j.coi.2010.02.013

101. **Mak TW**, Saunders ME. The Immune Response- Basic and Clinical Principles. Academic Press, 2006

102. **Luckheeram RV**, Zhou R, Verma AD, Xia B CD4+T Cells: Differentiation and Functions. Clinical and Developmental Immunology, March 2012; 2012: 925135. DOI: 10.1155/2012/925135.

103. **Romagnani S**. Th1/Th2 cells. Inflammatory Bowel Diseases, November 1999; 5(4):285-94

104. **Maynard CL**, Weaver CT. Effector CD4+ T Cells in the Intestines in Mucosal Immunology (Fourth Edition) Academic Press, April 2015

105. **Kaplan MH**. Th9 cells: differentiation and disease. Immunology Reviews, March 2013; 252(1): 104–115. DOI: 10.1111/imr.12028 1

106. **Awel O, Kaplan MH**. Translational Immunology- Mechanisms and Pharmacologic Approaches, Chapter 6: Th9 Cells as Targets for Immunotherapy. Academic Press, 2016; 165-184. DOI: 10.1016/B978-0-12-801577-3.00007-1

107. **Ouyang W, Kolls JK, Zheng Y**. The biological functions of T helper 17 cell effector cytokines in inflammation. Immunity, April 2008; 28(4): 454-67. DOI: 10.1016/j.immuni.2008.03.004.

108. **Crotty S**. Follicular Helper CD4 T Cells (TFH). Annual Review of Immunology. February 2011; 29:621-663. DOI: 10.1146/annurev-immunol-031210-101400

109. **Kanamori M**, Nakatsukasa H, Okada M, Lu Q, Yoshimura A. Induced Regulatory T Cells: Their Development, Stability, and Applications. Journal. Trends in Immunology September 09, 2016 DOI: 10.1016/j.it.2016.08.012

110. **Wissinger E**. Imperial College London, UK. British society for immunology. https://www.immunology.org/public-information/bitesized-immunology/células/cd8-t-cells (06.10.2019)

111. **Obar JJ**, Lefrançois L. Memory CD8+ T cell differentiation. Annals of the New York Academy of Sciences, Januar 2010; 1183: 251–266. DOI: 10.1111/j.1749-6632.2009.05126.x

112. **Gershon RK**, Kondo K. Cell interactions in the induction of tolerance: the role of thymic lymphocytes. Immunology. 1970; 18: 723-737.

113. **Chakraborty S**, Gaurisankar S. Development, maintenance and functions of CD8+ T-regulatory cells: Molecular orchestration of FOXP3 transcription. Journal of immunological sciences, May 2018; 2(2): 8-12

114. **Chen L**, Flies DB. Molecular mechanisms of T cell co-stimulation and co-inhibition. Nature Reviews Immunology, April 2013; 13(4): 227–242. DOI: 10.1038/nri3405

115. **Simpson TR**, Quezada SA, Allison JP. Regulation of CD4 T cell activation and effector function by inducible costimulator (ICOS). Current Opinions in Immunology, June 2010; 22(3): 326-32. DOI: 10.1016/j.coi.2010.01.001. 2010

116. **Astier A**. Co-Receptors: Function., University of Edinburgh, United Kingdom. www.immunology.org/public-information/bitesized-immunology/sistemas-y-procesos/co-receptors-function 12.10.2019

117. **Thaventhiran T**, Sethu S, Yeang HXA, Al-Huseini L, Hamdam J, Thaventhiran JG. T Cell Co-inhibitory Receptors: Functions and Signalling Mechanisms. Journal of Clinical and Cell Immunology, October 2012. DOI: 10.4172/2155-9899.S12-004

118. **Hutloff A**, Dittrich AM, Beier KC, Eljaschewitsch B, Kraft R, Anagnostopoulos I, Kroczek RA. ICOS is an inducible T-cell co-stimulator structurally and functionally related to CD28. Nature, January 1999; 397(6716):263-6

119. **Maawy AA**, Ito F. Immune Checkpoint Inhibitors in Cancer. Elsevier, 2019; Pages 227-243. DOI: 10.1016/B978-0-323-54948-6.00012-3

120. **Borrie AE**, Vareki SM. International Review of Cell and Molecular Biology. Academic press, 2018; 341: 201-276

121. **Wikenheiser DJ**, Stumhofer JS. ICOS Co-Stimulation: Friend or Foe? Review Frontiers in Immunology, August 2016. DOI: 10.3389/fimmu.2016.00304

122. **Slomovitz BM**, Coleman RL. The PI3K/AKT/mTOR Pathway as a Therapeutic Target in Endometrial Cancer. Clinical Cancer Research, November 2012; DOI: 10.1158/1078-0432.CCR-12-0662

123. **Fos C**, Salles A, Lang V, Carrette F, Audebert S, Pastor S, Ghiotto M, Olive D, Bismuth G, Nunès JA. ICOS Ligation Recruits the p50α PI3K Regulatory Subunit to the Immunological Synapse. Journal of Immunology, August 2008; 181 (3) 1969-1977. DOI: 10.4049/jimmunol.181.3.1969

124. **Dong C**, Juedes AE, Temann UA, Shresta S, Allison JP, Ruddle NH, Flavell RA. ICOS co-stimulatory receptor is essential for T-cell activation and function. Nature, January 2001; 409(6816): 97-101

125. **Tafuri A**, Shahinian A, Bladt F, Yoshinaga SK, Jordana M, Wakeham A, Boucher LM, Bouchard D, Chan VS, Duncan G, Odermatt B, Ho A, Itie A, Horan T, Whoriskey JS, Pawson T, Penninger JM, Ohashi PS, Mak TW. ICOS is essential for effective T-helper-cell responses. Nature. January 2001; 409(6816): 105-9.

126. **Naluai AT**, Nilsson S, Samuelsson L, Gudjónsdóttir AH, Ascher H, Ek J, Hallberg B, Kristiansson B, Martinsson T, Nerman O, Sollid LM, Wahlström J. The CTLA4/CD28 gene

region on chromosome 2q33 confers susceptibility to celiac disease in a way possibly distinct from that of type 1 diabetes and other chronic inflammatory disorders. Tissue Antigens, October 2000; 56(4):350-5

127. **van der Merwe P**, Bodian D, Daenke S, Linsley PS, Davis SJ. CD80 (B7-1) binds both CD28 and CTLA-4 with a low affinity and very fast kinetics. Journal of Experimental Medicine 1997; 185: 393–403. DOI: 10.1084/jem.185.3.393

128. **Rudd CE**, Alison Taylor A, Schneider H. CD28 and CTLA-4 coreceptor expression and signal transduction. Immunology Review, May 2009; 229(1): 12–26. DOI: 10.1111/j.1600-065X.2009.00770.x

129. **Schneider H**, Rudd CE. Diverse mechanisms regulate the surface expression of immunotherapeutic target CTLA-4. Review Frontiers in Immunology, December 2014. DOI: 10.3389/fimmu.2014.00619

130. **Chuang E**, Fisher TS, Morgan RW, Robbins MD, Duerr JM, Vander Heiden, MG Gardner JP, Hambor JE, Neveu MJ, Thomps CB. The CD28 and CTLA-4 receptors associate with the serine/threonine phosphatase PP2A. Immunity, 2000; 13: 313–22. DOI: 10.1016/S1074-7613(00)00031-5

131. **Schneider H**, Smith X,Liu H, Bismuth G, Rudd CE. CTLA-4 disrupts ZAP70 microcluster formation with reduced T cell/APC dwell times and calcium mobilization. European Journal of Immunology, January 2008; 38(1): 40–47. DOI: 10.1002/eji.200737423

132. **Hoff H**, Kolar P, Ambach A, Radbruch A, Brunner-Weinzierl MC. CTLA-4 (CD152) inhibits T-cell function by activating the ubiquitin ligase Itch. Molecular Immunology, 2010; 47:1875–81. DOI: 10.1016/j.molimm.2010.03.017

133. **Li D**, Gál I, Vermes C, Alegre ML, Chong ASF, Chen L, Shao Q, Adarichev V, Xu X, Koreny T, Mikecz T, Finnegan A, Glant TT, Zhang J. Cutting Edge: Cbl-b: One of the Key Molecules Tuning CD28- and CTLA-4-Mediated T Cell Costimulation. Journal of Immunology, December 2004; 173 (12) 7135-7139. DOI: 10.4049/jimmunol.173.12.7135

134. **Qureshi OS**, Zheng Y, Nakamura K, Attridge K, Manzotti C, Schmidt EM, Baker J, Jeffery LE, Kaur S, Briggs Z, Hou TZ, Futter CE, Anderson G, Walker LS, Sansom DM. Trans-

endocytosis of CD80 and CD86: a molecular basis for the cell-extrinsic function of CTLA-4. Science, April 2011; 332:600–3. DOI: 10.1126/science.1202947

135. **Friedline RH**, Brown DS, Nguyen H, Kornfeld H, Lee JH, Zhang Y, Appleby M, Der SD, Kang J, Chambers CA. CD4+ regulatory T cells require CTLA-4 for the maintenance of systemic tolerance. Journal of Experimental Medicine, February 2009; 206(2): 421–434. DOI: 10.1084/jem.20081811

136. **Walker LSK**. Treg and CTLA-4: Two intertwining pathways to immune toleranc. Journal of Autoimmunity, September 2013; 45(100): 49–57. DOI: 10.1016/j.jaut.2013.06.006 e

137. **Munn DH**, Shafizadeh E, Attwood JT, Bondarev I, Pashine A, Mellor AL. Inhibition of T cell proliferation by macrophage tryptophan catabolism. Journal of Experimental Medicine, May 1999; 189(9):1363-72.

138. **Grohmann U**, Orabona C, Fallarino F, Vacca C, Calcinaro F, Falorni A, Candeloro P, Belladonna ML, Bianchi R, Fioretti MC, Puccetti P. CTLA-4-Ig regulates tryptophan catabolism in vivo. Nature Immunology, November 2002; 3(11): 1097-101

139. **Fallarino F**, Grohmann U, Hwang KW, Orabona C, Vacca C, Bianchi R, Belladonna ML, Fioretti MC, Alegre ML, Puccetti P. Modulation of tryptophan catabolism by regulatory T cells. Nature Immunology, December 2003; 4(12): 1206-12

140. **Tivol EA**, Borriello F, Schweitzer AN, Lynch WP, Bluestone JA, Sharpe AH. Loss of CTLA-4 leads to massive lymphoproliferation and fatal multiorgan tissue destruction, revealing a critical negative regulatory role of CTLA-4. Immunity, 1995; 3: 541–547

141. **Chambers CA**, Sullivan TJ, Allison JP.Lymphoproliferation in CTLA-4-deficient mice is mediated by costimulation-dependent activation of CD4+ T cells. Immunity, December 1997; 7(6): 885-95. DOI: 10.1016/s1074-7613(00)80406-9

142. **Gajewski TF**, Fallarino F, Fields PE, Rivas F, Alegre ML. Absence of CTLA-4 lowers the activation threshold of primed CD8^{+} TCR-transgenic T cells: lack of correlation with Src homology domain 2-containing protein tyrosine phosphatase. Journal of Immunology, March 2001; 166 (6) 3900-3907; DOI: 10.4049/jimmunol.166.6.3900

143. **Banton MC**, Inder KL, Valk E, Rudd CE, Schneider H. Rab8 binding to immune cell-specific adaptor LAX facilitates formation of trans-Golgi network-proximal CTLA-4 vesicles for surface expression. Molecular Cell Biology, 2014; 34:1486–99. DOI: 10.1128/MCB.01331-13

144. **Zerial M**, McBride H. Rab proteins as membrane organizers. Nature Review Molecular Cell Biology, 2001; 2:107–17. DOI:10.1038/35052055

145. **Attanasio J**, Wherry EJ. Costimulatory and Coinhibitory Receptor Pathways in Infectious Disease Review Immunity, May 2016; 44 (5), P1052-1068, DOI: 10.1016/j.immuni.2016.04.022

146. **Terawaki S**, Chikuma S, Shibayama S, Hayashi T, Yoshida T, Okazaki T, Honjo T. IFN-α directly promotes programmed cell death-1 transcription and limits the duration of T cell-mediated immunity. Journal of Immunology, March 2011; 186(5):2772-9

147. **Zhang X**, Schwartz JC, Guo X, Bhatia S, Cao E, Lorenz M, Cammer M, Chen L, Zhang ZY, Edidin MA, Nathenson SG, Almo SC. Structural and functional analysis of the costimulatory receptor programmed death-1. Immunity, March 2004; 20(3): 337-47. DOI: 10.1016/s1074-7613(04)00051-2

148. **Keir ME**, Butte MJ, Freeman GJ, Sharpe AH. PD-1 and Its Ligands in Tolerance and Immunity. Annual Review in Immunology. 2008; 26: 677-704.
DOI: 10.1146/annurev.immunol.26.021607.090331.

149. **Francisco LM**, Sage PT, Sharpe, AH. The PD-1 pathway in tolerance and autoimmunity. Immunological Reviews, 2010: 236, 219–242

150. **Schildberg FA**, Klein SR, Freeman GJ, Sharpe AH. Coinhibitory pathways in the B7-CD28 ligand-receptor family. Immunity, May 2016; 44(5): 955–972.
DOI: 10.1016/j.immuni.2016.05.002

151. **Arasanz H**, Gato-Cañas M, Zuazo M, Ibañez-Vea M, Breckpot K, Kochan G, Escors D. Oncotarget, August 2017; 8(31): 51936–51945. DOI: 10.18632/oncotarget.17232

152. **Kulpa DA**, Lawani M, Cooper A, Peretz Y, Ahlers J, Sékaly RP. PD-1 Coinhibitory Signals: The Link Between Pathogenesis and Protection. Seminars in Immunology, October 2014; DOI: 10.1016/j.smim.2013.02.002

153. **Wu X**, Gu Z, Chen Y, Chen B, Chen W, Weng L, Liu X. Application of PD-1 Blockade in Cancer Immunotherapy. Computational and Structural Biotechnology Journal, May 2019; 17: 661-674. DOI: 10.1016/j.csbj.2019.03.006.

154. **Dana Farber Cancer Institute**. What is PD-1 and Immunotherapy? May, 2019. Retrieved on 7th October 2019.
https://blog.dana-farber.org/insight/2019/05/the-science-of-pd-1-and-immunotherapy/

155. **Page DB**, Postow MA, Callahan MK, Allison JP, Wolchok JD. Ludwig Center for Cancer Immunotherapy, Memorial Sloan-Kettering Cancer Center, New York, Annual Review of Medicine, January 2014; 65:185-202. DOI: 10.1146/annurev-med-092012-112807

156. **Brunner-Weinzier MC**, Rudd CE. CTLA-4 and PD-1 Control of T-Cell Motility and Migration: Implications for Tumor Immunotherapy. Frontiers in Immunology, November 2018 https://doi.org/10.3389/fimmu.2018.02737

157. **Keane MM**, Rivero-Lezcano OM, Mitchell JA, Robbins KC, Lipkowitz S. Cloning and characterization of cbl-b: a SH3 binding protein with homology to the c-cbl proto-oncogene. Oncogene, June 1995; 10(12): 2367-77.

158. **Lutz-Nicoladoni C**, Wolf D, Sopper S. Modulation of immune cell functions by the E3 ligase Cbl-b. Frontiers in Oncology, March 2015. DOI: 10.3389/fonc.2015.00058

159. **Metzger MB**, Pruneda JN, Klevit RE, Weissman AM. RING-type E3 ligases: Master manipulators of E2 ubiquitin-conjugating enzymes and ubiquitination Biochimica et Biophysica Acta (BBA)- Molecular Cell Research; January 2014; 1843(1): 47-60

160. **Morreale FE**, Walden H. SnapShot: Types of Ubiquitin ligases. Cell, March 2014; 165. DOI: 10.1016/j.cell.2016.03.003

161. **Jeon MS**, Atfield A, Venuprasad K, Krawczy C, Sarao R, Elly C, Yang C, Arya S, Bachmaier K, Su L, Bouchard D, Jones R, Gronski M, Ohashi P, Wada T, Bloom D, Fathman CG, Liu YC, Penninger JM. Essential Role of the E3 Ubiquitin Ligase Cbl-b in T Cell Anergy Induction. Journal of immunology, August 2004; 21(2): 167-177. DOI: 10.1016/j.immuni.2004.07.013

162. **Qiao G**, Li Z, Molinero L, Alegre ML, Ying H, Sun Z, Penninger JM, Zhang J. T-Cell Receptor-Induced NF-κB Activation Is Negatively Regulated by E3 Ubiquitin Ligase Cbl-b.

Molecular and cellular biology, American Society for Microbiology, April 2008; 28: 2470-2480. DOI: 10.1128/MCB.01505-07

163. **Fang D**, Liu YC. Proteolysis-independent regulation of PI3K by Cbl-b-mediated ubiquitination in T cells. Nature Immunology, September 2001; 2(9): 870-5. DOI: 10.1038/ni0901-870

164. **Liu Q**, Zhou H, Langdon WY, Zhang J. E3 ubiquitin ligase Cbl-b in innate and adaptive immunity. Cell Cycle, June 2014; 13(12): 1875–1884. DOI: 10.4161/cc.29213

165. **Bachmaier K**, Krawczyk C, Kozieradzki I, Kong YY, Sasaki T, Oliveira-dos-Santos A, Mariathasan S, Bouchard D, Wakeham A, Itie A, Le J, Ohashi PS, Sarosi I, Nishina H, Lipkowitz S, Penninger JM. Negative regulation of lymphocyte activation and autoimmunity by the molecular adaptor Cbl-b. Nature, January 2000; 403(6766): 211-6. DOI: 10.1038/35003228

166. **Chiang YJ**, Kole HK, Brown K, Naramura M, Fukuhara S, Hu RJ, Jang IK, Gutkind JS, Shevach E, Gu H. Cbl-b regulates the CD28 dependence of T-cell activation. Nature, January 2000; 403(6766):216-20. DOI: 10.1038/35003235

167. **Lin JT**, Lineberry NB, Kattah MG, Su LL, Utz PJ, Fathman CG, Wu L. Naive CD4 T Cell Proliferation Is Controlled by Mammalian Target of Rapamycin Regulation of GRAIL Expression. Journal of Immunology, May 2009; 182(10): 5919–5928.
DOI: 10.4049/jimmunol.0803986

168. **Kriegel MA,** Rathinam C, Flavell RA. E3 ubiquitin ligase GRAIL controls primary T cell activation and oral tolerance. Proceedings of the National Academy of Sciences of the United States of America, September 2009: 106 (39); 16770-16775. DOI: 10.1073/pnas.0908957106

169. **Nurieva RI**, Zheng S, Jin W, Chung Y, Zhang Y, Martinez GJ, Reynolds JM, Wang SL, Lin X, Sun SC,1 Lozano G, Dong C. The E3 ubiquitin ligase GRAIL regulates T cell tolerance and regulatory T cell function by mediating T cell receptor-CD3 degradation. Immunity, May 2010, 28; 32(5): 670-680. DOI: 10.1016/j.immuni.2010.05.002

170. **Melino G**, Gallagher E, Aqeilan RI, Knight R, Peschiaroli A, Rossi M, Scialpi F, Malatesta M, Zocchi L, Browne G, Ciechanover A, Bernassola F. Itch: a HECT-type E3 ligase regulating immunity, skin and cancer. Cell Death and Differeratiation, July 2008; 15(7): 1103-12. DOI: 10.1038/cdd.2008.60.

171. **Sluimer J**, Distel B. Regulating the human HECT E3 ligases. Cellular and Molecular Life Sciences, June 2018, 75(17): 3121–3141

172. **Aki D**, Zhang W, Liu YC. The E3 ligase Itch in immune regulation and beyond. Immunological Reviews John Wiley & Sons Ltd 2015; 266: 6–26

173. **Fang D**, Elly C, Gao B, Fang N, Altman Y, Joazeiro C, Hunter T, Copeland N, Jenkins N, Liu YC. Dysregulation of T lymphocyte function in itchy mice: a role for Itch in TH2 differentiation. Nature Immunology, MArch 2002; 3(3): 281-7. DOI: 10.1038/ni763

174. **Yang B**, Gay DL, MacLeod MK, Cao X, Hala T, Sweezer EM, Kappler J, Marrack P, Oliver PM. Nedd4 augments the adaptive immune response by promoting ubiquitin-mediated degradation of Cbl-b in activated T cells. Nature Immunology. December 2008; 9(12):1356-63. DOI: 10.1038/ni.1670. Epub 2008 Oct 19.

175. **Gay DL**, Ramón H, Oliver PM. Cbl- and Nedd4-family ubiquitin ligases: balancing tolerance and immunity. Immunologic Research, 2008;42(0): 51–64. DOI: 10.1007/s12026-008-8034-0

176. **Gruber T**, Hermann-Kleiter N, Hinterleitner R, Fresser F, Schneider R, Gastl G, Penninger JM, Baier G. PKC-theta modulates the strength of T cell responses by targeting Cbl-b for ubiquitination and degradation. Science Signaling, June 2009; 2(76): ra30. DOI: 10.1126/scisignal.2000046.

177. **Gruber T**, Hermann-Kleiter N, Pfeifhofer-Obermair C, Lutz-Nicoladoni C, Thuille N, Letschka T, Barsig J, Baudler M, Li J, Metzler B, Nüsslein-Hildesheim B, Wagner J, Leitges M, Baier G. PKC theta cooperates with PKC alpha in alloimmune responses of T cells in vivo. Molecular Immunology, June 2009; (10):2071-9. DOI: 10.1016/j.molimm.2009.02.030

178. **Pfeifhofer C**, Kofler K, Gruber T, Tabrizi NG, Lutz C, Maly K, Leitges M, BaierG. Protein Kinase C θ Affects Ca2+ Mobilization and NFAT Activation in Primary Mouse T Cells. Journal of Experimental Medicine, June 2003; 197(11): 1525–1535. DOI: 10.1084/jem.20020234

179. **Lin X**, O'Mahony A, Mu Y, Geleziunas R, Greene WC. Protein Kinase C-θ Participates in NF-κB Activation Induced by CD3-CD28 Costimulation through Selective Activation of IκB

Kinase β. Molecular and Cellular Biology, April 2000; 20(8): 2933–2940. DOI: 10.1128/mcb.20.8.2933-2940.2000

180. **Sun Z**, Arendt CW, Ellmeier W, Schaeffer EM, Sunshine MJ, Gandhi L, Annes J, Petrzilka D, Kupfer A, Schwartzberg PL, Littman DR. PKC-theta is required for TCR-induced NF-kappaB activation in mature but not immature T lymphocytes. Nature, March 2000; 404(6776): 402-7. DOI: 10.1038/35006090

181. **Salek-Ardakani S**, So T, Halteman BS, Altman A, Croft M. Protein kinase Ctheta controls Th1 cells in experimental autoimmune encephalomyelitis. Journal of Immunology, December 2005; 175(11): 7635-41. DOI: 10.4049/jimmunol.175.11.7635

182. **Salek-Ardakani S**, So T, Halteman BS, Altman A, Croft M. Differential regulation of Th2 and Th1 lung inflammatory responses by protein kinase C theta. Journal of Immunology, November 2004; 173(10): 6440-7.

183. **Brezar V**, Tu WJ, Seddiki N. PKC-Theta in Regulatory and Effector T-cell Functions. Frontiers in Immunology, October 2015; 6: 530. DOI: 10.3389/fimmu.2015.00530

184. **Walsh MC**, Lee JE, Choi Y. Tumor necrosis factor receptor associated factor 6 (TRAF6) regulation of development, function, and homeostasis of the immune system. Immunol Reviews, July 2015; 266(1): 72–92. DOI: 10.1111/imr.12302

185. **Shen J**, Qiao Y, Ran Z, Wang T. Different Activation of TRAF4 and TRAF6 in Inflammatory Bowel Disease. Mediators of Inflammation, 2013; DOI:10.1155/2013/647936

186. **Swaidani S**, Liu C, Zhao J, Bulek K and Li X. TRAF Regulation of IL-17 Cytokine Signaling. Frontiers in Immunology, June 2019. DOI: 10.3389/fimmu.2019.0129

187. **King CG**, Kobayashi T, Cejas PJ, Kim T, Yoon K, Kim GK, Chiffoleau E, Hickman SP, Walsh PT, Turka LA. TRAF6 is a T cell–intrinsic negative regulator required for the maintenance of immune homeostasis. Nature Medicine 2006; 12: 1088–1092

188. **Chiffoleau E**, Kobayashi T, Walsh MC, King CG, Walsh PT, Hancock WW, Choi Y, Turka LA. TNF receptor-associated factor 6 deficiency during hemopoiesis induces Th2-polarized inflammatory disease. Journal of Immunology, December 2003;171(11): 5751-9.

189. **Croft M**, Salek-Ardakani S, Song J, So T, Bansal-Pakala P. Regulation of T Cell Immunity by OX40 and OX40L. Madame Curie Bioscience Database. Austin, Texas: Landes Bioscience; 2000-2013.

190. **Willoughby J**, Griffiths J, Tews I, Cragg MS. OX40: Structure and function - What questions remain? Molecular Immunology, March 2017; 83:13-22.   DOI: 10.1016/j.molimm.2017.01.006.

191. **Webb GJ**, Hirschfield GM, Lane PJL. OX40, OX40L and Autoimmunity: a Comprehensive Review. Clinical Reviews in Allergy & Immunology. DOI 10.1007/s12016-015-8498-3

192. **Fu Y**, Lin Q, Zhang Z, Zhang L. Therapeutic strategies for the costimulatory molecule OX40 in T-cell mediated immunity. Acta Pharmaceutica Sinica B, September 2019. DOI: 10.1016/j.apsb.2019.08.010

193. **Takeda I**, Ine S, Killeen N, Ndhlovu LC, Murata K, Satomi S, Sugamura K, Ishii N. Distinct roles for the OX40-OX40 ligand interaction in regulatory and nonregulatory T cells. Journal of Immunology, March 2004; 172(6): 3580-9.

194. **Than NN**, Jeffery HC, Oo YH. Autoimmune Hepatitis: Progress from Global Immunosuppression to Personalised Regulatory T Cell Therapy. Canadian Journal of Gastroenterology and Hepatology, May 2016; 7181685. DOI: 10.1155/2016/7181685

195. **Benichou C**, Danan G, Flahault, A. Causality assessment of adverse reactions to drugs--II. An original model for validation of drug causality assessment methods: case reports with positive rechallenge. J Clin Epidemiol 1993; 46:1331-1336.

196. **Stürner KH**, Borgmeyer U, Schulze C, Pless O, Martin R. A multiple sclerosis-associated variant of CBLB links genetic risk with type I IFN function. J Immunol. 2014 Nov 1;193(9):4439-47. doi: 10.4049/jimmunol.1303077.

197. **Taubert R**, Hardtke-Wolenski M, Noyan F, Wilms A, Baumann AK, Schlue J, Olek S, Falk CS, Manns MP, Jaecke E. Intrahepatic regulatory T cells in autoimmune hepatitis are associated with treatment response and depleted with current therapies. Journal of Hepatology, November 2014 Nov; 61(5): 1106-14. DOI: 10.1016/j.jhep.2014.05.034

198. **Liberal R**, Grant CR, Mieli-Vergani G, Vergani D. Autoimmune hepatitis: a comprehensive review. Journal of Autoimmunity, March 2013; 41: 126-39. DOI: 10.1016/j.jaut.2012.11.002

199. **Crispe IN**. Liver antigen-presenting cells. Journal of Hepatology, February 2011; 54(2):357-65. DOI: 10.1016/j.jhep.2010.10.005

200. **Heneghan MA**, Yeoman AD, Verma S, Smith AD, Longhi MS. Autoimmune hepatitis. Lancet, October 2013; 382(9902): 1433-44. DOI: 10.1016/S0140-6736(12)62163-1

201. **Ebrahimkhani MR**, Mohar I, Crispe IN. Crosspresentation of antigen by diverse subsets of murine liver cells. Hepatology 54, 1379–1387 (2011).

202. **Ichiki Y**, Aoki CA, Bowlus CL, Shimoda S, Ishibashi H, Gershwin ME. T cell immunity in autoimmune hepatitis. Autoimmune Review 2005; 4(5): 315–321

203. **Vierling JM**. The pathogenesis of autoimmune hepatitis. In: Hirschfield GM, Heathcote EJ. Autoimmune Hepatitis: A Guide for Practicing Clinicians. New York: Humana Press, 2012

204. **Liberal R**, Longhi MS, Mieli-Vergani G, Vergani D. Pathogenesis of autoimmune hepatitis. Best Practice & Research. Clinical Gastroenterol, December 2011; 25(6): 653–664. DOI: 10.1016/j.bpg.2011.09.009.

205. **Sakaguchi S**, Miyara M, Costantino CM, Hafler DA. FOXP3+ regulatory T cells in the human immune system. Nat Rev Immunol, July 2010; 10(7): 490-500. DOI: 10.1038/nri2785. Epub 2010 Jun 18.

206. **Shevach EM**, Thornton AM tTregs, pTregs, and iTregs: similarities and differences. Immunology Rev. 2014 May; 259(1):88-102. DOI: 10.1111/imr.12160

207. **Longhi MS**, Ma Y, Grant CR, Samyn M, Gordon P, Mieli-Vergani G, Vergani D. T-regs in autoimmune hepatitis-systemic lupus erythematosus/mixed connective tissue disease overlap syndrome are functionally defective and display a Th1 cytokine profile. Journal of Autoimmunity 2013; 41: 146–151 37

208. **Muratori L**, Longhi MS. The interplay between regulatory and effector T cells in autoimmune hepatitis: Implications for innovative treatment strategies. J Autoimmun 2013; 46: 74–80

209. **Longhi MS**, Ma Y, Bogdanos DP, Cheeseman P, Mieli-Vergani G, Vergani D. Impairment of CD4(+)CD25(+) regulatory T-cells in autoimmune liver disease. J Hepatol 2004; 41: 31–37. 27

210. **Longhi MS**, Ma Y, Mitry RR, Bogdanos DP, Heneghan M, Cheeseman P, Mieli-Vergani G, Vergani D. Effect of CD4+ CD25+ regulatory T-cells on CD8 T-cell function in patients with autoimmune hepatitis. Journal of Autoimmunity, August 2005; 25(1):63-71.

211. **Ferri S**, Longhi MS, De Molo C, Lalanne C, Muratori P, Granito A, Hussain MJ, Ma Y, Lenzi M, Mieli-Vergani G, Bianchi FB, Vergani D, Muratori L. A multifaceted imbalance of T cells with regulatory function characterizes type 1 autoimmune hepatitis. Hepatology, August 2010. DOI: 10.1002/hep.23792

212. **Venuprasad K**. Cbl-b and Itch: Key regulators of peripheral T cell tolerance Cancer Research, April 2010; 70(8): 3009–3012. DOI: 10.1158/0008-5472.CAN-09-4076

213. **Tang R**, Langdon WY, Zhang J. Regulation of immune responses by E3 ubiquitin ligase Cbl-b PII: S0008-8749(18)30430-1 DOI: 10.1016/j.cellimm.2018.11.002

214. **Heissmeyer V**, Rao A. E3 ligases in T cell anergy--turning immune responses into tolerance. Sci STKE, July 2004; 2004(241):pe29.

215. **Schwartz RH**. T cell anergy. Annual Review of Immunology, 2003; 21:305-34.

216. **Klein L**, Kyewski B, Allen PM, Hogquist KA. Positive and negative selection of the T cell repertoire: what thymocytes see (and don't see). Nat Rev Immunol, June 2014; 14(6): 377-91. DOI: 10.1038/nri3667

217. **Hori S**, Takahashi T, Sakaguchi S. Control of autoimmunity by naturally arising regulatory CD4+ T cells. Advances in Immunology, 2003; 81: 331-71.

218. **Macian F**, Garcia-Cozar F, Im SH, Horton HF, Byrne MC, Rao A. Transcriptional mechanisms underlying lymphocyte tolerance. Cell, 2002; 109: 719–31

219. **Loeser S**, Penninger JM. Regulation of peripheral T cell tolerance by the E3 ubiquitin ligase Cbl-b, Semin Immunol. 19 (2007) 206-214, DOI: 10.1016/j.smim.2007.02.004

220. **Safford M**, Collins S, Lutz MA, Allen A, Huang CT, Kowalski J, Blackford A, Horton MR, Drake C, Schwartz RH, Powell JD. Egr-2 and Egr-3 are negative regulators of T cell activation. Nat Immunol. May 2005; 6(5):472-80. DOI: 10.1038/ni1193

221. **Naramura M**, Jang IK, Kole H, Huang F, Haines D, Gu H. c-Cbl and Cbl-b regulate T cell responsiveness by promoting ligand-induced TCR down-modulation. Nature Immunology, December 2002; 3(12): 1192-9

222. **Krawczyk C**, Bachmaier K, Sasaki T, Jones RG, Snapper SB, Bouchard D, Kozieradzki I, Ohashi PS, Alt FW, Penninger JM. Cbl-b is a negative regulator of receptor clustering and raft aggregation in T cells. Immunity, October 2000;13(4):463-73.

223. **Jeon MS**, Atfield A, Venuprasad K, Krawczyk C, Sarao R, Elly C, Yang C, Arya S, Bachmaier K, Su L, Bouchard D, Jones R, Gronski M, Ohashi P, Wada T, Bloom D, Fathman CG, Liu YC, Penninger JM. Essential role of the E3 ubiquitin ligase Cbl-b in T cell anergy induction. Immunity, Aigust 2004; 21(2): 167-77. DOI: 10.1016/j.immuni.2004.07.013

224. **Paolino M**, Thien CB, Gruber T, Hinterleitner R, Baier G, Langdon WY, Penninger JM. Essential role of E3 ubiquitin ligase activity in Cbl-b-regulated T cell functions. Journal of Immunology, February 2011; 186(4): 2138-47. DOI: 10.4049/jimmunol.1003390

225. **Adams CO**, Housley WJ, Bhowmick S, Cone RE, Rajan TV, Forouhar F, Clark RB. Cbl-b (-/-) T cells demonstrate in vivo resistance to regulatory T cells but a context-dependent resistance to TGF-beta. J Immunology, August 2010; 185(4): 2051-8.

226. **Wohlfert EA**, Callahan MK, Clark RB. Resistance to CD4+CD25+ regulatory T cells and TGF-beta in Cbl-b-/- mice. Journal of Immunology, July 2004; 173(2): 1059-65.

227. **Zhang J**, Bárdos T, Li D, Gál I, Vermes C, Xu J, Mikecz K, Finnegan A, Lipkowitz S, Glant TT. Cutting edge: regulation of T cell activation threshold by CD28 costimulation through targeting Cbl-b for ubiquitination. Journal of Immunology, September 2002; 169(5): 2236-40. DOI: 10.4049/jimmunol.169.5.2236

228. **Gruber T**, Hermann-Kleiter N, Hinterleitner R, Fresser F, Schneider R, Gastl G, Penninger JM, Baier G. PKC-theta modulates the strength of T cell responses by targeting Cbl-b for ubiquitination and degradation. Science Signalaling, June 2009; 2(76): ra30. DOI: 10.1126/scisignal.2000046

229. **St Rose MC**, Qui HZ, Bandyopadhyay S, Mihalyo MA, Hagymasi AT, Clark RB, Adler AJ. The E3 ubiquitin ligase Cbl-b regulates expansion but not functional activity of self-reactive CD4 T cells. Journal of Immunology, October 2009; 183(8): 4975-83. DOI: 10.4049/jimmunol.0901243

230. **Leng Q,** Borkow G, Bentwich Z. Attenuated signaling associated with immune activation in HIV-1-infected individuals. Biochem Biophys Res Commun, November 2002; 298(4): 464-7. DOI: 10.1016/s0006-291x(02)02460-9

231. **Leng Q**, Bentwich Z, Borkow G. Increased TGF-beta, Cbl-b and CTLA-4 levels and immunosuppression in association with chronic immune activation. Int Immunology, May 2006; 18(5): 637-44. DOI: 10.1093/intimm/dxh375

232. **Oestreich KJ**, Yoon H, Ahmed R, Boss JM. NFATc1 regulates PD-1 expression upon T cell activation. Journal of Immunology, October 2008; 181(7): 4832-9.

233. **Bally APR**. Austin JW, Boss JM. Genetic and epigenetic regulation of PD-1 expression. Journal of Immunology, March 2016; 196(6): 2431–2437. DOI: 10.4049/jimmunol.1502643

234. **Oikawa T**, Takahashi H, Ishikawa T, Hokari A, Otsuki N, Azuma M, Zeniya M, Tajiri H. Intrahepatic expression of the co-stimulatory molecules programmed death-1, and its ligands in autoimmune liver disease. Pathol Int. 2007 Aug;57(8):485-92. DOI: 10.1111/j.1440-1827.2007.02129.x

235. **Agina HA**, Ehsan NA, Abd-Elaziz TA, Abd-Elfatah GA, Said EM, Sira MM. Hepatic expression of programmed death-1 (PD-1) and its ligand, PD-L1, in children with autoimmune hepatitis: relation to treatment response. Clin Exp Hepatology, September 2019; 5(3):256-264. doi: 10.5114/ceh.2019.87642

236. **Kassel R**, Cruise MW, Iezzoni JC, Taylor NA, Pruett TL, Hahn YS Chronically inflamed livers up-regulate expression of inhibitory B7 family members. Hepatology, November 2009; 50(5):1625-37. DOI: 10.1002/hep.23173.

237. **Behairy OG**, Behiry EG, El Defrawy MS, El Adly AN. Diagnostic value of soluble programmed cell death protein-1 in type-1 autoimmune hepatitis in Egyptian children. Scand J Clin Lab Invest, November 2019; 1-7. DOI: 10.1080/00365513.2019.1695283

238. **Li YG**, Chen LE, Chen GF, Wang FS. Expressions and significance of B7-H1 and programmed death-1 in lymphocytes from patients with chronic hepatitis B virus infection. Chin. J. Hepatolology, 2007; 738–741

239. **Boni C**, Fisicaro P, Valdatta C, Amadei B, Di Vincenzo P, Giuberti T, Laccabue D, Zerbini A, Cavalli A, Missale G, Bertoletti A, Ferrari C. Characterization of hepatitis B virus (HBV)-specific T-cell dysfunction in chronic HBV infection. J Virol, 2007; 81(8): 4215-25. DOI: 10.1128/JVI.02844-06

240. **Peng G**, Li S, Wu W, Tan X, Chen Y, Chen Z. PD-1 upregulation is associated with HBV-specific T cell dysfunction in chronic hepatitis B patients. Mol Immunol. 2008 Feb;45(4):963-70. DOI: 10.1016/j.molimm.2007.07.038

241. **Golden-Mason L**, Klarquist J, Wahed AS, Rosen HR. Cutting edge: Programmed death-1 expression is increased on immunocytes in chronic hepatitis C virus and predicts failure of response to antiviral therapy: Race-dependent differences. Journal of Immunology, 2008; 180: 3637–3641

242. **Gruener NH**, Lechner F, Jung MC, Diepolder H, Gerlach T, Lauer G, Walker B, Sullivan J, Phillips R, Pape GR, Klenerman P. Sustained dysfunction of antiviral CD8+ T lymphocytes after infection with hepatitis C virus. J Virol. 2001 Jun;75(12):5550-8. DOI: 10.1128/JVI.75.12.5550-5558.2001

243. **Penna A**, Pilli M, Zerbini A, Orlandini A, Mezzadri S, Sacchelli L, Missale G, Ferrari C. Dysfunction and functional restoration of HCV-specific CD8 responses in chronic hepatitis C virus infection. Hepatology 2007, 45, 588–601.

244. **Nakamoto N**, Kaplan DE, Coleclough J, Li Y, Valiga ME, Kaminski M, Shaked A, Olthoff K, Gostick E, Price DA, Freeman GJ, Wherry EJ, Chang KM. Functional restoration of HCV-specific CD8 T cells by PD-1 blockade is defined by PD-1 expression and compartmentalization. Gastroenterology, June 2008;134(7): 1927-37, 1937.e1-2. DOI: 10.1053/j.gastro.2008.02.033. Epub 2008 Feb 17.

245. **Cho H**, Kang H, Lee HH, Kim CW. Int. Review Programmed Cell Death 1 (PD-1) and Cytotoxic T Lymphocyte-Associated Antigen 4 (CTLA-4) in Viral Hepatitis. J. Mol. Sci. 2017, 18(7), 1517. DOI: 10.3390/ijms18071517

246. **Schietinger A**, Greenberg PD. Tolerance and Exhaustion: Defining Mechanisms of T cell Dysfunction. Trends in Immunology, February 2014; 35(2): 51–60. DOI: 10.1016/j.it.2013.10.001

247. **Li C**, Xu X, Wang H, Wei B. PD-1 and CTLA-4 Mediated Inhibitory Signaling for T cell Exhaustion during Chronic Viral Infections. J Clin Cell Immunology, November 2012. DOI:10.4172/2155-9899.S12-010

248. **Bernard NJ**. Some PD-1+ CD8+ T cells are not exhausted. Nature Reviews Rheumatology, September 2018; 14: 624

249. **Petrelli A**, Mijnheer G, Hoytema van Konijnenburg DP1, van der Wal MM, Giovannone B, Mocholi E, Vazirpanah N, Broen JC, Hijnen D, Oldenburg B, Coffer PJ, Vastert SJ, Prakken BJ, Spierings E, Pandit A, Mokry M, van Wijk F. PD-1+CD8+ T cells are clonally expanding effectors in human chronic inflammation. J Clin Invest, October 2018; 128(10): 4669-4681. DOI: 10.1172/JCI96107

250. **Leng Q**, Bentwich Z, Magen E, Kalinkovich A, Borkow G. CTLA-4 upregulation during HIV infection: association with anergy and possible target for therapeutic intervention. AIDS, March 2002; 16(4): 519-29.

251. **Arasanz H**, Gato-Cañas M, Zuazo M, Ibañez-Vea M, Breckpot K, Kochan G, Escors D. PD1 signal transduction pathways in T cells. Oncotarget, April 2017; 8(31): 51936-51945. DOI: 10.18632/oncotarget.17232

252. **Karwacz K**, Bricogne C, MacDonald D, Arce F, Bennett CL, Collins M, Escors D. PD-L1 co-stimulation contributes to ligand-induced T cell receptor down-modulation on CD8+ T cells. EMBO Mol Med, October 2011; 3(10): 581–592. DOI: 10.1002/emmm.201100165

253. **Löhning M**, Hutloff A, Kallinich T, Mages HW, Bonhagen K, Radbruch A, Hamelmann E, Kroczek RA. Expression of ICOS In Vivo Defines CD4+ Effector T Cells with High Inflammatory Potential and a Strong Bias for Secretion of Interleukin 10. J Exp Med. 2003 Jan 20; 197(2): 181–193. DOI: 10.1084/jem.20020632

254. **Yu D**, Tan AH, Hu X, Athanasopoulos V, Simpson N, Silva DG, Hutloff A, Giles KM, Leedman PJ, Lam KP, Goodnow CC, Vinuesa CG. Roquin represses autoimmunity by limiting

inducible T-cell co-stimulator messenger RNA. Nature, November 2007; 450(7167): 299-303. DOI: 10.1038/nature06253.

255. **Bertino SA**, Craft J. Immunity. Roquin Paralogs Add a New Dimension to ICOS Regulation. Immunity, April 2013; 38(4): 624–626. DOI: 10.1016/j.immuni.2013.03.007

256. **Tilg H**, Wilmer A, Vogel W, Herold M, Nolchen B, Judmaier G, Huber C. Serum levels of cytokines in chronic liver diseases. Gastroenterology 1992; 103: 264-274

257. **Maggiore G**, De Benedetti F, Massa M, Pignatti P, Martini A: Circulating levels of interleukin-6, interleukin-8, and tumor necrosis factor-α in children with autoimmune hepatitis. J Pediatr Gastroenterol Nutr 1995; 20:23-27

258. **Czaja AJ**, Sievers C, Zein NN. Nature and Behavior of Serum Cytokines in Type 1 Autoimmune Hepatitis. Digestive Diseases and Sciences, May 2000; 45(5): 1028–1035

259. **Wang M**, Zhang H. The pathogenesis of autoimmune hepatitis. Frontiers in Laboratory Medicine, March 2018; 2(1): 36-39. DOI: 10.1016/j.flm.2018.03.002

260. **Bovensiepen CS**, Schakat M, Sebode M, Zenouzi R, Hartl J, Peiseler M, Li J, Henze L, Woestemeier A, Schramm C, Lohse AW, Herkel J, Weiler-Normann C. TNF-Producing Th1 Cells Are Selectively Expanded in Liver Infiltrates of Patients with Autoimmune Hepatitis. Journal of Immunology, December 2019; 203(12): 3148-3156. DOI:10.4049/jimmunol.1900124

261. **Lopetuso LR**, Mocci G, Marzo M, D'Aversa F, Rapaccini GL, Guidi L, Armuzzi A, Gasbarrini A, Papa A. Harmful Effects and Potential Benefits of Anti-Tumor Necrosis Factor (TNF)-α on the Liver Int J Mol Sci. 2018 Jul 27;19(8). DOI: 10.3390/ijms19082199

262. **Terziroli Beretta-Piccoli B**, Mieli-Vergani G, Vergani D. Autoimmune hepatitis: Standard treatment and systematic review of alternative treatments. World J Gastroenterol, September 2017; 23(33):6030-6048. doi: 10.3748/wjg.v23.i33.6030.

263. **Ghabril M**, Bonkovsky HL, Kum C, Davern T, Hayashi PH, Kleiner DE, Serrano J, Rochon J, Fontana RJ, Bonacini M. Liver injury from tumor necrosis factor-α antagonists: analysis of thirty-four cases.US Drug-Induced Liver Injury Network. Clin Gastroenterol Hepatology, January 2013 May;11(5):558-564.e3. doi: 10.1016/j.cgh.2012.12.025

264. **Behfarjam F**, Nasseri-Moghaddam S, Jadali Z. Enhanced Th17 Responses in Patients with Autoimmune Hepatitis. Middle East J Dig Dis, April 2019; 11(2): 98–103. DOI:10.15171/mejdd.2018.134

265. **Zhao L**, Tang Y, You Z, Wang Q, Liang S, Han X, Qiu D, Wei J, Liu Y, Shen L, Chen X, Peng, Zhiping Li Y, Ma X. Interleukin-17 Contributes to the Pathogenesis of Autoimmune Hepatitis through Inducing Hepatic Interleukin-6 Expression. Plos one, April 2011. DOI: 10.1371/journal.pone.0018909

266. **Liang SC**, Tan XY, Luxenberg DP, Karim R, Dunussi-Joannopoulos K, Collins M, Fouser LA. Interleukin (IL)-22 and IL-17 are coexpressed by Th17 cells and cooperatively enhance expression of antimicrobial peptides. J Exp Med, October 2006; 203(10): 2271–2279.DOI: 10.1084/jem.20061308

267. **Stritesky GL**, Yeh N, Kaplan MH. IL-23 promotes maintenance but not commitment to the Th17 lineage. J Immunol, November 2008; 181(9): 5948–5955. DOI: 10.4049/jimmunol.181.9.5948

268. **Tesmer LA**, Lundy SK, Sarkar S, Fox DA. Th17 cells in human disease. Immunol Rev, June 2008; 223: 87–113. DOI: 10.1111/j.1600-065X.2008.00628.x

269. **Yeoman AD**, Heneghan MA. Anti TNF-α therapy can be a novel treatment option in patients with autoimmune hepatitis: authors' reply. Aliment Pharmacol Ther, 2010; 32 (1):116-117

270. **Passos ST**, Silver JS, O'Hara AC, Sehy D, Stumhofer JS, Hunter CA. IL-6 promotes NK cell production of IL-17 during toxoplasmosis. J Immunol, February 2010;184(4):1776-83. DOI: 10.4049/jimmunol.0901843

6.2 Abbreviations

AIH	autoimmune hepatitis
Ab	antibody
AF488	alexa fluor 488
ALT	alanine transaminase
AMA	anti-mitochondrial antibodies
ANA	ant- inuclear antibodies
ANOVA	analysis of variance
AP (ALP)	alkaline Phosphatase
APCs	antigen presenting cells
APC	allophycocyanin
ASMA	anti-smooth muscle antibodies
AST	aspartate transaminase
Bili	bilirubin
BSA	bovine serum albumin
BV	brilliant violet
CBL-B	casitas B-lineage lymphoma proto-oncogene-b
CD	cluster of differentiation
cDNA	complementary deoxyribonucleic acid
CTLA-4	cytotoxic T-lymphocyte-associated Protein 4
DAB	3, 3- diaminobenzidine
DC	dendritic cells
DILI	drug induced liver injury
DMSO	dimethylsulfoxide
DNA	deoxyribonucleic acid
dNTPs	deoxyribonucleotide triphosphate
DPBS	Dulbecco's Phosphate-Buffered Saline
EDTA	ethylenediaminetetraacetic acid
ELISA	enzyme-linked immunosorbent assay
FACS	fluorescence-activated cell sorting
FC	flow cytometry

FCS	fetal calf serum
FFPE	formalin-fixed paraffin-embedded
FITC	fluorescein isothiocyanate
FOXP3	forhead Box Protein 3
g	gramme
GRAIL	gene related to anergy in lymphocytes
h	hour
HLA	human leukocyte antigen
HPRT1	hypoxanthine posphoribosyl transferase 1
IBD	inflammatory bowel disease
ICOS	inducible T-cell co-stimulator
IF	immunofuorescence
IFN	interferon
Ig	immunoglobulin
IHC-P	immunohistochemistry on fixed and in paraffin embedded tissue
IL	interleukin
ITAMs	immunoreceptor tyrosine- based activation motifs
ITCH	itchy E3 Ubiquitin Protein Ligase
ITIM	immunoreceptor tyrosine-based inhibition motif
ITISM	immunoreceptor tyrosine-based switch motif
MACS	magnetic activated cell sorting
mg	miligram
mHAI	modified hepatic activity index
MHC	major histocompatibility complex
min	minute
mL	millilitre
mM	millimolar
mRNA	messenger ribonucleic acid
NASH	non-alcoholic steatohepatitis
NEDD4	neural precursor cell expressed developmentally down-regulated protein 4
NGS	normal goat serum

P13K	class IA phosphatidylinositol 3-kinase
pANCA	perinuclear anti- neutrophil cytoplasmic antibodies
PBC	primary biliary cholangitis
PBS	phosphate-buffered saline
PCR	polymerase chain reaction
PD-1	programmed cell death protein 1
PE	phycoerythrin
PKC -Ө	protein kinase C theta
PP2A	protein Phosphatase 2A
PSC	primary sclerosing cholangitis
RNA	ribonucleic acid
rpm	rotation per minute
RPMI	Roswell Park Memorial Institute
RT	room temperature
SHP-2	Src homology region 2 domain- containing phosphatase
TCR	T cell receptor
T_h	T helper cell
TMB	3,3',5,5'- tetramethylbenzidine
TNF	tumor necrosis factor
TNFRSF4 (OX40)	Tumor necrosis factor receptor superfamily, member 4
TRAF6	TNF receptor associated factor 6
T reg	regulatory T cell
W	watt
xg	times gravity
ZAP-70	zeta-assoziierten Proteins 70

6.3 Congress Participations

The International Liver Congress™ European Association for the Study of the Liver (EASL)

Vienna, Austria. Poster presentation:

Activation regulators of peripheral blood and intrahepatic T effector cells in autoimmune hepatitis**.**

Pamela Filpe[1], Sören Weidemann[2], Christina Weiler-Normann[1], Ansgar W Lohse[1], Christoph Schramm[1,3], Johannes Herkel[1], Marcial Sebode[1]

[1] I. Department of Medicine, University Medical Centre Hamburg-Eppendorf, Hamburg, Germany

[2] Department of Pathology, University Medical Centre Hamburg-Eppendorf, Hamburg, Germany

[3] Martin Zeitz Centre for Rare Diseases, University Medical Centre Hamburg-Eppendorf, Hamburg, Germany

European Network of Immunology Institutes (ENII)

Sardinia, Italy. Invited speaker:

Activation regulators of peripheral blood and intrahepatic T effector cells in autoimmune hepatitis.

Pamela Filpe[1], Sören Weidemann[2], Christina Weiler-Normann[1], Ansgar W Lohse[1], Christoph Schramm[1,3], Johannes Herkel[1], Marcial Sebode[1]

[1] I. Department of Medicine, University Medical Centre Hamburg-Eppendorf, Hamburg, Germany

[2] Department of Pathology, University Medical Centre Hamburg-Eppendorf, Hamburg, Germany

[3] Martin Zeitz Centre for Rare Diseases, University Medical Centre Hamburg-Eppendorf, Hamburg, Germany

German Association of the Study of the Liver (GASL)

Mainz, Germany. Poster presentation

Aberrant expression of activation regulators CBL-B, CTLA-4 and PD-1 in intrahepatic T effector cells in autoimmune hepatitis.

Pamela Filpe[1], Anna Wöstemeier[2], Eleonora De Martin[3,4], Sören Weidemann[5], Richard Taubert[6,4], Christoph Schramm[1,4], Ansgar W Lohse[1,4], Johannes Herkel[1], Marcial Sebode[1,4]

1 I. Department of Medicine, University Medical Centre Hamburg-Eppendorf, Hamburg, Germany

2 Department of General, Visceral and Thoracic Surgery, University Medical Centre Hamburg

3 Department of Hepatology, AP-HP Hôpital Paul-Brousse, Centre Hépato-Biliaire, Villejuif, France

4 European Reference Network on Hepatological Diseases (ERN RARE-LIVER)

5 Department of Pathology, University Medical Centre Hamburg-Eppendorf, Hamburg, Germany

6 Department of Gastroenterology, Hepatology and Endocrinology, Hannover Medical School, Hannover, Germany

6.4   Publications

Activation regulators of peripheral blood and intrahepatic T effector cells in autoimmune hepatitis**.**

Pamela Filpe[1], Sören Weidemann[2], Christina Weiler-Normann[1], Ansgar W Lohse[1], Christoph Schramm[1,3], Johannes Herkel[1], Marcial Sebode[1]

[1] I. Department of Medicine, University Medical Centre Hamburg-Eppendorf, Hamburg, Germany

[2] Department of Pathology, University Medical Centre Hamburg-Eppendorf, Hamburg, Germany

[3] Martin Zeitz Centre for Rare Diseases, University Medical Centre Hamburg-Eppendorf, Hamburg, Germany

(EASL 2019-Congress publication)

Autoaggression of $FOXO1_{low}CXCR6^{hi}CD8^+$ T cells causing liver pathology in NASH. Michael Dudek[1], Dominik Pfister[2], Sainitin Donakonda[1], **Pamela Filpe**[3], Rupert Öllinger[1], Roland Rad[1], Ansgar Lohse[3], Mathias Heikenwälder[2], Percy A. Knolle[1]

[1]Institute of Molecular Immunology and Experimental Oncology, Technical University of Munich, Munich, Germany;

[2]German Cancer Research Center, DKFZ, Munich, Germany

[3]I. Department of Medicine, University Medical Centre Hamburg-Eppendorf, Hamburg, Germany

[4]European Reference Network on Hepatological Diseases (ERN RARE-LIVER)

(German Society for Immunology DGfI 2019-Congress publication)

6.5   Acknowledgement

6.6   Declaration in lieu of an oath/ Eidesstattliche Versicherung

I hereby declare on oath that I have written the present dissertation myself and have used no other than the specified sources and resources.

/

Hiermit erkläre ich an Eides statt, dass ich die vorliegende Dissertationsschrift selbst verfasst und keine anderen als die angegebenen Quellen und Hilfsmittel benutzt habe.

_____	_____	_____
place/ Ort	date/ Datum	signature/ Unterschrift